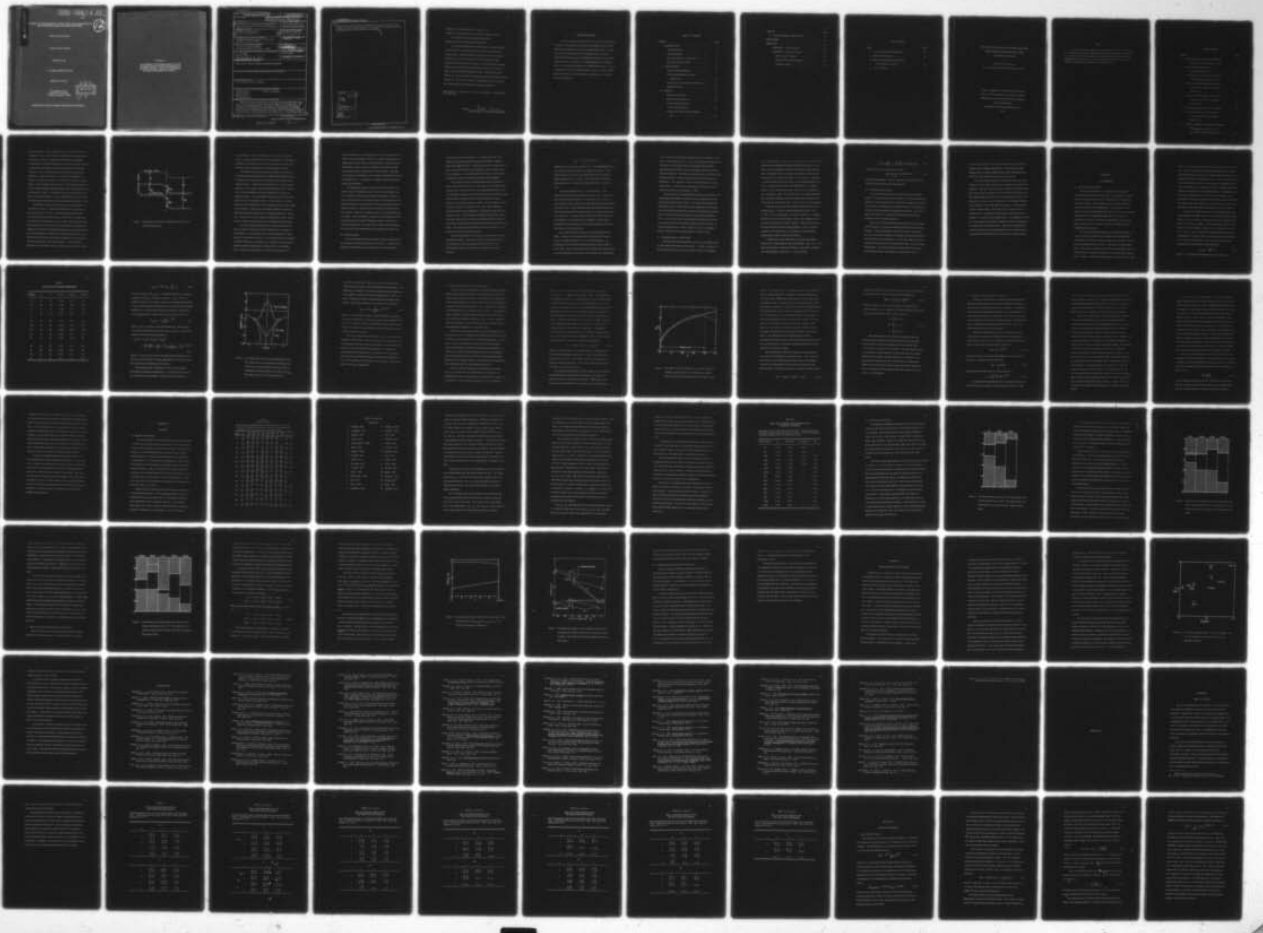
AD-A032 078 COLORADO UNIV BOULDER F/G 20/12
A MODEL FOR THE PREDICTION OF SEMICONDUCTOR HETEROJUNCTION DISC--ETC(U)
SEP 76 W R FRENSLEY DAHC04-74-G-0114
UNCLASSIFIED ARO-12061.4-EL NL

1 OF 2
ADA032078



AD A032078

AQO-12061.4-EL

A MODEL FOR THE PREDICTION OF SEMICONDUCTOR HETEROJUNCTION DISCONTINUITIES USING BULK BAND STRUCTURES

12

Interim Technical Report

William Robert Frensley

September 1976

U. S. ARMY RESEARCH OFFICE

DAHC04-74-G-0114

DDC
RECEIVED
NOV 16 1976
B

The Regents of the
University of Colorado
Boulder, Colorado 80309

APPROVED FOR PUBLIC RELEASE; DISTRIBUTION UNLIMITED.

Disclaimer

THE FINDINGS IN THIS REPORT ARE NOT TO BE CONSTRUED AS AN OFFICIAL DEPARTMENT OF THE ARMY POSITION, *UNLESS SO DESIGNATED* BY OTHER AUTHORIZED DOCUMENTS.

UNCLASSIFIED

SECURITY CLASSIFICATION OF THIS PAGE (When Data Entered)

REPORT DOCUMENTATION PAGE	READ INSTRUCTIONS BEFORE COMPLETING FORM
1. REPORT NUMBER	2. GOVT ACCESSION NO. (9) Doctoral thesis, 3. RECIPIENT'S CATALOG NUMBER
4. TITLE (and Subtitle) (6) A Model for the Prediction of Semiconductor Heterojunction Discontinuities Using Bulk Band Structures	5. TYPE OF REPORT & PERIOD COVERED Interim Technical Report
	6. PERFORMING ORG. REPORT NUMBER
7. AUTHOR(s) (10) William Robert Frensley	8. CONTRACT OR GRANT NUMBER(s) (15) DAHC04-74-G-0114
9. PERFORMING ORGANIZATION NAME AND ADDRESS The Regents of the University of Colorado Boulder, Colorado 80309	10. PROGRAM ELEMENT, PROJECT, TASK AREA & WORK UNIT NUMBERS P-12061-E
11. CONTROLLING OFFICE NAME AND ADDRESS U.S. Army Research Office Research Triangle Park, N.C. 27709	12. REPORT DATE (11) September 1976 13. NUMBER OF PAGES 150 (12) 151 p.
14. MONITORING AGENCY NAME & ADDRESS (if different from Controlling Office) (18) ARO (19) 12061.4-EL	15. SECURITY CLASS. (of this report) Unclassified
	15a. DECLASSIFICATION/DOWNGRADING SCHEDULE

16. DISTRIBUTION STATEMENT (of this Report)

Approved for public release; distribution unlimited.

17. DISTRIBUTION STATEMENT (of the abstract entered in Block 20, if different from Report)

18. SUPPLEMENTARY NOTES

Ph.D. Thesis of W. R. Frensley

19. KEY WORDS (Continue on reverse side if necessary and identify by block number)

Heterojunctions
Semiconductors
Band structure
Pseudopotentials
Electron affinities

20. ABSTRACT (Continue on reverse side if necessary and identify by block number)

The problem of theoretically predicting the energy band discontinuities at a semiconductor heterojunction is studied in a simple model. The bulk band structures and their relationship to the periodic electrostatic potential are calculated by a self-consistent pseudopotential technique. A simple matching scheme determines the lineup of the electrostatic potentials at the interface, and this determines the band lineup. The predicted band

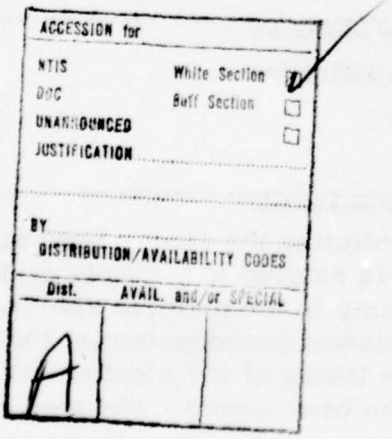
DD FORM 1 JAN 73 1473 EDITION OF 1 NOV 65 IS OBSOLETE

UNCLASSIFIED

SECURITY CLASSIFICATION OF THIS PAGE (When Data Entered)

088 400 Dnc

lineups are in good qualitative agreement with experimentally known lineups, and the model is applied to the prediction of discontinuities for heterojunctions for which no data are available.



Frensley, William Robert (Ph.D., Physics)

A Model for the Prediction of Semiconductor Heterojunction Discontinuities Using Bulk Band Structures

Thesis directed by Professor Herbert Kroemer

The problem of theoretically predicting the energy band discontinuities at a semiconductor heterojunction is studied in a simple model. The bulk band structures and their relationship to the periodic electrostatic potential are calculated by a self-consistent pseudopotential technique. A simple matching scheme determines the lineup of the electrostatic potentials at the interface, and this determines the band lineup. The predicted band lineups are in good qualitative agreement with experimentally known lineups, and the model is applied to the prediction of discontinuities for heterojunctions for which no data are available.

This abstract is approved as to form and content. I recommend its publication.

Signed Herbert Kroemer

Faculty member in charge of dissertation

ACKNOWLEDGMENTS

I wish to express my appreciation to my advisor, Prof. Herbert Kroemer, for his generous assistance and guidance, and to Henry Schauer, for numerous discussions concerning this work. I would also like to thank Professors R. H. Garstang and S. Geller for helping me find various bits of information necessary for this work, and Professors R. E. Hayes, K. T. Mahanthappa, W. O'Sullivan, and J. F. Scott for their suggestions concerning the thesis. I wish to thank Ann Cofer for doing the typing. Finally, I want to express particular appreciation to my fiancée, Susan Rinker, for her help and encouragement.

TABLE OF CONTENTS

CHAPTER	PAGE
I. INTRODUCTION	1
Heterojunctions	1
Pseudopotentials	5
Pseudopotentials in Other Fields	8
The Heterojunction Model	10
II. CALCULATIONS	12
The Ionic Pseudopotential	12
Self-Consistent Band Structure Calculations	20
Evaluation of the Electrostatic Potential . . .	25
Matching Scheme	28
III. RESULTS	31
Band Structure Results	31
Heterojunction Predictions	38
Heterojunctions Involving Semiconductor Alloys	44
Comparison with the Electron-Affinity Rule	50

CHAPTER PAGE

IV. DISCUSSION AND CONCLUSIONS 52

BIBLIOGRAPHY 59

APPENDICES 68

APPENDIX A. Free Ion Spectra 69

APPENDIX B. Computer Programs 80

Band Structure Program 80

Electrostatic Potential Program 85

Program Listings 86

LIST OF TABLES

TABLE		PAGE
I.	Ionic Pseudopotential Parameters	16
II.	Band Structure Results	32
III.	Band Edge Energies with Respect to the Reference Potential	37
IV.	Free Ion Spectra	73

A MODEL FOR THE PREDICTION OF SEMICONDUCTOR HETEROJUNCTION DISCONTINUITIES USING BULK BAND STRUCTURES

by

William Robert Frensley

B.S., California Institute of Technology, 1973

A thesis submitted to the Faculty of the Graduate School of the University of Colorado in partial fulfillment of the requirements for the degree of

Doctor of Philosophy

Department of Physics and Astrophysics

1976

NOTE

This Interim Technical Report is a verbatim copy of the Ph.D. thesis of Dr. William R. Frensley. Although parts of it will eventually be published, it is issued in this form because it is believed to be desirable to make the complete thesis available as soon as possible to those who might wish to employ the procedures developed here in their own work.

LIST OF FIGURES

FIGURE		PAGE
1.	The Anderson model for the energy band profile of an abrupt heterojunction	3
2.	The components of the ionic pseudopotential for Ge	18
3.	The cube root of the charge density and the quadratic approximation (II.9)	22
4.	The relative band energies for the semiconductors with lattice constants near 5.45 Å	39
5.	The relative band energies for the semiconductors with lattice constants near 5.65 Å	41
6.	The relative band lineup for InP and CdS	43
7.	The relative band lineup for the semiconductors with lattice constants around 6.1 Å	45
8.	Conduction band and valence band energies of $Ga_{0.48y}In_{1-0.48y}As_yP_{1-y}$ as a function of composition parameter y	48

FIGURE PAGE

9. The band edge energies of the quaternary alloy systems (Ga,In)(As,P) and (Al,Ga)(As,Sb) as a function of lattice constant 49

10. The electron affinity vs. the conduction band energy relative to our reference potential 55

11. The potential difference between the two interstitial points vs. the difference in Phillips electronegativity. 57

CHAPTER I

INTRODUCTION

A. Heterojunctions

Semiconductor heterojunctions are junctions between chemically different semiconductors, such as between GaAs and AlAs, or between GaAs and Ge. The two semiconductors which form a heterojunction may have significantly different properties, so the use of such junctions promises to increase vastly the flexibility available in the design of electronic devices. However, the technology involved in fabricating heterojunctions is complex, and often is not readily transferable from one material to another. Thus there is a need to be able to predict the properties of a heterojunction between two given semiconductors before that heterojunction is in fact fabricated. In this work we describe a theoretical model which successfully gives the energy band lineups of known heterojunctions, and which is readily applied to unknown ones.

Sharma and Purohit have published an exhaustive review of heterojunction work up to about 1973 [Sharma, 1974], so only a brief historical account will be given here. The first proposal to use different semiconductors in the same electronic device was

made by Shockley in the patent on the bipolar junction transistor [Shockley, 1951]. Real interest in heterojunction technology did not develop, however, until Kroemer showed that significant improvements in transistor performance could be achieved by using a wider-gap semiconductor for the emitter than that of the base [Kroemer, 1957]. Anderson fabricated the first heterojunctions [Anderson, 1960] and presented a theoretical model [Anderson, 1962] for the band lineup which is commonly used today to explain abrupt, lattice-matched heterojunctions. Heterojunction work was further stimulated when Kroemer suggested the double-heterostructure laser [Kroemer, 1963]. Currently the most important application of heterojunction technology is in such opto-electronic devices, and they are rapidly approaching commercial production [Kressel, 1976].

The Anderson model of the band lineup at a heterojunction is illustrated in Figure 1, with band energy plotted as a function of position through the junction. Anderson assumes that the bulk semiconductor band structures exist up to the junction where they discontinuously change from one to the other. The magnitude of the discontinuity in the conduction band is assumed to be given by the difference in the electron affinities between the two semiconductors. The electron affinity χ is defined as the energy required to move an electron from the bottom of the conduction band to a point just outside the semiconductor (the "vacuum level"). Thus the basic assumption in the Anderson model is that the vacuum levels line up

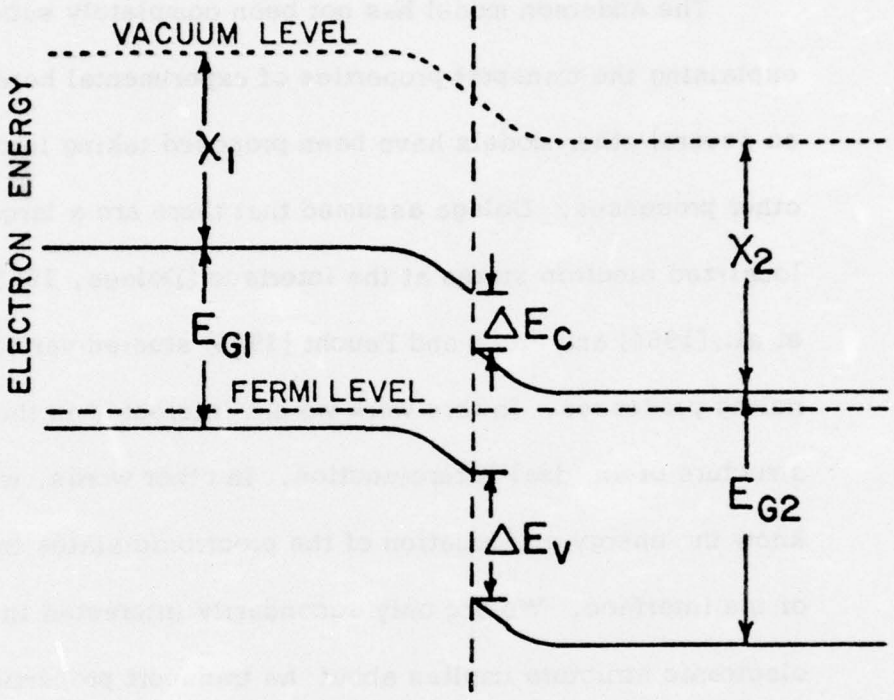


Figure 1. The Anderson model for the energy band profile of an abrupt heterojunction.

at the interface. Once the heterojunction is formed, the Fermi levels in the two semiconductors must be equalized. This involves a transfer of electrons from one side of the junction to the other, creating a space charge with the consequent band bending.

The Anderson model has not been completely successful in explaining the transport properties of experimental heterojunctions, so several other models have been proposed taking into account other processes. Dolega assumed that there are a large number of localized electron states at the interface [Dolega, 1963]. Rediker, et al.,[1964] and Riben and Feucht [1966] studied various tunneling processes. In this work we are interested in the electronic structure of an ideal heterojunction. In other words, we wish to know the energy and location of the electronic states in the vicinity of the interface. We are only secondarily interested in what the electronic structure implies about he transport properties. Therefore, we assume most of the features of Anderson's model: discontinuous change in band structure at the interface and rigid bands.

Our only significant departure from the Anderson model has been to regard the conduction band discontinuity as a property of the interface, to be calculated with a model appropriate to heterojunctions, rather than assuming it to be determined by the difference in electron affinities, as Anderson did. Kroemer has discussed the arguments against accepting the electron affinity rule [Kroemer, 1975]. Essentially the problem is that the electron affinity is

largely dependent on the surface dipole set up by the electron distribution at a free surface. There is no reason to believe that at a heterojunction these dipoles will add linearly, since the electron distribution is almost certain to resemble more nearly the bulk semiconductor than a superposition of free surfaces. Therefore, in the absence of information on the electron distribution, the electron affinity rule is, in principle, incapable of predicting heterojunction band lineups.

Our approach has been to replace the electron affinity rule with one that is somewhat similar, but involving a different quantity. Instead of expressing the energy of the bands in terms of a vacuum level defined at a location outside of the crystal, we refer the band energies to a level defined by the electrostatic potential within the crystal. We have chosen a reference level which we have reason to believe is continuous across most heterojunctions of interest. Thus the problem is reduced to the calculation of both the band structures and the electrostatic potential in terms of a common energy scale. We have done so using a self-consistent pseudopotential technique which will be described in detail later.

B. Pseudopotentials

The pseudopotential method for band structure calculations is the foundation upon which most of this work rests. It was chosen because of the relative ease with which one can obtain results

applicable to real semiconductors, in contrast with more formal methods like the orthogonalized plane wave (OPW) or augmented plane wave (APW) methods. It has also been the only method which has so far proved feasible for calculations of the electronic structure of surfaces, so it would be the obvious choice if one wished to extend this work to detailed calculations of the interface.

An excellent review of pseudopotential work is available in Heine [1970] and Cohen [1970] so again only a short summary will be given here. The motivation for the pseudopotential method was the difficulty of treating the extended (valence and conduction band) electron states with the same set of basis functions as those required for the tightly bound core states. The core states are best described in terms of localized, atomic-like states, while the extended states are best described, in the region outside the core, by plane waves. The OPW method of Herring [1940] tried to overcome these difficulties by setting up the calculation on a basis of plane waves which had been orthogonalized with respect to the core states. This method requires rather massive computations, so its application has been somewhat limited.

The pseudopotential concept was first proposed by Phillips and Kleinman [1959]. They noted that the orthogonalizing terms in the OPW method could be grouped with the potential in the Schroedinger equation, giving rise to an effective (=pseudo) potential

$$V_{eff} = V + \sum_{|c\rangle} (E-E_c)|c\rangle\langle c| \qquad (I.1)$$

where the sum is over all core states $|c\rangle$. The orthogonality terms are expected to have the effect of a repulsive potential, so the pseudopotential should be much weaker than the true potential. Cohen and Heine [M. H. Cohen, 1961] considered the Phillips-Kleinman form in more detail and showed that this is indeed the case.

Heine and Abarenkov [Heine, 1964; Abarenkov, 1965] developed a model pseudopotential for the ion core, consisting of the Coulomb potential outside of a given core radius, and a constant potential inside, which was fitted separately for each angular momentum value. These parameters were determined by fitting the spectroscopically observed energy levels of the closed-shell-plus-one-electron ion. Animalu and Heine [1965 and 1966] determined the parameters for a large number of elements. These pseudopotentials have been widely used as initial potentials which were then varied to fit empirical data.

Brust [1964] applied the empirical pseudopotential method (EPM), in which the pseudopotential form factors are treated as freely adjustable parameters, to silicon and germanium. He developed the calculational techniques which are still commonly used. This involves using a basis set of plane waves with a cutoff at a given magnitude of wavevector and treating other plane waves

by a modification of the Löwdin perturbation theory [Löwdin, 1951]. Cohen and Bergstresser [M. L. Cohen, 1966] applied the EPM to the calculation of the band structures of fourteen semiconductors, demonstrating the power of the pseudopotential method in dealing with real materials. The EPM has since been used to calculate such diverse properties of bulk semiconductors as dielectric functions [Richardson, 1971; Vinsome, 1971], electronic densities of states [Chelikowsky, 1974b], and the temperature dependence of X-ray reflection intensities [Chelikowsky, 1974a].

The extension of pseudopotential calculations to systems more complicated than perfect crystals was made possible by the self-consistent pseudopotential method, first suggested by Appelbaum and Hamann [1973]. The motivation for developing this technique was the study of the electronic structure of semiconductor surfaces, and in this application it has been quite successful [Appelbaum, 1975]. The self-consistent pseudopotential method has also been successfully applied to calculation of the electronic structure of vacancy defects [Louie, 1976a], metal-semiconductor interfaces [Louie, 1976b], and even molecules [M. L. Cohen, 1975].

C. Pseudopotentials in Other Fields

The use of the pseudopotential concept is by no means limited to solid-state band structure calculations. However, to make contact with other applications, we must first consider a formulation

due to Heine [1970]. It makes use of the fact that, if we know the amplitude for scattering an electron off the closed-shell ion, we have all of the information needed to calculate the band structure. These amplitudes may be expressed as the phase shifts for each partial wave as a function of energy. If, for a given ℓ, there are n_ℓ electron states occupied in the ion, the scattering states must have n_ℓ radial nodes in order to be orthogonal to the occupied states. In the scattering amplitude, this is just a contribution of $n_\ell \pi$ to the phase shift. We can remove the $n_\ell \pi$ without affecting the scattering amplitude, and then construct that potential which would give the same phase shifts. This is just the pseudopotential.

With this in mind, we see that the optical potential used in nuclear physics is really a pseudopotential [McCarthy, 1968, p. 255]. In its simplest form, the optical potential is a constant potential inside the nuclear radius, with a small imaginary part to account for scattering into other channels. (Note the similarity to the Heine-Abarenkov model pseudopotential.) This is a pseudopotential in the sense that it is an effective potential which approximates a rather complicated situation.

In field theory, the Lamb shift is calculated with what is effectively a pseudopotential technique [Bjorken, 1964, pp. 177-9]. The electron-proton scattering amplitude is calculated, including vacuum-polarization corrections. It can be written

$$-u^{\dagger}(p+q)\left\{\frac{Ze^2}{|\vec{q}|^2}\left[1-\frac{\alpha}{3\pi}\frac{|\vec{q}|^2}{m^2}(\text{constant})\right]\right\}u(p) \qquad (I.2)$$

which can also be derived from a potential

$$-\frac{Ze^2}{r}+\frac{4\alpha}{3}\frac{Z\alpha}{m^2}(\text{constant})\,\delta^3(r). \qquad (I.3)$$

This "pseudopotential" is used to calculate the energy levels of the bound state problem (the hydrogen atom).

D. The Heterojunction Model

The model by which we have studied heterojunction band lineups is logically divisible into two parts. The first concerns the problem of calculating the bulk semiconductor energy band locations with respect to the periodic electrostatic potential. This has been done by a self-consistent pseudopotential technique. The second part of the model is our scheme for matching the electrostatic potentials across the heterojunction.

The self-consistent pseudopotential technique was developed with an emphasis on preserving information about the electrostatic potential. The pseudopotential of the ion core was constructed from the electrostatic potential of a charge distribution derived from atomic Hartree-Fock calculations. To this was added a so-called pseudizing potential which approximated the effect of the core state orthogonality. The valence electron charge density was derived from calculated pseudo wavefunctions, and this was used to

calculate an electrostatic potential and an exchange interaction, using a local exchange approximation. The calculations were iterated until the valence charge density self-consistently reproduced the pseudopotential from which it was derived.

The self-consistent valence charge density was used along with the ion core charge distribution to calculate the electrostatic potential. This was used to calculate a reference potential, which was chosen to be the average of the electrostatic potentials at the two large interstitial vacancies in the zinc blende structure. The reason for this choice is that charge density calculations [Walter, 1971] show that much of the interstitial space in a semiconductor crystal is nearly empty. Thus much of the interfacial area of a heterojunction, along which the electrostatic potentials must be matched, is a region of low charge density. We therefore think that it is most appropriate to define a reference potential in that part of the crystal with low charge density. With these considerations, our final prescription for predicting heterojunction band lineups is to assume that the reference levels line up at the heterojunction.

CHAPTER II

CALCULATIONS

A. The Ionic Pseudopotential

Since we are interested in calculating the electrostatic potential along with the band structure, it is important to construct the ionic pseudopotential in such a way that we can recover the electrostatic part. This consideration has not been important in other pseudopotential work [Appelbaum, 1973; Schlüter, 1975] where the ionic pseudopotential was taken to be of some convenient analytical form with adjustable parameters. In our work it is desirable to start with a reasonable approximation to the electrostatic potential of the ion, and to add terms to approximate the orthogonality requirement.

The ionic pseudopotential needs to satisfy three criteria. It must be sufficiently weak that the lowest bound electron states correspond to the valence, rather than the core, electrons. It must be a well-behaved function, with no singularities in magnitude or slope. This allows rapid fall-off of the Fourier transform, which is necessary for the proper convergence of the band structure calculations. Finally, it must be localized in the vicinity of the ion. This

imposes a relationship between the zero wavevector Fourier component, which does not affect the band gaps (but which does affect the band energy with respect to the electrostatic potential), and the nonzero wavevector components, which do. Thus, in adjusting the ionic pseudopotential to fit the band structure, the nonzero wavevector components act to determine the $\vec{k}=0$ component, which can therefore be regarded as a meaningful quantity. Consequently, we must use an analytic form for the ionic pseudopotential, with adjustability provided by parameters within the analytic expression. We cannot adjust individual Fourier components, as is done in the EPM and in some OPW methods [see Herman, 1967, for example].

We begin the construction of the ionic pseudopotential with the electrostatic potential of the ion. We know that for very small distances from the nucleus, the potential must be of the form Ze/r, where Z is the atomic number. For large distances, the potential must be of the form $(Z-Q)e/r$, where Q is the number of core electrons. Now, in order to satisfy the smoothness criterion for the pseudopotential, the Ze/r behavior at the origin must be cancelled out in the pseudizing process. This is easily done if we can assume that the core electrons are distributed as

$$\rho_{core}(r) = \frac{Q\alpha^2}{4\pi r} e^{-\alpha r} \qquad \text{(II.1)}$$

where α is a parameter characterizing the size of the ion.

We must now consider the validity of this form for the core charge distribution. There are a number of criteria that could be applied to test whether this provides a good approximation to calculated ionic charge distributions, but the one which was chosen was that the model should reproduce the Fourier components for low wavevectors. The reason for this choice is that the band structure calculations are performed in k-space, using a limited number of plane waves, so the Fourier components of the potential with small k are the important quantities. It is also very easy to apply this test, because the Fourier components of atomic and ionic electron distributions ("form factors") from Hartree-Fock calculations are tabulated in the International Tables for X-ray Crystallography [MacGillavry, 1962, pp. 201-6]. The Fourier transform of our assumed charge distribution is

$$\rho_{\text{core}}(k) = \frac{Q\alpha^2}{k^2+\alpha^2} \approx Q\left(1 - \frac{k^2}{\alpha^2} + \cdots\right) \qquad \text{(II.2)}$$

which would fit the form factors for just about any localized distribution, for sufficiently small k. However, this expression is capable of fitting the tabulated form factors to within 5 percent for wavevectors less than four or five reciprocal Bohr radii. The largest wavevectors included in the band structure calculations were about 2.5 a_0^{-1}. Therefore, it appears that for our purposes, the expression (II.1) for the ionic charge distribution is quite adequate.

The parameter α in (II.1) must be determined from Hartree-Fock calculations for the ions. The International Tables for X-ray Crystallography do not list form factors for all of the elements of interest in semiconductor work, so, having demonstrated the validity of our assumed form, it was necessary to find a more complete set of data. This is readily provided by the work of Desclaux, where the results of relativistic Hartree-Fock calculations are presented for atoms with Z=1 to Z=120 [Desclaux, 1973]. It is most important to do all of our calculations in exactly the same way, so we have taken all of our ionic data from this work. The charge distribution data in Desclaux are presented in terms of various radial moments for each atomic shell. We used the average second moment $\langle r^2 \rangle$ for the occupied shells of the ion to determine α according to

$$\alpha^2 = \frac{6}{\langle r^2 \rangle} . \qquad \text{(II.3)}$$

The values of α thus determined, along with the other parameters of the ionic pseudopotential, are given in Table I.

The electrostatic potential energy of an electron in the field of the ion, using our model charge distribution, is (in c.g.s. notation)

$$V_{es}(r) = -\frac{e^2}{r}\left[(Z-Q) + Qe^{-\alpha r}\right] . \qquad \text{(II.4)}$$

As mentioned earlier, the Ze/r singularity at the origin must be removed in the pseudizing process. This is easily done by choosing part of the pseudizing potential to be

TABLE I

IONIC PSEUDOPOTENTIAL PARAMETERS

Element	Z	Q	α (a.u.)	γ (a.u.)	V_0 (Ry.)
Al	13	10	4.04	1.7	43
Si	14	10	4.52	2.25	44
P	15	10	4.99	2.5	41
S	16	10	5.47	2.6	41
Zn	30	28	3.33	2.0	25
Ga	31	28	3.64	2.0	28
Ge	32	28	3.94	2.06	36.8
As	33	28	4.22	2.2	42
Se	34	28	4.49	2.25	44
Cd	48	46	3.02	1.8	46
In	49	46	3.24	2.0	52
Sb	51	46	3.63	1.8	56
Te	52	46	3.81	1.8	58

$$V_{ps1}(r) = \frac{Ze^2}{r} \exp\left(-\sqrt{\frac{Q}{Z}}\,\alpha r\right). \qquad \text{(II.5)}$$

The sum of $V_{es}(r)$ and $V_{ps1}(r)$ is a potential well that is smoothly rounded at the origin, as shown in Figure 2, with a $-(Z-Q)e^2/r$ behavior at large r, as desired. There are no adjustable parameters in V_{ps1}, and it leaves the potential at the origin still fairly strongly attractive, so we must add another term to produce a satisfactory ionic pseudopotential. This term was chosen to be of the form

$$V_{ps2}(r) = V_0 \frac{\gamma^3}{(2\pi)^{3/2}} e^{-\frac{\gamma^2 r^2}{2}} \qquad \text{(II.6)}$$

where V_0 and γ are freely adjustable parameters. The complete ionic pseudopotential for Ge is also shown in Figure 2. The Fourier transform of the ionic pseudopotential is

$$V_{ion}(k) = V_{es}(k) + V_{ps1}(k) + V_{ps2}(k)$$

$$= -\frac{8\pi}{\Omega}\left[\frac{(Z-Q)}{k^2} + \frac{Q}{k^2+\alpha^2}\right] + \frac{8\pi}{\Omega}\,\frac{Z}{k^2+(Q/Z)\alpha^2} + \frac{V_0}{\Omega}\, e^{-(k^2/2\gamma^2)} \qquad \text{(II.7)}$$

where Ω is the unit cell volume (the appropriate normalization in a periodic crystal) and the 8π really represents $4\pi e^2$, but $e^2=2$ when the chosen units are Rydbergs and Bohr radii.

The expression (II.7) diverges as $\vec{k} \to 0$, as any potential arising from a nonzero net charge must. In the semiconductor crystal, this poses no real problem, since the Coulomb potential is

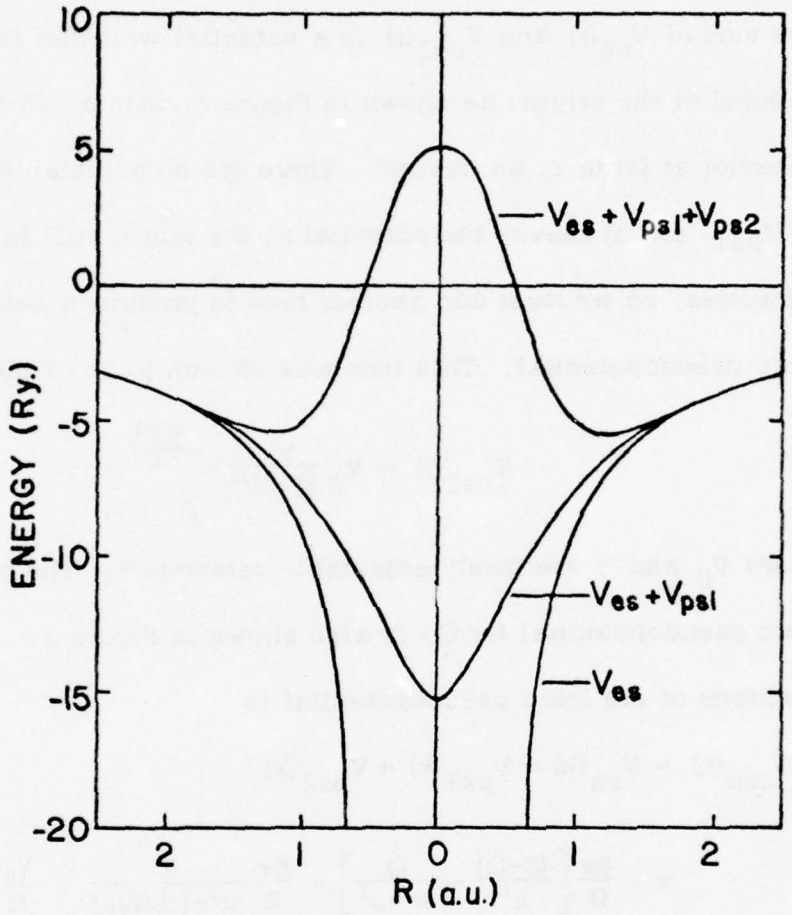


Figure 2. The components of the ionic pseudopotential for Ge. The lowest curve is the electrostatic potential; the center curve is the electrostatic potential after the singularity has been removed by the addition of V_{ps1}. The upper curve is the final pseudopotential.

screened by the valence electrons, but we need a well-defined, finite value for $V_{ion}(\vec{k}=0)$ for the band structure calculations. The solution is to introduce a fictitious screening charge distribution in the $V_{ion}(\vec{k}=0)$ calculation for bookkeeping purposes, and to subtract a corresponding charge distribution from the valence band charge. This charge distribution was chosen to be of the form

$$\rho_F(r) = (Z-Q) \frac{\beta^3}{(2\pi)^{3/2}} e^{-(\beta^2 r^2)/2} \qquad \text{(II.8)}$$

where β is an arbitrary parameter. When the effect of this fictitious charge distribution is taken into account, the $(Z-Q)/k^2$ term in (II.7) is replaced, for $\vec{k}=0$, by $(Z-Q)/2\beta^2$. This scheme will be discussed in greater detail when we consider the actual calculation of the electrostatic potential.

The initial values of the parameters V_0 and γ were chosen by fitting the energy levels of the closed-shell-plus-one-electron ion. The parameters were then adjusted in response to the band structure results, until an acceptable fit was obtained. The final ionic pseudopotential was again used to calculate the ionic spectrum, to ensure that the pseudopotential was a reasonable representation of the ion. The method of calculating the ionic spectra, and the final results, are given in Appendix A.

B. Self-Consistent Band Structure Calculations

With our ionic pseudopotential, we can calculate the energy band structure self-consistently. The procedure is to choose an initial valence charge distribution, derive from it the electrostatic and exchange potentials, and add these to the ionic pseudopotential to obtain the total pseudopotential. This is then used to calculate the wavefunctions for a suitable number of states. The appropriate linear combinations of the absolute squares of the wavefunctions give the valence electron distribution. This is used to generate a new pseudopotential, and the entire process is repeated until the pseudopotential converges to a consistent value.

The choice of the initial valence electron distribution is not particularly critical. Appelbaum and Hamann [1973] simply assumed a linear dielectric response to the ionic pseudopotential. We have tried to speed convergence by using an initial valence charge density calculated from published empirical pseudopotentials. In certain cases, where such potentials were not readily available, we have started the calculation with the self-consistent charge distribution for a related compound. (For example, we initiated the CdSe calculation with the ZnSe charge distribution.)

Since the charge distribution is represented as a Fourier series, calculating the electrostatic (Hartree) potential is a straightforward matter of dividing each component by the square of its wavevector. The exchange interaction is more complicated.

We have used the generalized Slater approximation, commonly known as the "$X\alpha$" approximation [Slater, 1974]. In this approach, the exchange interaction is approximated by a local potential which is proportional to the cube root of the charge density. In our calculations, the exact evaluation of this approximation would require summing the Fourier series for the charge density at a number of points, taking the cube root at each point, and re-analyzing the series. Instead of this rather time-consuming procedure, we have used a polynomial approximation to the cube root, which can be evaluated by direct manipulations on the series. The valence charge densities in semiconductors are limited to a range of about one to forty electrons per unit cell [Walter, 1971]. Fitting a quadratic polynomial to the cube root over this range gives

$$\rho^{\frac{1}{3}} \approx 0.847 + 0.142\rho - 0.00209\rho^2 \qquad \text{(II.9)}$$

which is shown in Figure 3. In the first round of calculations we used a pure Slater approximation with α=1, but for the final calculations we used α=0.8. This value has been used successfully in surface calculations [Schlüter, 1975], and it gave improved band structures in our own calculations.

The pseudo wavefunctions and their energies were calculated using established pseudopotential techniques. The Hamiltonian matrix was set up on a basis of plane waves $|\vec{k}+\vec{G}\rangle$ where $\vec{k}$ is a vector in the reduced Brillouin zone and $\vec{G}$ is a reciprocal lattice

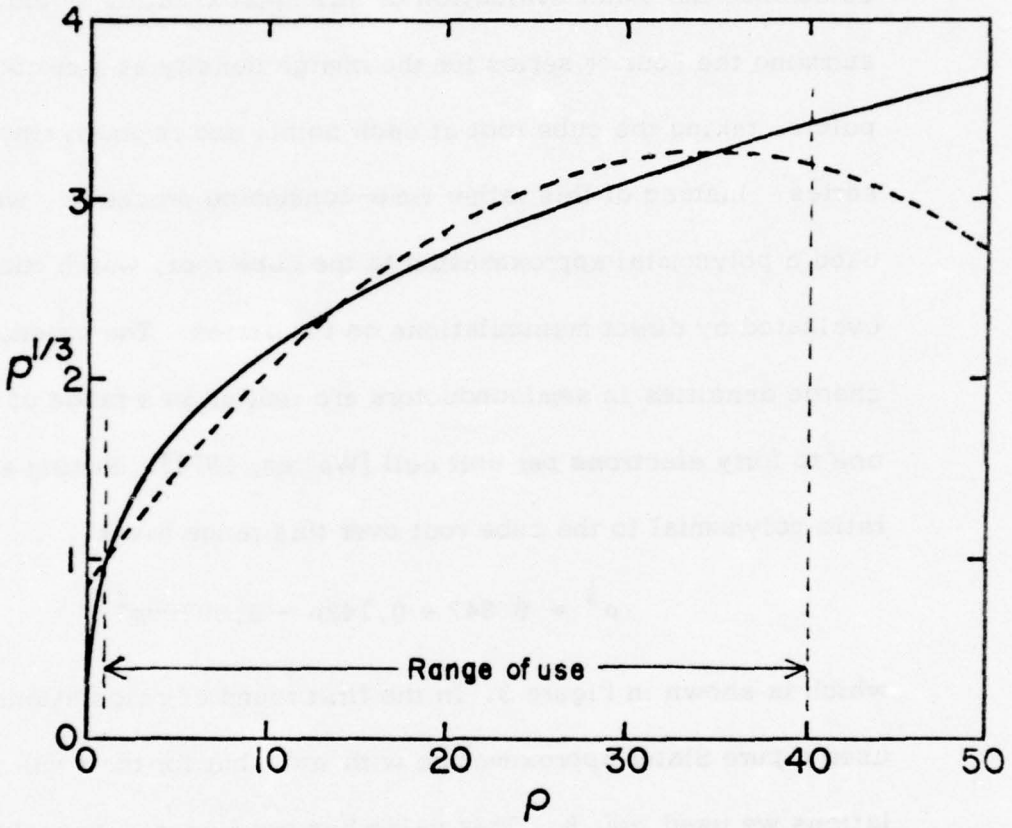


Figure 3. The cube root of the charge density (solid line) and the quadratic approximation (II.9) (dotted line), and the range over which this approximation was actually used.

vector. For each value of $\vec{k}$, all plane waves such that $|\vec{k}+\vec{G}|^2 \leq E_1$ were included in the direct calculation, and the remaining plane waves such that $|\vec{k}+\vec{G}|^2 \leq E_2$ were included via the second-order perturbation scheme of Löwdin [1951] as modified by Brust [1964]. We found that setting $E_1=7$ and $E_2=14$ (in units of $(2\pi/a)^2$) yielded good band structure results without requiring excessive computation. The criterion for "good" band structures, in this regard, is that the band energies should not change excessively as $\vec{k}$ moves through a point where the set of included $\vec{G}$'s changes. If the basis set is too small, the sudden inclusion of different pseudopotential components leads to significant changes in the eigenvalues. The eigenvalues were calculated by numerically diagonalizing the Hamiltonian, and the wavefunctions were derived from the eigenvectors of the foldec-down Hamiltonian by a partial unfolding of the Löwdin scheme.

The pseudocharge density was calculated using the Chadi-Cohen three-point Brillouin zone sample [Chadi, 1973]. This has been shown to give charge densities which agree to within about 1 percent with calculations involving many more points in the Brillouin zone. The expression used to calculate the charge density is

$$\rho(\vec{r}) = \tfrac{1}{4}\rho_{\Delta}(\vec{r}) + \tfrac{1}{4}\rho_{W}(\vec{r}) + \tfrac{1}{2}\rho_{\Sigma}(\vec{r}) \qquad \text{(II.10)}$$

where the $\rho_{\vec{k}}(\vec{r})$ are the charge densities from the various $\vec{k}$ points, symmetrized with respect to the point-group operations:

$$\rho_{\vec{k}}(\vec{r}) = \sum_i \frac{1}{n_G} \sum_R |\psi^{(i)}_{R\vec{k}}(\vec{r})|^2 \qquad \text{(II.11)}$$

where the index i refers to the band and is summed over the valence bands, R is an element of the crystal point group G which has n_G such elements. The k vectors used are

$$\Delta = \frac{2\pi}{a} \left(\tfrac{1}{2}, 0, 0\right)$$

$$W = \frac{2\pi}{a} \left(1, \tfrac{1}{2}, 0\right) \qquad \text{(II.12)}$$

$$\Sigma = \frac{2\pi}{a} \left(\tfrac{1}{2}, \tfrac{1}{2}, 0\right).$$

The simple procedure of iterating the band structure and charge density calculations converges quickly for the Group IV semiconductors, but for the heteropolar (III-V and II-VI) semiconductors the convergence is oscillatory. This was easily damped out by taking a linear combination of the "new" and "old" charge densities as the input to the next iteration; a contribution of one-half from each worked very well. The average root-mean-square change in the electrostatic potential was calculated at each iteration. The iterations were terminated when this reached a level of 0.001 or 0.002 Rydbergs.

C. Evaluation of the Electrostatic Potential

With the ion model and the valence charge distribution from the band structure calculations, we have complete information on the microscopic charge distribution in the crystal. In principle the calculation of the electrostatic potential is a straightforward solution of Poisson's equation. In practice, some care must be taken if the calculation is to produce meaningful results. The difficulties arise in the methods of representing the potential, so we must digress briefly to discuss these problems.

There are fundamentally two ways to represent a periodic scalar function (such as the charge density or the potential) in a crystal [Kittel, 1963, ch. 1]. A function F can be represented as a Fourier series in the reciprocal lattice vectors $\vec{G}$:

$$F(\vec{r}) = \sum_i a_i e^{i\vec{G}_i \cdot \vec{r}} . \qquad \text{(II.13)}$$

The same function can also be represented as a sum of "atomic" functions f centered at lattice points $\vec{R}_j$:

$$F(\vec{r}) = \sum_j f(\vec{r}-\vec{R}_j) \qquad \text{(II.14)}$$

The relationship between the two representations is

$$a_i = \frac{1}{\Omega} \int d^3\vec{x}\ f(\vec{x}) e^{-i\vec{G}_i \cdot \vec{x}} . \qquad \text{(II.15)}$$

In applying these representations to numerical computations, we see that each is suited to a particular kind of function. The

Fourier series works well for smooth functions which need not be well localized. However, it is incapable of representing singularities when truncated at any finite number of terms, as it must be in any practical computation. The atomic functions, on the other hand, may be quite singular, but they must be well localized.

In the case of the crystal electrostatic potential, we make use of both representations. The Coulomb singularity at the nucleus cannot be treated with a truncated Fourier series. On the other hand, the valence charge distribution exists as a Fourier series and representing it in terms of atomic functions would require some very tedious fitting to Equation (II.15). Therefore, we use atomic functions to represent the ionic charge distribution, while a Fourier series is used for the valence charge. This creates a problem in itself, for we cannot solve Poisson's equation in either representation if the net charge involved is nonzero. With the Fourier series, this means that the $\vec{G}=0$ component is nonzero. Dividing by $\vec{G}^2$ gives an undefined result. In the atomic-function representation, a net charge implies a Coulomb tail. Since the number of lattice points at a radius R is proportional to R^2, the 1/R Coulomb term is not sufficient to cause the series to converge. These difficulties are clearly an artifact of the mathematical formulation, because the crystal itself is neutral. In fact, they are a corollary to the problem of the divergence of $V_{ion}(\vec{k}=0)$ discussed earlier.

The solution to these difficulties is to remove an arbitrary charge distribution from the valence charge and add it onto the ion, so that both the valence and ionic distributions are neutral overall. This fictitious distribution is given in Equation (II.8). (The choice of a Gaussian is essentially required because we need rapid convergence in both r and k space.) The Fourier transform of this charge distribution (with the appropriate structure factors) is subtracted from the valence charge, allowing us to solve Poisson's equation and set the $\vec{G}=0$ Fourier component of the potential equal to zero (the usual boundary condition). The fictitious charge distribution is added to the ionic charge distribution, cancelling the Coulomb tail and allowing us to calculate the ionic contribution to the electrostatic potential according to (II.14). The two contributions are then added to obtain the total electrostatic potential.

There is one remaining subtle point in this procedure. The boundary conditions are defined so that the Fourier series makes no contribution to the average ($\vec{G}=0$) electrostatic potential. However, the fictitious charge plus the (Z-Q) part of the nuclear charge contribute a term

$$\frac{8\pi}{\Omega} \frac{(Z-Q)}{2\beta^2} \qquad \text{(II.16)}$$

to the average electrostatic potential, which must be included in the $\vec{G}=0$ component of the pseudopotential, as noted previously. Thus the arbitrary parameter β affects both the electrostatic

potential and the band energy, but it cannot affect the relation between the two. (It effectively sets the zero on the energy scale.) The existence of this arbitrary but irrelevant parameter has proved to be quite useful in detecting program errors. (If it is not irrelevant, there is an error.)

There are practical limits on the value of β imposed by the desire for rapid convergence. In the Fourier series, we included $\vec{G}$'s up to about 3 a.u. If we want the terms at the cutoff to be smaller than 10^{-4} Ry., we should use $\beta < 1.8$. In the summation over a cluster of lattice points, the cutoff was at a distance of 10 a.u. Applying the same criterion for the size of the terms at cutoff, we find that we should use $\beta > 0.3$. Most of the calculations actually used $\beta = 0.5$ a.u.

D. Matching Scheme

The matching scheme, which specifies how the electrostatic potentials should line up at the heterojunction, could be developed at a number of levels of sophistication. In the earlier stages of this investigation, we thought that it would probably be necessary to model the detailed charge distribution at the interface, probably by assuming some sort of dielectric response. The extreme case of a matching scheme would be to do the full quantum-mechanical interface calculation, as is currently being done for surfaces [Appelbaum, 1975; Schlüter, 1975]. We have found, however, that

a very simple matching scheme gives remarkably good heterojunction predictions.

Our matching scheme is suggested by considering a muffin-tin potential [Harrison, 1970, p. 87]. This potential, which is commonly used for APW band structure calculations, consists of spherically symmetric wells within a certain core radius from the ions, and is constant everywhere else. If the electrostatic potential in a semiconductor were really of a muffin-tin form, then the matching scheme would be completely obvious: the flat parts of the potentials would line up.

Our calculations indicate that, for the cubic semiconductors, the electrostatic potential is indeed flat to within about a volt inside the large interstitial spaces in the crystal structure. These spaces are centered on the points $a(\frac{1}{2},\frac{1}{2},\frac{1}{2})$ and $a(\frac{3}{4},\frac{3}{4},\frac{3}{4})$ if the atoms are at $a(0,0,0)$ and $a(\frac{1}{4},\frac{1}{4},\frac{1}{4})$. For the zincblende semiconductors the two interstitial points are not equivalent, but the potential difference is typically less than one volt. Therefore, we have simply taken the average of the potentials at the two interstitial points as our reference potential. Then, following the muffin-tin analogy, the matching scheme is simply to line up the reference potentials.

This scheme can be expected to work best for heterojunctions grown on nonpolar {110} crystal faces. In this case, the interstitial points lie in the atomic planes adjacent to the junction, with equal

numbers of each type. For a heterojunction on a {111} polar face, the interstitial points are slightly displaced from the heterojunction plane, with the two types displaced in opposite directions. Therefore, it would probably be more appropriate to use a slightly different weighting factor for the two points in such cases. Experimentally, the only investigation of orientation effects is that by Fang and Howard [1964]. They found differences of about 0.2 eV in band lineup between the two {111} orientations of Ge-GaAs junctions. This probably indicates the accuracy we can expect from our matching scheme as long as we neglect orientation effects.

It should be emphasized that this matching scheme is primarily appropriate to ideally abrupt heterojunctions. If the composition is graded over more than a few atomic layers, the reference levels of the pure semiconductors cease to be important and the equalization of the Fermi levels begins to dominate. Also, this matching scheme explicitly neglects interface states. We believe, for physical reasons, that the interface states at heterojunctions can result only from imperfections and dislocations at the junction. Therefore, our model is limited to predictions for well lattice-matched heterojunctions.

CHAPTER III

RESULTS

A. Band Structure Results

We have applied the model described in the previous chapter to fifteen semiconductors with cubic structures. The ionic pseudopotentials were adjusted to fit the band structures, with particular emphasis on the fundamental direct and indirect gaps, but the pseudopotential for a given ion was the same for all compounds involving that ion. Of the Group IV semiconductors, only silicon and germanium were calculated, since these are the ones of technological interest. There is a great deal of interest in the III-V quaternary alloy systems (Ga,In)(As,P) and (Al,Ga)(As,Sb), so we calculated the pure compounds for each of these systems. Of the II-VI compounds, we calculated all of the possible combinations of Zn and Cd with S, Se, and Te.

Table II gives the band gaps which are usually considered in discussing band structures. The experimental data are given for comparison with the calculated values. The symmetry labels are those appropriate to the zincblende structure. In quoting the experimental data, we have chosen electroreflectance data when available, preferably at low temperature. We have used the

TABLE II

BAND STRUCTURE RESULTS

The calculated (upper) and experimental (lower) band splittings are given in eV. a is the lattice constant and Δ_0 and Δ_1 are the spin-orbit splittings of the valence band at Γ and L, respectively. The letters refer to the source of the experimental data.

Semi-conductor	a (Å)	Γ_{15V} $-\Gamma_{1C}$	Γ_{15V} $-\Gamma_{15C}$	Γ_{15V} $-\Lambda_{1C}$	Γ_{15V} $-\Delta_{1C}$	Λ_{3V} $-\Lambda_{1C}$	Λ_{3V} $-\Lambda_{3C}$	X_{5V} $-X_{1C}$	X_{1C} $-X_{3C}$	Δ_0	Δ_1
Si	5.431	4.21	2.96	2.53	1.07	3.7	5.4	4.28			
	a	4.20	3.45	2.23	1.18	3.40	5.50	4.60	—	0.04	—
		c	d,e	e	f,c	d,e	d	d		c	
Ge	5.657	0.96	3.00	0.84	0.90	2.0	5.2	3.76			
	a	0.99	3.24	0.86	—	2.34	5.8	4.50	—	0.30	0.18
		g	g	h		g	d	g		g	g
AlAs	5.659	2.84	4.85	2.81	2.05	3.6	6.1	4.19	0.50		
	b	3.04	4.43	—	2.32	3.93	—	4.54	0.35	0.28	0.20
		i	i		j	i		i	i	i	i
AlSb	6.135	2.53	3.78	2.16	1.84	2.9	5.1	3.79	0.04		
	a	2.47	4.15	—	1.94	3.01	—	4.25	0.5	0.75	0.40
		k	k		l,k	k		k	k	k	k
GaP	5.451	2.89	5.03	2.55	2.23	3.5	6.6	4.62	0.10		
	a	2.90	4.84	2.6	2.36	3.81	6.7	5.27	0.29	0.08	0.05
		m	k	n,o,m	o,m	m	p	k	o	m	m
GaAs	5.653	1.63	4.49	1.75	1.86	2.6	6.1	4.11	0.21		
	a	1.63	4.72	2.2	2.06	3.15	6.62	4.98	0.40	0.34	0.22
		q	q	q,r,s	q,r	q	t	q	q	q	q
GaSb	6.095	1.09	3.61	1.18	1.32	2.0	5.2	3.27	0.67		
	a	1.08	3.55	1.16	1.7	2.26	5.5	4.20	0.37	0.73	0.46
		u	v	w,u	x,k,u	k	k	k	k	u	k
InP	5.869	1.46	5.13	2.82	2.61	3.4	6.2	4.37	0.28		
	a	1.45	4.80	2.0	2.34	3.20	—	5.14	0.5	0.10	0.15
		y	k	s	k,s	k		k	k	y	k
InAs	6.058	0.54	4.53	2.14	2.27	2.8	5.7	3.98	0.27		
	a	0.55	4.5	1.2	2.4	2.64	6.3	4.70	0.48	0.43	—
		aa	k	bb	x,k	k	p	k	k	k	
ZnS	5.43	3.83	8.12	4.99	4.19	5.4	8.6	5.88	0.90		
	a	3.82	8.35	—	—	5.80	9.78	6.99	0.42	0.07	—
		cc	dd			dd	dd	dd	dd	cc	
ZnSe	5.669	2.88	7.17	4.07	3.72	4.5	7.8	5.33	0.64		
	a	2.81	—	—	—	4.93	8.3	6.7	0.5	0.43	0.35
		cc				ee	p	p	p	cc	ee
ZnTe	6.101	2.54	5.78	3.18	3.20	3.7	6.6	4.64	0.13		
	a	2.56	5.71	—	—	3.90	7.20	5.4	0.6	0.93	0.57
		k	k			k	ff	p	p	k	k
CdS	5.825	2.31	8.08	4.88	4.22	5.0	8.3	5.48	1.22		
	a	2.42	6.20	—	—	5.49	9.18	7.95	0.4	--	--
		k	dd			dd	dd	dd	dd		
CdSe	6.05	1.76	7.23	4.30	3.80	4.3	7.5	5.01	0.99		
	a	—	—	—	—	—	—	—	—	--	--
CdTe	6.477	1.80	5.93	3.63	3.35	3.7	6.4	4.45	0.52		
	a	1.80	5.61	—	—	3.58	7.20	5.49	0.50	0.92	0.59
		k	k			k	ff	ff	ff	k	k

TABLE II (continued)

References

a	Donnay, 1963	q	Aspnes, 1973b
b	Ettenberg, 1970	r	Balslev, 1968
c	Aspnes, 1972	s	Pitt, 1973
d	Zucca, 1970	t	Pandey, 1974
e	Chelikowsky, 1974b	u	Piller, 1973
f	Dean, 1969	v	Parsons, 1971
g	Aspnes, 1973a	w	Harland, 1966
h	Fischer, 1970	x	Ley, 1974
i	Onton, 1970	y	Lösch, 1976
j	Monemar, 1973	z	Onton, 1972
k	Cardona, 1967	aa	Adachi, 1968
l	Rowe, 1969	bb	Kwan, 1968
m	Stowkowski, 1972	cc	Dimmock, 1967
n	Pitt, 1974	dd	Pollak, 1967
o	Dean, 1967	ee	Aven, 1961
p	Guizzetti, 1974	ff	Cardona, 1963

"traditional" assignment of the optical structures. The E_0 and E_0' peaks in Cardona's notation [Cardona, 1969] are assigned to the Γ_{15v}-Γ_{1c} and Γ_{15v}-Γ_{15c} transitions, respectively. The E_1 and E_1' sets of peaks are assigned to Λ_{3v}-Λ_{1c} and Λ_{3v}-Λ_{3c} transitions, and the E_2 peaks are assigned to transitions from X_{5v} to X_{1c} and X_{3c}. With the refinement of both theory and experiment, it now appears that this scheme is too naive. The optical structures arise from transitions over sizeable volumes of the Brillouin zone, and detailed critical-point analyses are needed to properly interpret the optical structure [see Saravia, 1968, for example]. However, the assigned locations in the Brillouin zone have not changed radically, and we think that the older interpretation is adequate for our work.

We made no provision for calculating the spin-orbit splitting, so the experimental data have been corrected for this. To all gaps involving Γ_{15v}, one-third of the spin-orbit splitting of this level (Δ_0) has been added. The Λ_{3v} levels have been corrected by adding one-half of Δ_1. The spin-orbit splitting at X is almost always negligible.

The calculated values given in Table II have been obtained from calculations sampling the Brillouin zone primarily along the $\Lambda\langle 111\rangle$ and $\Delta\langle 100\rangle$ directions. The Γ point is the center of the zone. The indirect gaps, Γ_{15v}-Λ_{1c} and Γ_{15v}-Δ_{1c} are from the top of the valence band to the local minima along the respective

directions. The direct gaps along Λ were obtained by finding either the minimum gap or a region where the gap is approximately constant, in an attempt to guess where the critical point might be. Accordingly, these gaps are only given to 0.1 eV. In the Δ direction, the direct gaps are calculated at the point X.

An examination of Table II shows that we have generally been able to fit the first direct gap at Γ and the lowest gap of the indirect gap materials to within about 0.1 eV. The worst fit to these levels is that for AlAs, where the direct gap is 0.2 eV low and the indirect gap is 0.3 eV low. (However, the experimental data were taken on n-type samples with carrier concentration in the high-10^{18}-cm^{-3} range [Monemar, 1973], so there could possibly be a Burstein shift of the order of 0.1 eV in this gap.) Other indirect gaps show a reasonable agreement with the data, except the Γ_{15v}-Λ_{1c} gap in InAs. The data for InAs are from high-pressure Hall-effect experiments, which found a local minimum in the conduction band 0.7 eV above the band edge, which was interpreted to be along the Λ direction. However, it is difficult to see how such a minimum might occur, considering the direct gaps and typical curvatures of the upper valence band, so we should not be too worried by this discrepancy.

The Λ_{3v}-Λ_{1c} gaps generally fit the experimental data to about 0.3 eV and the same may be said of the Γ_{15v}-Γ_{15c} gap, although there are a few cases where the disagreement is considerably

larger. The upper conduction bands are not very well fitted; the average error for the Λ_{3v}-Λ_{3c} gap is about 0.5 eV. The direct gaps at X are particularly difficult to fit with our model. The disagreement in the X_{5v}-X_{1c} gap runs around 1 eV and there are some particularly glaring errors in the gap between the two conduction bands at X.

It appears that no experimental data exist for cubic cadmium selenide, but the band gap is in reasonable agreement with that of the hexagonal crystal. For those II-VI compounds which exist in both structures, the band gaps are usually about the same.

The remarkable thing about our model is that we can fit the fundamental gaps for this number of semiconductors with the same ionic pseudopotentials (which have only <u>two</u> adjustable parameters). There are limits to this, however. We have the pseudopotentials necessary to calculate AlP and InSb, but these give direct band gaps which are in error by 0.6 and 0.8 eV, respectively.

The object of our band structure calculations has of course been to calculate the energies of the bands in relation to our reference potential. These results are given in Table III. In this case the calculations have been corrected for spin-orbit splitting by adding one-third of the experimentally observed splitting Δ_0 to the valence band energies. Also given is the difference in the electrostatic potential (ΔV) between the two interstitial points used to define V_{ref}.

TABLE III

BAND EDGE ENERGIES WITH RESPECT TO THE REFERENCE POTENTIAL

The energies of the edge of the valence band, including spin-orbit splitting, and the conduction bands are given. ΔV is the difference in potential between the two interstitial points.

Semiconductor	E_v	E_c(direct)	E_c(indirect)	ΔV
Si	-3.16	-0.21	-2.10	0
Ge	-3.25	-2.39	-2.51	0
AlAs	-3.96	-1.21	-2.00	0.74
AlSb	-3.94	-1.66	-2.35	0.42
GaP	-4.12	-1.26	-1.92	0.66
GaAs	-3.96	-2.44	--	0.48
GaSb	-3.98	-3.04	--	0.19
InP	-4.58	-3.15	--	0.81
InAs	-4.38	-3.98	--	0.64
ZnS	-5.34	-1.53	--	0.92
ZnSe	-5.07	-2.33	--	0.74
ZnTe	-4.74	-2.51	--	0.46
CdS	-5.42	-3.11	--	1.07
CdSe	-5.29	-3.53	--	0.99
CdTe	-4.90	-3.41	--	0.71

B. Heterojunction Predictions

For purposes of making heterojunctions, the semiconductors we have considered can be divided into four groups, based on lattice constant. Those semiconductors with a lattice constant of about 5.45 Å are Si, GaP, and ZnS. Around 5.65 Å we have Ge, GaAs, AlAs, and ZnSe. There are only InP and CdS at 5.85 Å, but the group around 6.1 Å includes GaSb, AlSb, InAs, ZnTe, and CdSe. If a heterojunction between pure semiconductors is to be lattice-matched, both semiconductors must be chosen from the same group.

The relative band edge energies for the silicon group are shown in Figure 4. Our model predicts that most of the discontinuity will be in the valence band for all heterojunctions within this group. The best experimental data available for this group are those of Zeidenbergs and Anderson [1967], who fabricated isotype (n-n) heterojunctions between Si and GaP. These junctions exhibited ohmic current-voltage characteristics at temperatures as low as 77 K. This indicates that there is a negligible conduction band discontinuity, in qualitative agreement with our predictions. Lendvay, et al., [1970] have prepared n-n Si-ZnS heterojunctions, and measured their electrical properties. These junctions do show a diode characteristic, with a polarity such that the ZnS conduction band must lie above that of Si, but the data are not sufficient to determine the height of the barrier.

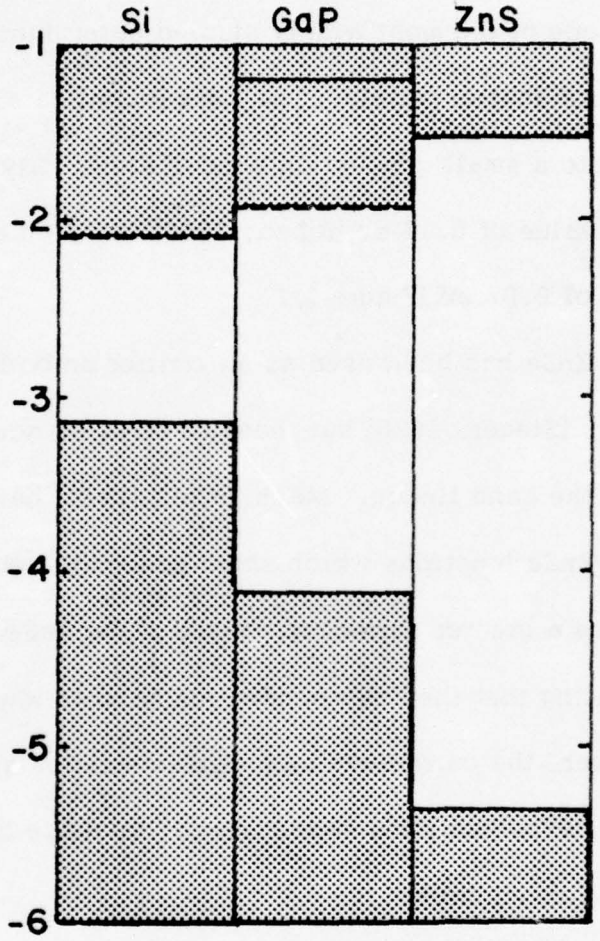


Figure 4. The relative band energies for the semiconductors with lattice constants near 5.45 Å. The energies are in eV and dashed lines indicate indirect conduction band edges.

The greatest amount of experimental work has been done on heterojunctions within the Ge group. The Ge-GaAs system has been one of the most widely studied heterojunctions. Unfortunately, the data scatter widely. The more recent data, however, tend to indicate a small conduction band discontinuity. Riben and Feucht get a value of 0.11 eV [Riben, 1966], in good agreement with our value of 0.07 eV (Figure 5).

ZnSe has been used as an emitter on both Ge and GaAs transistors [Sleger, 1970] but these devices do not really tell us much about the band lineup. Mach, et al., [1970] have studied n-n GaAs-ZnSe junctions which show nonohmic behavior. In these devices a greater current is passed if the ZnSe is made positive, indicating that the ZnSe conduction band is lower than that of GaAs. However, the current-voltage characteristics are far from the exponential expected for a simple diode, so these data cannot be considered conclusive.

Undoubtedly the best experimental data available are those of Dingle, et al., [1974 and 1975] for the GaAs-AlAs system. They fabricated periodic arrays of heterojunctions between layers sufficiently thin that they exhibited quantized "square well" electron and hole states. These states were observed spectroscopically and from their energies, the barrier heights (band discontinuities) were determined. These structures were grown by molecular beam epitaxy and are very abrupt; the grading distance is less than 5 Å.

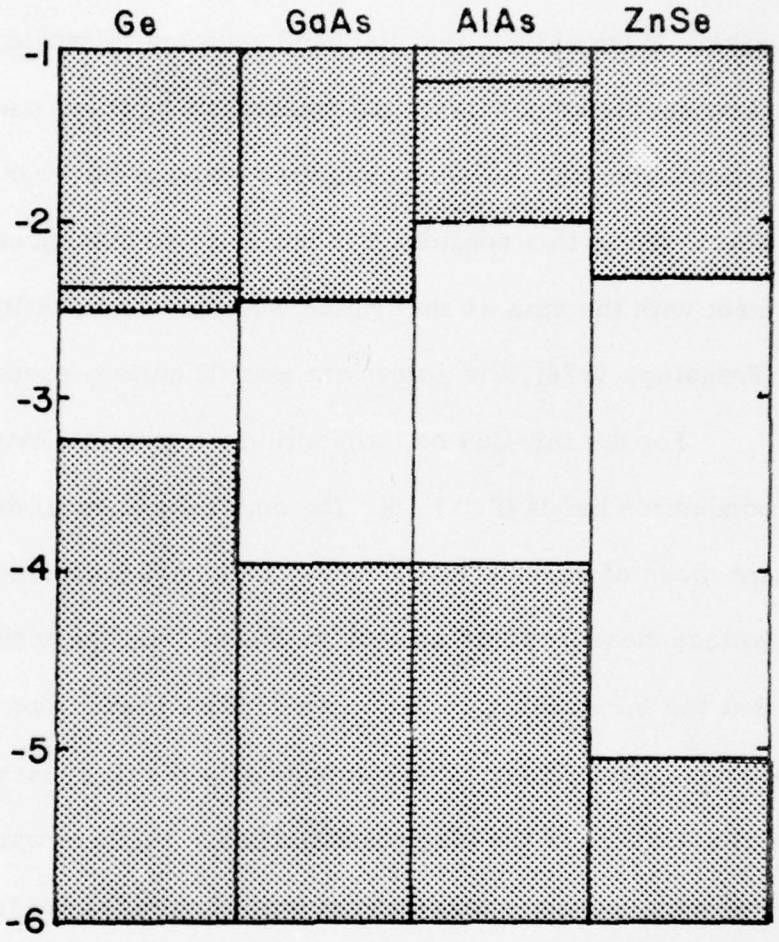


Figure 5. The relative band energies for the semiconductors with lattice constants near 5.65 Å. The energies are in eV and the dashed lines indicate indirect conduction band edges.

These heterostructures were actually fabricated of GaAs and $Al_xGa_{1-x}As$ with x in the range 0.2 to 0.3. The observed valence band discontinuity is 0.15 ± 0.03 of the total difference in band-gaps. If we assume that the band energies interpolate linearly, this ratio should be constant, independent of composition. Our calculations give zero valence band discontinuity between pure GaAs and AlAs. While this prediction is not quite so spectacularly in agreement with the data as that which we obtained in earlier calculations [Frensley, 1976], the agreement is still quite reasonable.

For the InP-CdS heterojunction we predict almost continuous conduction bands (Figure 6). The only experimental data available are those of Shay, et al., [1976]. They have performed capacitance-voltage measurements on p-n junctions, and the results indicate that the InP conduction band lies 0.56 eV higher than the CdS conduction band. They further support this result by making theoretical estimates of the electron affinities. The heterojunctions were grown by vacuum evaporation at quite low substrate temperatures (200-250°C), so capacitance-voltage measurements should be reliable. The origin of the discrepancy is possibly the presence of an oxidized layer at the interface. The substrates were exposed to the atmosphere while being prepared, so such a layer would have formed. Kroemer [1975] has noted that the one case in which the electron affinity rule can be expected to hold is when an oxidized layer is present. Another possibility is that our calculations may

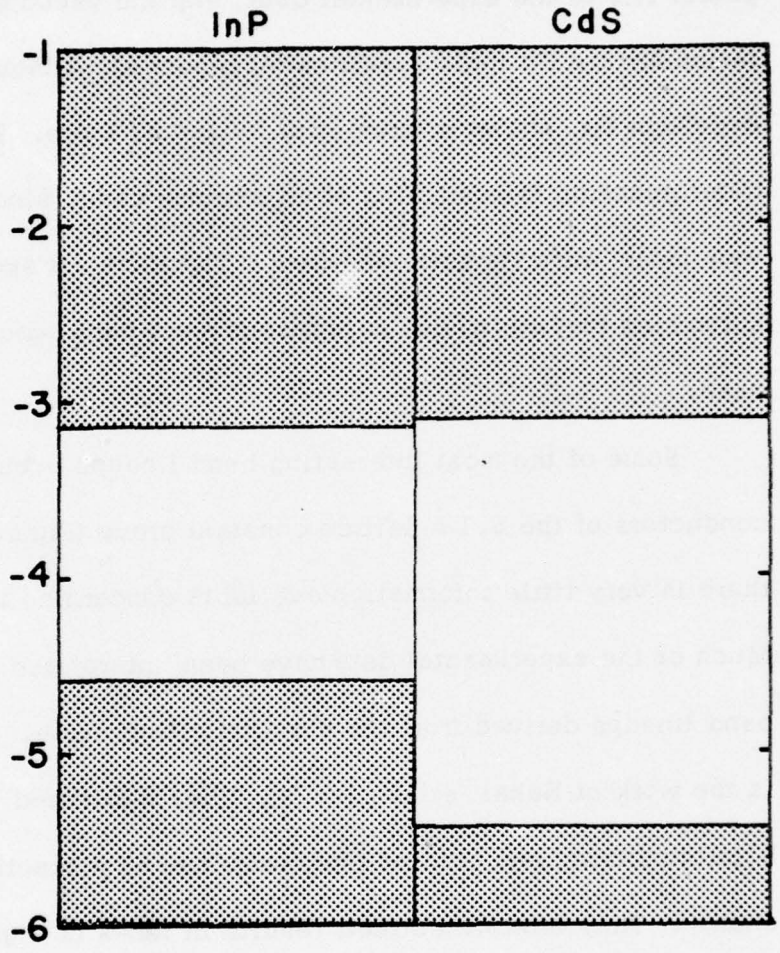


Figure 6. The relative band lineup for InP and CdS. The energies are in eV.

not be accurate in this case. The CdS band structure is one of our poorer fits to the experimental data, and the pseudopotential calculation for the Cd ionic spectrum (Appendix A), although an otherwise excellent fit, shows a large error for the 5s state. The InP-CdS heterojunction is something of an extreme case, since it involves a very ionic wurtzite semiconductor. Therefore, it should not be too surprising that our model is apparently not very successful in this case.

Some of the most interesting band lineups occur between semiconductors of the 6.1 Å lattice constant group (Figure 7). However, there is very little information available concerning these lineups. Much of the experimental data have been interpreted in terms of band lineups derived from the electron affinity rule. One exception is the work of Nakai, et al., [1976]. They fabricated p-p ZnTe-GaSb heterojunctions and studied photoresponse as a function of photon energy. They interpreted their results in terms of a graded-gap heterojunction with an overall valence band barrier of 1.0 eV. This compares favorably with our predicted value of 0.76 eV, but one should remember that our model is not particularly suited to graded junctions.

C. Heterojunctions Involving Semiconductor Alloys

There is a great deal of current interest in heterojunctions involving semiconductor alloys. The reason for this is that the

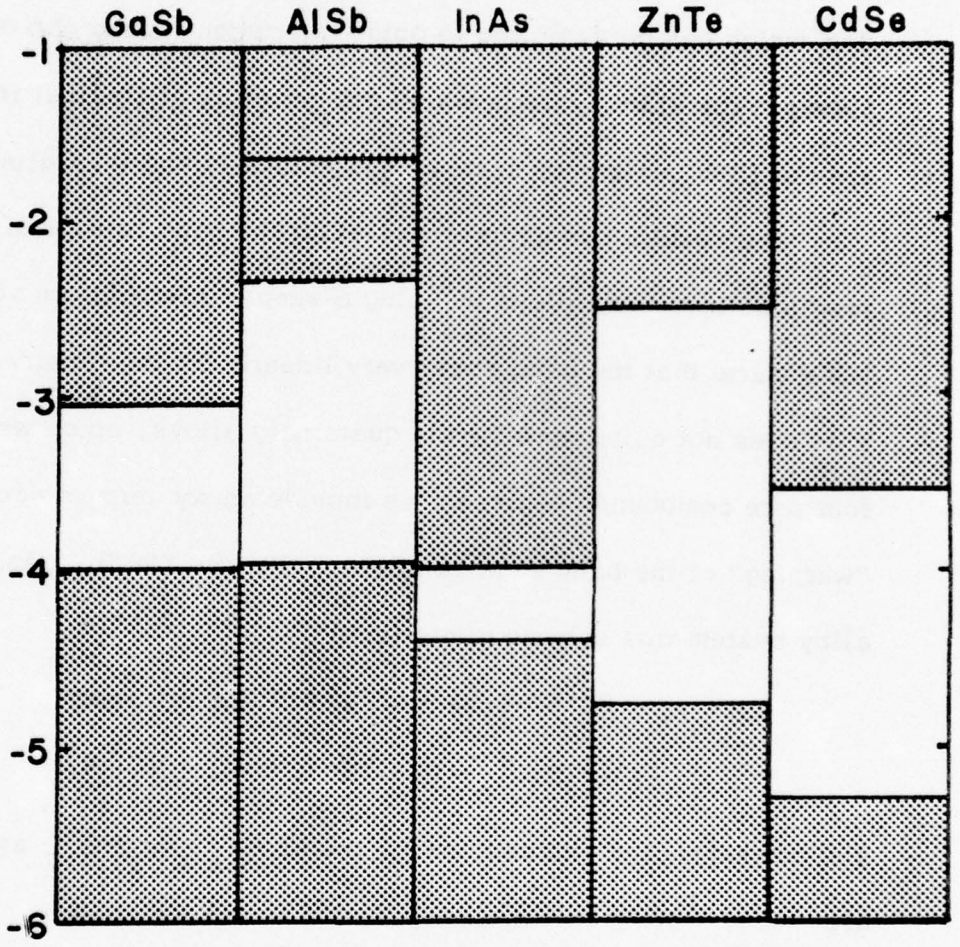


Figure 7. The relative band lineup for the semiconductors with lattice constants around 6.1 Å. The energies are in eV and the dashed line indicates the indirect conduction band edge of AlSb.

composition of the alloy can be adjusted so as to achieve a very good lattice match. In the case of quaternary alloys, there are two compositional parameters, so there is an additional degree of freedom which can be exploited to obtain an optimum band gap or band lineup. The alloy systems which are currently of greatest interest are the III-V quaternary systems (Ga,In)(As,P) and (Al,Ga)(As,Sb).

Our results can be used to predict the band lineups of heterojunctions involving alloys by using a simple interpolation scheme. We assume that the band edges vary linearly for the ternary alloys. This does not quite work for the quaternary alloys, since we have four pure compounds to fit, so we include an xy term to account for "warping" of the band edge "surface." For the $Ga_xIn_{1-x}As_yP_{1-y}$ alloy system this scheme gives (in eV)

$$\begin{aligned} E_v &= -4.58 + 0.46x + 0.20y - 0.04xy \\ E_c(\Gamma) &= -3.15 + 1.89x - 0.83y - 0.35xy. \end{aligned} \tag{III.1}$$

The corresponding expressions for the $Al_xGa_{1-x}As_ySb_{1-y}$ system are

$$\begin{aligned} E_v &= -3.98 + 0.04x + 0.02y - 0.04xy \\ E_c(\Gamma) &= -3.04 + 1.38x + 0.60y - 0.15xy \\ E_c(X) &= -2.81 + 0.46x + 0.60y - 0.25xy. \end{aligned} \tag{III.2}$$

This phenomenological interpolation is certainly inaccurate to the extent that alloys actually exhibit a small nonlinearity in the band gap vs. composition curve. We have attempted to calculate

the alloy band structures directly, both in the virtual crystal approximation and with a perturbative correction to it similar to that proposed by Baldereschi and Maschke [1975]. However, neither technique successfully reproduced the band gaps for all of the alloy systems of interest. It therefore appears that it will require a significantly different approach to treat the alloys properly, a circumstance already noted by Van Vechten and Bergstresser [1970].

We have already considered the GaAs-$Al_xGa_{1-x}As$ heterojunction. There is a great deal of current interest in the InP-$Ga_{0.48y}In_{1-0.48y}As_yP_{1-y}$ junction. The band energies as a function of y may be evaluated using (Equations (III.1). The results are shown in Figure 8. Our model predicts a very small conduction band discontinuity for all compositions. In some very preliminary experimental results, n-n heterojunctions of this system have been fabricated and they show nearly ohmic behavior [R. E. Hayes, private communication], in qualitative agreement with our prediction.

The predictions for heterojunctions involving the III-V quaternary alloy systems (Ga,In)(As,P) and (Al,Ga)(As,Sb) are summarized in Figure 9, where the band energies are plotted as a function of lattice constant. Our model predicts that heterojunctions within the (Ga,In)(As,P) system will generally have most of the discontinuity in the valence band. Those within the (Al,Ga)(As,Sb) system will have essentially all of the discontinuity in the conduction band.

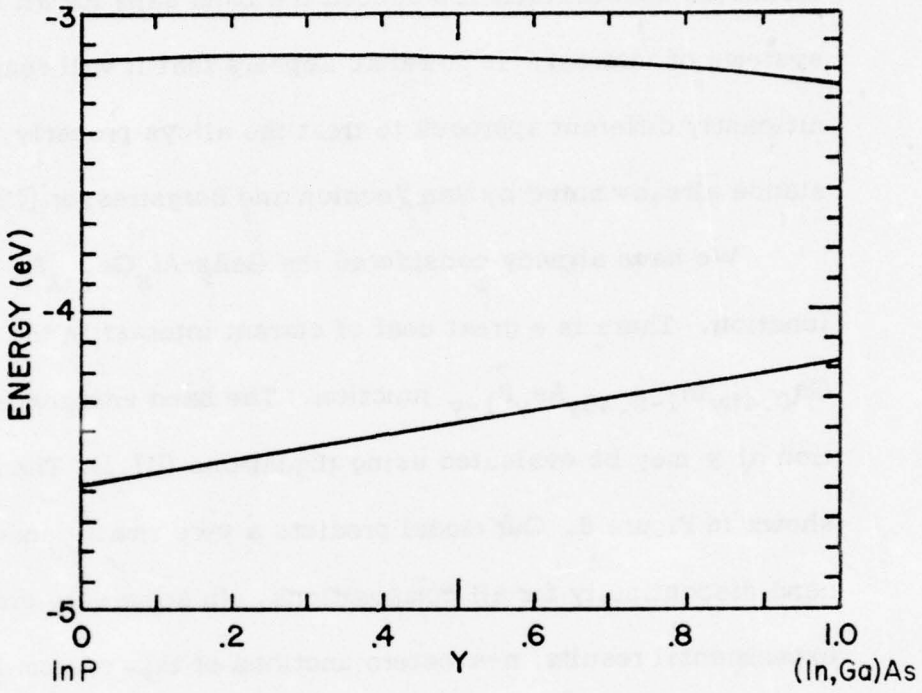


Figure 8. Conduction band (upper curve) and valence band (lower) curve) energies of $Ga_{0.48y}In_{1-0.48y}As_yP_{1-y}$ as a function of composition parameter y.

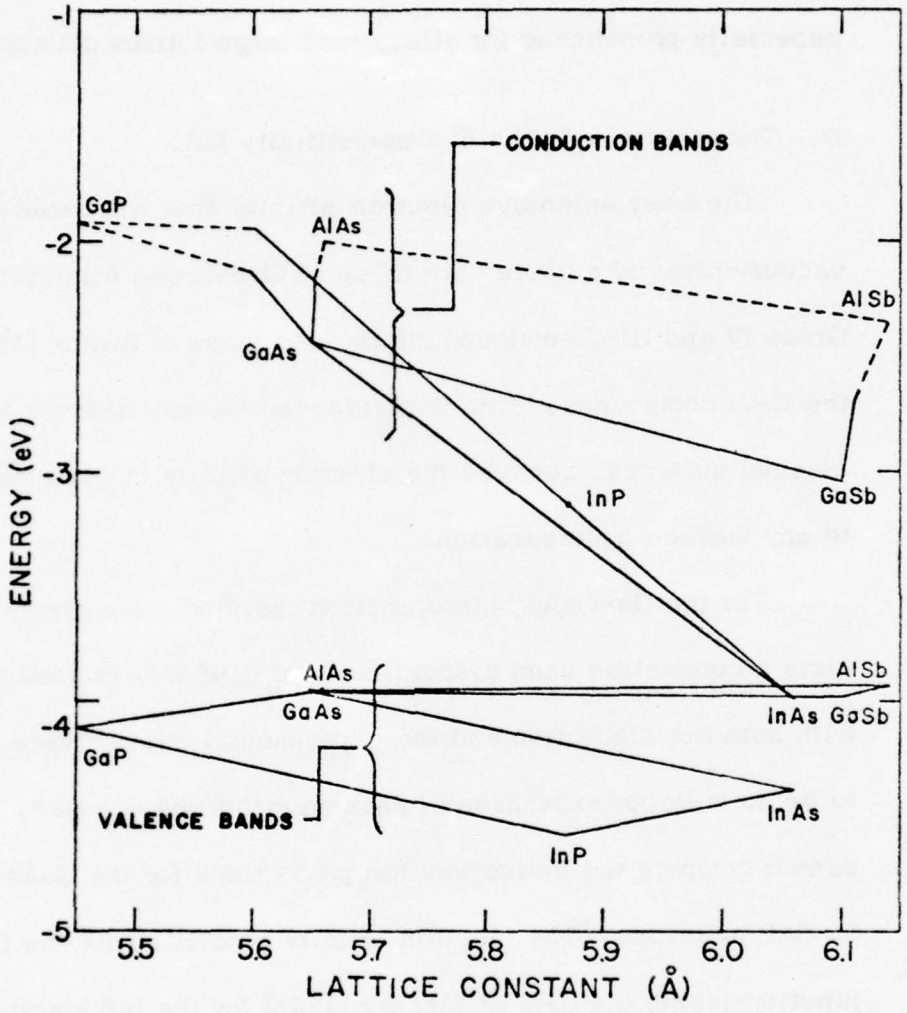


Figure 9. The band edge energies of the quaternary alloy systems (Ga,In)(As,P) and (Al,Ga)(As,Sb) as a function of lattice constant. The dotted lines indicate indirect conduction band edges.

Lattice-matched (Ga,In)(As,P)-(Al,Ga)(As,Sb) heterojunctions should show a stagger in band lineup, with the stagger becoming especially pronounced for alloys with large lattice constants.

D. Comparison with the Electron-Affinity Rule

The most extensive electron-affinity data available for vacuum-cleaved surfaces are those of Gobeli and Allen [1966] for Group IV and III-V semiconductors, and those of Swank [1967] for the II-VI compounds. It is important to use only data for vacuum-cleaved surfaces, because the electron affinity is quite sensitive to any surface contamination.

For the Ge-GaAs heterojunction the electron-affinity rule predicts a conduction band discontinuity of 0.06 eV, in good agreement with both our prediction and the experimental data. There appear to be no suitable experimental data on either AlAs or GaP, so we cannot compare the heterojunction predictions for the GaAs-AlAs and Si-GaP junctions. The electron affinity prediction for the InP-CdS junction (using the data of Fischer [1966] for the InP electron affinity) gives a conduction band discontinuity of 0.39 eV, with the InP band higher, in better agreement with Shay, et al., [1976] than with our prediction. For the InP-(Ga,In)As heterojunction the electron affinity rule predicts a conduction-band discontinuity of 0.10 eV, with the alloy conduction band being the higher one. Our model predicts a discontinuity of the same magnitude, but in the

opposite direction. Finally, our model and the electron-affinity rule are in qualitative agreement on the band lineup of the InAs-GaSb junction.

It therefore appears that our model and the electron-affinity rule generally disagree by no more than a few tenths of an electron volt. This level of disagreement is not much greater than the expected accuracy of our predictions (and the expected accuracy of the electron-affinity rule is certainly debatable) so it is not clear that the differences are significant. Our model has the advantage of being able to provide a more complete set of predictions than the available electron-affinity data, particularly for heterojunctions involving GaP and AlAs. It is also more readily adapted to detailed studies of the electronic structure of the interface.

CHAPTER IV

DISCUSSION AND CONCLUSIONS

Perhaps the most significant result of this work has been the demonstration that it is possible to define a meaningful "absolute" energy scale for band structure calculations. The relationship between the band structure and the electrostatic potential is certainly unique, if somewhat difficult to determine computationally, and the success of our simple matching scheme demonstrates the sort of understanding that can be gained from a knowledge of this relationship. Our calculations are certainly not the last word on this subject. We have achieved surprisingly good band structures for a model with only two adjustable parameters per ion, but it would be very desirable to apply more sophisticated band structure methods, such as nonlocal pseudopotential and OPW methods, to this sort of calculation. Perhaps others will try to derive the electrostatic potential from their calculations, now that we have shown that this is useful information.

The matching scheme deserves a great deal more attention and development. The success of our two-point scheme indicates that the physics of the heterojunction interface is likely to be

considerably simpler than one might at first expect. However, it would be quite desirable to have a more detailed theory. It appears to us that the most feasible way to investigate this question, beyond our simple scheme, would be through some sort of dielectric-response model of the detailed charge distribution at the interface. Such a scheme would presumably be sufficiently simple that it could be applied to a wide variety of heterojunctions. On a more elaborate level one could apply the techniques currently being used to calculate surfaces, and both groups presently doing such calculations [Appelbaum, 1975; Schlüter, 1975] have expressed an intention to do just that. This will certainly improve our understanding of heterojunction physics, but it will not invalidate the simpler models, which are likely to contribute more to our understanding of such aspects as chemical trends in heterojunction properties.

With our present two-point matching scheme, our model shares the property of transitivity with the electron affinity model. That is, if we know the band lineups for heterojunctions A-B and B-C, we can derive the lineup for A-C. Much of our original objection to the electron affinity rule concerned the fact that there is no fundamental reason to believe that heterojunctions should display this property. Only a great deal of further experimental work can determine the extent to which the transitivity property

actually holds. (Note that nontransitive theories necessarily involve the structure of the interface itself.)

Our results can also be viewed as part of a theory of electron affinities. There is a correlation between our conduction band energies and measured electron affinities, but there is a great deal of scatter in the data (Figure 10). The electron affinity should involve three contributions: the conduction band energy with respect to the electrostatic potential, the surface dipole (defined as the difference between the reference potential in the bulk and the vacuum level), and the image potential. Our calculations give the first of these contributions. As our understanding of surfaces improves, it may be possible to derive a phenomenological approximation for the surface dipole. We investigated the effect of image forces at heterojunctions and found it to be generally negligible [Frensley, 1975], but this is probably not the case at semiconductor surfaces.

We should note, at this point, that our results for the relationship between the reference potential and the energy bands depend sensitively on the choice of the parameter α in the local exchange approximation, although the relative lineup between semiconductors (which is what is important for heterojunction lineups) is much less sensitive. Therefore, any attempt to relate our results to absolute quantities such as the electron affinity will run squarely into the issue of the proper choice of α. Viewed differently, a

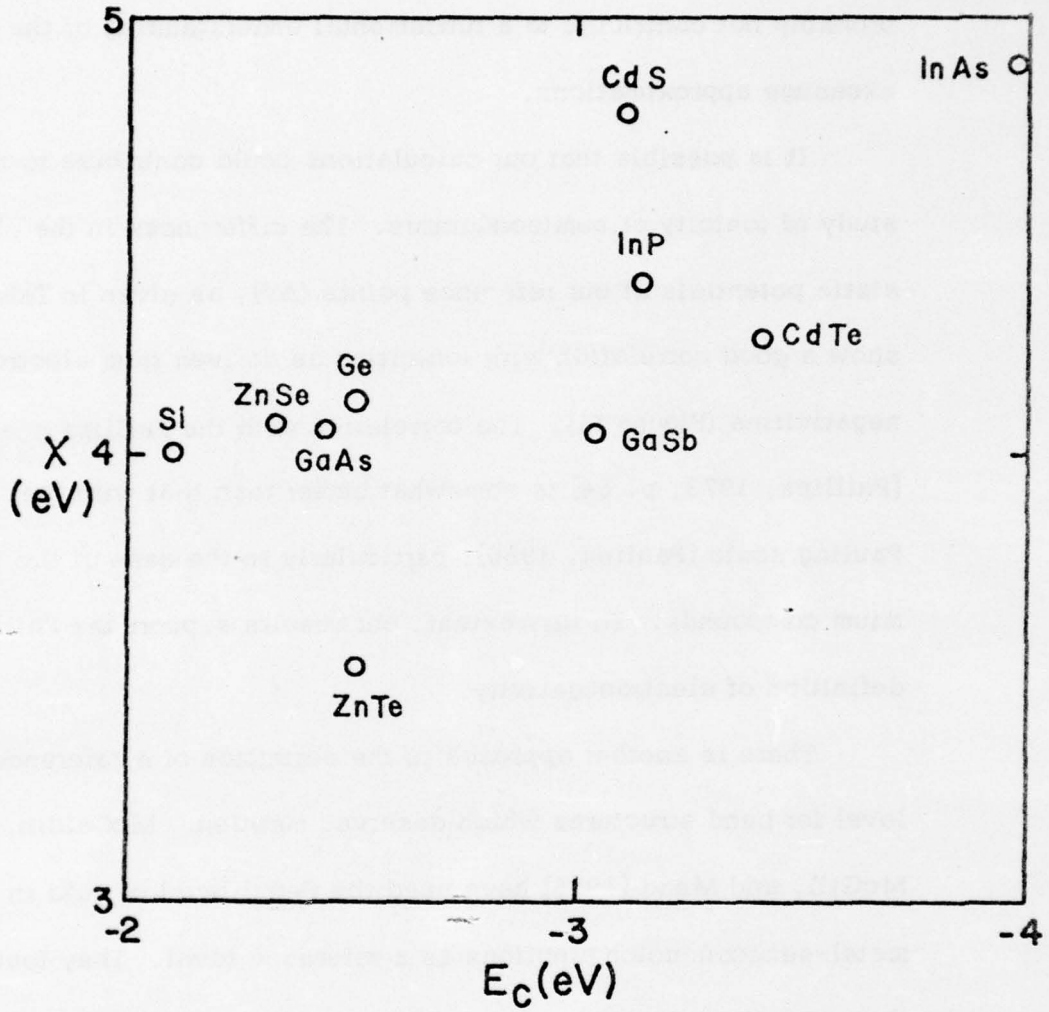


Figure 10. The electron affinity [Gobeli, 1966, and Swank, 1967] vs. the conduction band energy relative to our reference potential.

theory of electron affinities could contribute to our understanding of the appropriate parameter in such approximations, though it would probably not contribute to a fundamental understanding of the local exchange approximations.

It is possible that our calculations could contribute to the study of ionicity of semiconductors. The differences in the electrostatic potentials at our reference points (ΔV), as given in Table III, show a good correlation with ionicities as derived from electronegativities (Figure 11). The correlation with the Phillips scale [Phillips, 1973, p. 54] is somewhat better than that with the Pauling scale [Pauling, 1960], particularly in the case of the cadmium compounds. To this extent, our results support the Phillips definition of electronegativity.

There is another approach to the definition of a reference level for band structures which deserves mention. McCaldin, McGill, and Mead [1976] have used the Fermi level of gold in metal-semiconductor junctions as a reference level. They found that the valence band location with respect to this level is only dependent upon the anion species and furthermore correlates strongly with the anion electronegativity. Our results show a similar correlation, but with much more scatter than McCaldin, et al. report. This subject deserves a great deal more study, particularly to determine why Schottky barriers using copper show more scatter than those using gold, and how this is related to the

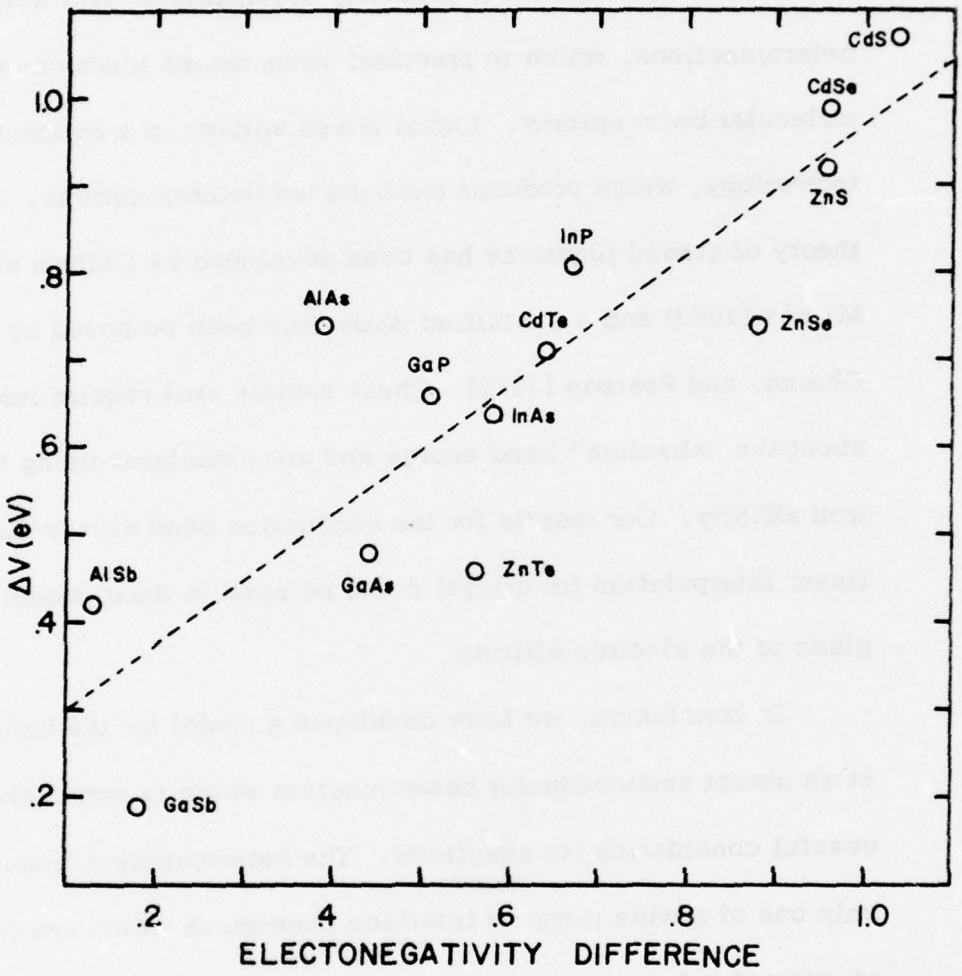


Figure 11. The potential difference between the two interstitial points vs. the difference in Phillips electronegativity [Phillips, 1973, p. 54].

detailed electronic structure of a metal-semiconductor interface as studied by Louie, et al. [1976b].

Our present model is primarily applicable to very abrupt heterojunctions, which in practical terms means junctions grown by molecular beam epitaxy. Liquid phase epitaxy is a better developed technology, which produces more graded heterojunctions. The theory of graded junctions has been developed by Oldham and Milnes [1963] and a simplified model has been proposed by Cheung, Chiang, and Pearson [1975]. These models still require information about the "absolute" band energy and are formulated using the electron affinity. Our results for the conduction band energy (assuming linear interpolation for alloys) could be used in these models in place of the electron affinity.

In conclusion, we have developed a model for the band lineup at an abrupt semiconductor heterojunction which is remarkably successful considering its simplicity. The heterojunction lineup is only one of a wide range of interface phenomena which are currently of interest. A semiconductor heterojunction is one of the "gentlest" possible interfaces, and this apparently accounts for the success of our model. One may hope that the understanding we have gained can be applied to the solution of other interface problems.

BIBLIOGRAPHY

Abarenkov, I. V. and V. Heine, 1965, "The Model Potential for Positive Ions," Philos. Mag. 12, 529.

Adachi, E., 1968, "Energy Band Parameters of InAs at Various Temperatures," J. Phys. Soc. Japan 24, 1178.

Anderson, R. L., 1960, "Germanium-Gallium Arsenide Heterojunctions," IBM J. Res. Dev. 4, 283.

Anderson, R. L., 1962, "Experiments on Ge-GaAs Heterojunctions," Solid-State Electron. 5, 341.

Animalu, A. O. E. and V. Heine, 1965, "The Screened Model Potential for 25 Elements," Philos. Mag. 12, 1249.

Animalu, A. O. E., 1966, "The Total Electronic Band Structure Energy for 29 Elements," Proc. R. Soc. Lond. Ser. A 294, 376.

Appelbaum, J. A. and D. R. Hamann, 1973, "Self-Consistent Pseudopotential for Si," Phys. Rev. B 8, 1777.

Appelbaum, J. A., G. A. Baraff, and D. R. Hamann, 1975, "The Si (100) Surface. II. A Theoretical Study of the Relaxed Surface," Phys. Rev. B 12, 5749.

Aspnes, D. E. and A. A. Studna, 1972, "Direct Observation of the E_0 and $E_0+\Delta_0$ Transitions in Silicon," Solid State Commun. 11, 1375.

Aspnes, D. E., 1973a, "Interband Masses of Higher Interband Critical Points in Ge," Phys. Rev. Lett. 31, 230.

Aspnes, D. E. and A. A. Studna, 1973b, "Schottky-Barrier Electroreflectance: Application to GaAs," Phys. Rev. B 7, 4605.

Aven, M., D. T. F. Marple, and B. Segall, 1961, "Some Electrical and Optical Properties of ZnSe," J. Appl. Phys. 32, 2261.

Baldereschi, A. and K. Maschke, 1975, "Band Structure of Semiconductor Alloys Beyond the Virtual Crystal Approximation. Effect of Compositional Disorder on the Energy Gaps in GaP_xAs_{1-x}," Solid State Commun. 16, 99.

Balslev, I., 1968, "Optical Absorption Due to Inter-Conduction-Minimum Transitions in Gallium Arsenide," Phys. Rev. 173 762.

Bjorken, J. D. and S. D. Drell, 1964, Relativistic Quantum Mechanics (McGraw-Hill Book Co., New York).

Brust, D., 1964, "Electronic Spectra of Crystalline Germanium and Silicon," Phys. Rev. 134, A1337.

Cardona, M. and D. L. Greenway, 1963, "Fundamental Reflectivity and Band Structure of ZnTe, CdTe, and HgTe," Phys. Rev. 131, 98.

Cardona, M., K. L. Shaklee, and F. H. Pollak, 1967, "Electroreflectance at a Semiconductor-Electrolyte Interface," Phys. Rev. 154, 696.

Cardona, M., 1969, Modulation Spectroscopy, Supplement 11 to Solid State Phys., edited by F. Seitz, D. Turnbull, and H. Ehrenreich (Academic Press, New York).

Chadi, D. J. and M. L. Cohen, 1973a, "Electronic Structure of $Hg_{1-x}Cd_xTe$ Alloys and Charge-Density Calculations Using Representative $\underline{k}$ Points," Phys. Rev. B 7, 692.

Chadi, D. J. and M. L. Cohen, 1973b, "Special Points in the Brillouin Zone," Phys. Rev. B 8, 5747.

Chelikowsky, J. R. and M. L. Cohen, 1974a, "Electronic Charge Densities and the Temperature Dependence of the Forbidden (222) Reflection in Silicon and Germanium," Phys. Rev. Lett. 33, 1339.

Chelikowsky, J. R. and M. L. Cohen, 1974b, "Electronic Structure of Silicon," Phys. Rev. B 10, 5095.

Cheung, D. T., S. Y. Chiang, and G. L. Pearson, 1975, "A Simplified Model for Graded-Gap Heterojunctions," Solid-State Electron. 18, 263.

Cohen, M. H. and V. Heine, 1961, "Cancellation of Kinetic and Potential Energy in Atoms, Molecules, and Solids," Phys. Rev. 122, 1821.

Cohen, M. L. and T. K. Bergstresser, 1966, "Band Structures and Pseudopotential Form Factors for Fourteen Semiconductors of the Diamond and Zinc-blende Structures," Phys. Rev. 141, 789.

Cohen, M. L. and V. Heine, 1970, "The Fitting of Pseudopotentials to Experimental Data and Their Subsequent Application," Solid State Phys., edited by H. Ehrenreich, F. Seitz, and D. Turnbull (Academic Press, New York), Vol. 24, p. 37.

Cohen, M. L., et al., 1975, "Self-Consistent Pseudopotential Method for Localized Configurations: Molecules," Phys. Rev. B 12, 5575.

Dean, P. J., G. Kaminsky, and R. B. Zetterstrom, 1967, "Intrinsic Optical Absorption of Gallium Phosphide Between 2.33 and 3.12 eV," J. Appl. Phys. 38, 3551.

Dean, P. J., Y. Yafet, and J. R. Haynes, 1969, "Valley-Orbit Splitting of the Indirect Free Exciton in Silicon," Phys. Rev. 184, 837.

Desclaux, J. P., 1973, "Relativistic Dirac-Fock Expectation Values for Atoms with Z=1 to Z=120," At. Data and Nucl. Data Tables 12, 311.

Dimmock, J. O., 1967, "Optical Absorption and Band Edge Parameters of Group II-VI Semiconductors," II-VI Semiconductor Compounds, 1967 International Conference (W. A. Benjamin, Inc., New York), p. 277.

Dingle, R., W. Wiegmann, and C. H. Henry, 1974, "Quantum States of Confined Carriers in Very Thin $Al_xGa_{1-x}As$-GaAs-$Al_xGa_{1-x}As$ Heterostructures," Phys. Rev. Lett. 34, 827.

Dingle, R., A. C. Gossard, and W. Wiegmann, 1975, "Direct Observation of Superlattice Formation in a Semiconductor Heterostructure," Phys. Rev. Lett. 34, 1327.

Dolega, U., 1963, "Theorie des pn-Kontaktes zwischen Halbleitern mit verschiedenen Kristallgittern," Z. Naturforschg. 18a, 653.

Donnay, J. D. H. and G. Donnay, editors, 1963, Crystal Data, Determinative Tables (American Crystallographic Association).

Ettenberg, M. and R. J. Paff, 1970, "Thermal Expansion of AlAs," J. Appl. Phys. 41, 3926.

Fang, F. F. and W. E. Howard, 1964, Effects of Crystal Orientation on Ge-GaAs Heterojunctions," J. Appl. Phys. 35, 612.

Fischer, J. E., 1970, "Transverse Electroreflectance and the Band Structure of Germanium," Proc. of the 10'th Internat. Conf. on the Physics of Semiconductors, Cambridge, 1970 (USAEC, Springfield, Va.), p. 427. (CONF-700801).

Fischer, T. E., 1966, "Photoelectric Emission and Work Function of InP," Phys. Rev. 142, 519.

Frensley, W. R., H. A. Schauer, and H. Kroemer, 1975, "Contribution of Dielectric Image Force to the Conduction Band Discontinuity in Semiconductor Heterojunctions," Bull. Am. Phys. Soc., Ser. II 20, 426.

Frensley, W. R. and H. Kroemer, 1976, "Prediction of Semiconductor Heterojunction Discontinuities from Bulk Band Structures," J. Vac. Sci. Technol. 13, 810.

Gobeli, G. W. and F. G. Allen, 1966, "Photoelectric Threshold and Work Function," Semiconductors and Semimetals, edited by R. K. Willardson and A. C. Beer (Academic Press, New York), Vol. 2, p. 263.

Guizzetti, G., et al., 1974, "Thermoreflectance Spectra of Diamond and Zinc-Blende Semiconductors in the Vacuum-Ultraviolet Region," Phys. Rev. B 9, 640.

Harland, H. B. and J. C. Woolley, 1966, "Conduction Band of GaSb," Can. J. Phys. 44, 2715.

Harrison, W. A., 1970, Solid State Theory (McGraw-Hill Book Co., New York).

Heine, V. and I. V. Abarenkov, 1964, "A New Method for the Electronic Structure of Metals," Philos. Mag. 9, 451.

Heine, V., 1970, "The Pseudopotential Concept," Solid State Physics, edited by H. Ehrenreich, F. Seitz, and D. Turnbull (Academic Press, New York), Vol. 24, p. 1.

Herman, F., et al., 1967, "Energy Band Structure and Optical Spectrum of Several II-VI Compounds," II-VI Semiconducting Compounds, 1967 International Conference (W. A. Benjamin, Inc., New York), p. 503.

Herring, C., 1940, "A New Method for Calculating Wave Functions in Crystals," Phys. Rev. 57, 1169.

Kittel, C., 1963, Quantum Theory of Solids (John Wiley and Sons, Inc., New York).

Kressel, H., 1976, "Light Sources," Phys. Today 29, No. 5, p. 38.

Kroemer, H., 1957, "Theory of a Wide-Gap Emitter for Transistors," Proc. IRE 45, 1535.

Kroemer, H., 1963, "A Proposed Class of Heterojunction Injection Lasers," Proc. IEEE 51, 1782.

Kroemer, H., 1975, "Problems in the Theory of Heterojunction Discontinuities," CRC Crit. Rev. Solid State Sci. 5, 555.

Kwan, C. C. Y. and J. C. Woolley, 1968, "Conduction Band of InAs," Can. J. Phys. 46, 1669.

Lendvay, E., et al., 1970, "Preparation and Some Properties of Si-ZnS Heterojunctions," Proc. of the Int. Conf. on the Physics and Chemistry of Semiconductor Heterojunctions and Structures (Akademiai Kiado, Budapest), Vol. I, p. 263.

Ley, L., et al., 1974, "Total Valence-Band Densities of States of III-V and II-VI Compounds from X-ray Photoemission Spectroscopy," Phys. Rev. B 9, 600.

Lösch, K. and J. U. Fischbach, 1976, "Measurement of High Near-Edge Absorption Coefficients in Surface Layers of InP," Phys. Status Solidi A 33, 473.

Louie, S. G., et al., 1976a, "Self-Consistent Electronic States for Reconstructed Si Vacancy Models," Phys. Rev. B 13, 1654.

Louie, S. G. and M. L. Cohen, 1976b, "Electronic Structure of a Metal-Semiconductor Interface," Phys. Rev. B 13, 2461.

Löwdin, P. O., 1951, "A Note on the Quantum-Mechanical Perturbation Theory," J. Chem. Phys. 19, 1396.

McCaldin, J. O., T. C. McGill, and C. A. Mead, 1976, "Correlation for III-V and II-VI Semiconductors of the Au Schottky Barrier Energy with Anion Electronegativity," Phys. Rev. Lett. 36, 56.

McCarthy, I. E., 1968, Introduction to Nuclear Theory (John Wiley and Sons, Inc., New York).

MacGillavry, C. H. and G. Riech, editors, 1962, International Tables for X-ray Crystallography. Vol. III. Physical and Chemical Tables (Kynoch Press, Birmingham).

Mach, R., et al., 1970, "Epitaxial Growth and the Conduction Properties of ZnSe-GaAs Heterojunctions," Phys. Status Solidi A 2, 701.

Monemar, B., 1973, "Fundamental Energy Gaps of AlAs and AlP from Photoluminescence Exc tation Spectra," Phys. Rev. B 8, 5711.

Moore, C. E., 1949, Atomic Energy Levels (U. S. Government Printing Office, Washington), Vol. I.

Moore, C. E., 1952, Atomic Energy Levels (U. S. Government Printing Office, Washington), Vol. II.

Moore, C. E., 1958, Atomic Energy Levels (U. S. Government Printing Office, Washington), Vol. III.

Nakai, J., et al., 1970, "ZnTe-GaSb Heterojunctions," Proc. of the Int. Conf. on the Physics and Chemistry of Semiconductor Heterojunctions and Layer Structures (Akademaia Kiado, Budapest), Vol. I, p. 319.

Oldham, W. G. and A. G. Milnes, 1963, "n-n Semiconductor Heterojunctions," Solid-State Electron. 6, 121.

Onton, A., 1970, "AlAs and AlP: Raman Scattering and Electric Field Modulated Reflectance," Proc. of the 10'th Int. Conf. on the Physics of Semiconductors, Cambridge, 1970 (USAEC, Springfield, Va.), p. 107. (CONF-700801)

Onton, A., Y. Yacoby, and R. J. Chicotka, 1972, "Direct Optical Observation of the Subsidiary X_{1c} Conduction Band and Its Donor Levels in InP," Phys. Rev. Lett. 28, 966.

Pandey, K. C. and J. C. Phillips, 1974, "Fine Structure of E_1' Peak in Ge and GaAs," Phys. Rev. B 9, 1560.

Parsons, B. J. and H. Piller, 1971, "An Electroreflectance Study of Gallium Antimonide in the 3.0-4.2 eV Region," Solid State Commun. 9, 767.

Pauling, L., 1960, The Nature of the Chemical Band (Cornell Univ. Press, Ithaca, N.Y.).

Phillips, J. C. and L. Kleinman, 1959, "New Method for Calculating Wave Functions in Crystals and Molecules," Phys. Rev. 116, 287.

Phillips, J. C., 1973, Bonds and Bands in Semiconductors (Academic Press, New York).

Piller, H., C. K. So, and R. C. Whited, 1973, "Infrared Modulated Reflectance Spectra of n and p Type Gallium Antimonide and n Type Indium Antimonide," Surface Sci. 37, 639.

Pitt, G. D., 1973, "The Conduction Band Structures of GaAs and InP," J. Phys. C 6, 1586.

Pitt, G. D., M. K. R. Vyas, and A. W. Mabbit, 1974, "The Conduction Band Structure of the $In_{1-x}Ga_xP$ Alloy System," Solid State Commun. 14, 621.

Pollak, F. H., 1967, "Experimental Studies of Interband Transitions Above the Fundamental Edge in the II-VI Semiconducting Compounds," II-VI Semiconductor Compounds, 1967 International Conference (W. A. Benjamin, Inc., New York), p. 552.

Rediker, R. H., S. Stopek, and J. H. R. Ward, 1964, "Interface-Alloy Epitaxial Heterojunctions," Solid-State Electron. 7, 621.

Riben, A. R. and D. L. Feucht, 1966, "n Ge-p GaAs Heterojunctions," Solid-State Electron. 9, 1055.

Richardson, D. and P. K. W. Vinsome, 1971, "Dielectric Function in Semiconductors," Phys. Lett. A 36, 3.

Rowe, J. E., M. Cardona, and K. L. Shaklee, 1969, "Derivative Spectrum of Indirect Excitons in AlSb," Solid State Commun. 7, 411.

Saravia, L. R. and D. Brust, 1968, "High Resolution Study of the One-Electron Spectrum of Si," Phys. Rev. 171, 916.

Schlüter, M., et al., 1975, "Self-Consistent Pseudopotential Calculations for Si (111) Surfaces: Unreconstructed (1×1) and Reconstructed (2×1) Model Structures," Phys. Rev. B 12, 4200.

Sharma, B. L. and R. K. Purohit, 1974, Semiconductor Heterojunctions (Pergamon Press, Oxford).

Shay, J. L., S. Wagner, and J. C. Phillips, 1976, "Heterojunction Band Discontinuities," Appl. Phys. Lett. 28, 31.

Shockley, W., 1951, U.S. Patent No. 2,569,347.

Slater, J. C., 1974, The Self-Consistent Field for Molecules and Solids: Quantum Theory of Molecules and Solids, Vol. IV (McGraw-Hill Book Co., New York).

Sleger, K. J., A. G. Milnes, and D. L. Feucht, 1970, "ZnSe-GaAs and ZnSe-Ge Heterojunction Transistors," Proc. of the Int. Conf. on the Physics and Chemistry of Semiconductor Heterojunctions and Layer Structures (Akademiai Kiado, Budapest), Vol. I, p. 73.

Stowkowski, S. E. and D. D. Sell, 1972, "Reflectivity and (dR/dE)/R of GaP between 2.5 and 6.0 eV," Phys. Rev. B 5, 1636.

Swank, R. K., 1967, "Surface Properties of II-VI Compounds," Phys. Rev. 153, 844.

Van Vechten, J. A. and T. K. Bergstresser, 1970, "Electronic Structures of Semiconductor Alloys," Phys. Rev. B 1, 3351.

Vinsome, P. K. W. and D. Richardson, 1971, "The Dielectric Function in Zincblende Semiconductors," J. Phys. C 4, 2650.

Walter, J. P. and M. L. Cohen, 1971, "Pseudopotential Calculations of Electronic Charge Densities in Seven Semiconductors," Phys. Rev. B 4, 1877.

Zeidenbergs, G. and R. L. Anderson, 1967, "Si-GaP Heterojunctions," Solid-State Electron. 10, 113.

Zucca, R. R. and Y. R. Shen, 1970, "Wavelength Modulation Spectra of Some Semiconductors," Phys. Rev. B 1, 2668.

APPENDICES

APPENDIX A

FREE ION SPECTRA

The ionic pseudopotential is supposed to represent the effective interaction between the closed-shell ion and an electron. Therefore, a natural test to apply is to calculate the energy levels of an electron in the field of an isolated ionic pseudopotential, and compare the results to the spectroscopically observed levels. This test is very useful in the initial choice of parameters, and, after we have fitted the band structures, a reasonable fit to the ionic levels increases our confidence that we have chosen a good pseudopotential.

Since the ionic pseudopotential which we are using is a simple, spherically symmetric potential, calculation of the electronic levels is a matter of solving the radial part of the Schroedinger equation. This is conveniently done by the technique of finite-difference equations.[1] The wavefunction is calculated at a finite number of points and the differential equation is transformed into a tridiagonal matrix equation.

---

[1]The author wishes to express his appreciation to Mr. David G. Unger for calling this technique to his attention.

We wish to find the eigenvalues E of the radial Schroedinger equation

$$-\frac{1}{r^2}\frac{d}{dr}\left(r^2\frac{d\psi}{dr}\right)+\frac{\ell(\ell+1)}{r^2}\psi(r)+V(r)\psi(r)=E\psi(r) \qquad (A.1)$$

where V(r) is our ionic pseudopotential. The first step is to transform the independent variable to

$$x=\frac{r}{a+r}\,. \qquad (A.2)$$

Whereas r runs from 0 to ∞, x runs from 0 to 1. a is effectively a scale factor. The radial equation then becomes

$$-\frac{(1-x)^4}{a^2}\frac{1}{x}\frac{d^2}{dx^2}(x\psi(x))+\frac{(1-x)^2}{a^2}\frac{\ell(\ell+1)}{x^2}\psi(x)+V[r(x)]\psi(x)=E\psi(x)\,. \qquad (A.3)$$

If we define $f(x)=x\psi(x)$, we have the simpler form

$$\frac{(1-x)^2}{a^2}\left\{-(1-x)^2\frac{d^2}{dx^2}+\frac{\ell(\ell+1)}{x^2}\right\}f(x)+V[r(x)]=Ef(x) \qquad (A.4)$$

Now we consider a finite mesh of n equally spaced points $x_j=j\Delta$ where $\Delta=1/(n+1)$. The $f(x_j)$ form an n-dimensional vector, and if we approximate the derivative by finite differences, the Hamiltonian becomes a tridiagonal matrix of order n, with nonzero elements

$$H_{jj}=\frac{(1-x_j)^2}{a^2}\left\{\frac{2(1-x_j)^2}{\Delta^2}+\frac{\ell(\ell+1)}{x_j^2}\right\}+V[r(x_j)] \qquad (A.5)$$

$$H_{j,j-1}=H_{j,j+1}=-\frac{(1-x_j)^4}{a^2\Delta^2}\,.$$

This matrix can then be diagonalized to find the eigenvalues of the original Hamiltonian.

A computer program was written, which straightforwardly evaluated the expressions (A.5) and used library subroutines to diagonalize the resulting matrix. A mesh of one hundred points was used, and the scale factor a was set to 2 a.u. The program was tested with a Coulomb potential with charge Z=4. The calculated energies were within 0.003 Ry. of the exact values for all states with principal quantum number n less than eight, except for the 1s state, which receives a significant contribution from the Coulomb singularity. This problem will not occur for our pseudopotential, since it is smooth and continuous. We therefore believe that the program is capable of accurately calculating the energy levels of our ionic pseudopotential.

The calculated ionic spectra for the pseudopotentials actually used in the band structure calculations are given in Table IV, along with the experimental values. The calculated values generally agree with the experimental ones to within about 5 percent, which is probably about as good as one could expect with a local, energy-independent pseudopotential. The values for the Si row of the periodic table illustrate the limits of a local pseudopotential. The d states are uniformly lower in energy than the calculated values. This is because there are no occupied d states in the

core, so the d states are not "pseudized," a point discussed by Chelikowsky and Cohen [1974b].

The importance of fitting the free ion spectra is illustrated by the fact that we found it possible to obtain reasonable band structures for the antimonide compounds with a different pseudopotential than that which was finally used. This potential had a narrower, taller central peak, and gave a value for the Sb 5s state which was several eV too low. It also led to band energies with respect to the reference potential which were about 0.3 eV different from the final values. Therefore, we think that it is quite important to apply such a test in self-consistent pseudopotential calculations.

TABLE IV

FREE ION SPECTRA DERIVED FROM
THE IONIC PSEUDOPOTENTIAL

The experimental values are shown directly above the calculated ones. Experimental data are from Moore, 1949, 1952, and 1958. Energies are in eV.

Al

n	s	p	d
	-28.45	-21.77	-14.07
3	-28.95	-21.21	-12.94
	-12.81	-10.63	-7.89
4	-13.27	-10.46	-7.31
	-7.29	-6.32	-5.03
5	-7.54	-6.26	-4.72
	-4.71	-4.19	-3.48
6	-4.86	-4.17	-3.30

Si

n	s	p	d
	-45.14	-36.26	-25.26
3	-46.54	-35.81	-22.69
	-21.09	-18.07	-14.14
4	-21.75	-17.87	-12.83
	-12.23	-10.85	-9.00
5	-12.57	-10.76	-8.29
	-7.99	-7.24	-6.22
6	-8.19	-7.21	-5.82

TABLE IV (continued)

FREE ION SPECTRA DERIVED FROM
THE IONIC PSEUDOPOTENTIAL

The experimental values are shown directly above the calculated ones. Experimental data are from Moore, 1949, 1952, and 1958. Energies are in eV.

	P		
n	s	p	d
	-65.02	-53.97	-39.71
3	-67.34	-52.95	-34.69
	-31.18	-27.29	-22.20
4	-32.31	-26.85	-19.69
	-18.33	-16.52	-14.11
5	-18.91	-16.32	-12.76
	-12.06	-11.08	-9.75
6	-12.41	-10.99	-8.96

	S		
n	s	p	d
	-88.05	-74.82	-57.37
3	-89.08	-71.49	-48.53
	-43.05	-38.28	-32.04
4	-44.03	-36.97	-27.67
	-25.55	-23.31	-20.35
5	-26.15	-22.69	-17.99
	-16.91	-15.69	-14.05
6	-17.30	-15.37	-12.67

TABLE IV (continued)

FREE ION SPECTRA DERIVED FROM
THE IONIC PSEUDOPOTENTIAL

The experimental values are shown directly above the calculated ones. Experimental data are from Moore, 1949, 1952, and 1958. Energies are in eV.

	Zn		
n	s	p	d
	-17.96	-11.88	-5.95
4	-17.79	-11.37	-5.99
	-7.00	-5.38	-3.34
5	-7.21	-5.30	-3.37
	-3.77	-3.09	-2.14
6	-3.89	-3.07	-2.17
	-2.36	-2.04	-1.49
7	-2.43	-2.01	-1.52

	Ga		
n	s	p	d
	-30.71	-22.49	-12.84
4	-32.42	-22.67	-13.17
	-13.26	-10.73	-7.25
5	-14.29	-10.97	-7.43
	-7.46		
6	-7.98	-6.49	-4.78

TABLE IV (continued)

FREE ION SPECTRA DERIVED FROM
THE IONIC PSEUDOPOTENTIAL

The experimental values are shown directly above the calculated ones. Experimental data are from Moore, 1949, 1952, and 1958. Energies are in eV.

Ge

n	s	p	d
	-45.71	-35.40	-22.06
4	-47.21	-35.68	-22.58
	-21.01	-17.56	-12.65
5	-22.25	-17.88	-12.79
	-12.23	-10.54	
6	-12.84	-10.78	-8.26

As

n	s	p	d
	-62.63	-50.24	-33.22
4	-64.47	-50.91	-34.02
	-29.95		
5	-31.64	-26.19	-19.38
6	-18.68	-16.01	-12.59

TABLE IV (continued)

FREE ION SPECTRA DERIVED FROM
THE IONIC PSEUDOPOTENTIAL

The experimental values are shown directly above the calculated ones. Experimental data are from Moore, 1949, 1952, and 1958. Energies are in eV.

Se

n	s	p	d
	-81.7	-67.3	-46.6
4	-83.98	-67.84	-47.15
	-40.3		
5	-42.75	-35.74	-27.06
6	-25.67	-22.13	-17.67

Cd

n	s	p	d
	-16.91	-11.23	-5.78
5	-15.33	-10.67	-5.95
	-6.62	-5.11	-3.24
6	-6.51	-5.06	-3.35
	-3.60	-2.97	-2.09
7	-3.60	-2.97	-2.16
	-2.27	-1.95	-1.46
8	-2.28	-1.96	-1.51

TABLE IV (continued)

FREE ION SPECTRA DERIVED FROM
THE IONIC PSEUDOPOTENTIAL

The experimental values are shown directly above the calculated ones. Experimental data are from Moore, 1949, 1952, and 1958. Energies are in eV.

In

n	s	p	d
	-28.03	-20.58	-12.08
5	-28.02	-21.18	-12.99
	-12.30	-10.00	-6.88
6	-12.76	-10.41	-7.33
	-7.03	-5.60	-4.46
7	-7.29	-6.22	-4.73
	-4.55		
8	-4.73	-4.15	-3.31

Sb

n	s	p	d
	-55.7	-44.9	-30.6
5	-57.11	-46.31	-32.44
	-27.9	-23.9	
6	-29.33	-24.53	-18.64
7	-17.69	-15.24	-12.20

TABLE IV (continued)

FREE ION SPECTRA DERIVED FROM
THE IONIC PSEUDOPOTENTIAL

The experimental values are shown directly above the calculated ones. Experimental data are from Moore, 1949, 1952, and 1958. Energies are in eV.

	Te		
n	s	p	d
	-72.3	-59.8	-42.7
5	-74.39	-61.20	-44.39
	-37.8	-33.0	
6	-39.94	-33.38	-25.82
7	-24.55	-21.03	-17.01

APPENDIX B

COMPUTER PROGRAMS

1. Band Structure Program

The primary task of the band structure program is to calculate the wavefunctions and energies of one-electron states in a periodic potential. We therefore make use of Bloch's theorem [Kittel, 1963, ch. 9] to write the wavefunctions as

$$\psi(\vec{x}) = e^{i\vec{k}\cdot\vec{x}} \sum_{\vec{G}} a_{\vec{G}} e^{i\vec{G}\cdot\vec{x}} \qquad (B.1)$$

where $\vec{k}$ is a vector from the first Brillouin zone, the $\vec{G}$'s are reciprocal lattice vectors, and the $a_{\vec{G}}$'s are complex coefficients. For computational purposes the wavefunction is most conveniently represented by the one-dimensional vector of the $a_{\vec{G}}$'s. With this representation of the wavefunction the Hamiltonian becomes a matrix

$$H_{\vec{k}+\vec{G},\vec{k}+\vec{G}'} = |\vec{k}+\vec{G}|^2 \delta_{\vec{G},\vec{G}'} + v(\vec{G}-\vec{G}'). \qquad (B.2)$$

The first term is the kinetic energy (the units are Rydbergs and reciprocal Bohr radii, which are used for all internal calculations). The second term is the Fourier coefficient of the potential for the reciprocal lattice vector $\vec{G}-\vec{G}'$.

At this point it should be obvious that in order to represent our states and Hamiltonian as subscripted arrays, we must number the reciprocal lattice vectors so that they may be used as indicies. This is done by the subroutine FCCLAT, which constructs the reciprocal lattice vectors for the face-centered cubic lattice. All vectors with $G^2 \leq 32$ are constructed, sorted in order of increasing $\vec{G}^2$, and stored in the TABLE common block. A cross-table which will give an index when entered with the three components of $\vec{G}$ is then constructed and stored in TABLE.

The potential is constructed by either FRMFCTR or MODELV, depending upon whether an empirical pseudopotential, such as those of Cohen and Bergstresser [1966], or the self-consistent potential described in Chapter II is to be used. It is convenient to choose the origin of the coordinate system at the point halfway between the two atoms in the unit cell. The potential can then be written as

$$v(\vec{G}) = v_s(\vec{G}) \cos \vec{G}\cdot\vec{\tau} + i v_a(\vec{G}) \sin \vec{G}\cdot\vec{\tau} \qquad (B.3)$$

where $\vec{\tau} = a(\frac{1}{8},\frac{1}{8},\frac{1}{8})$, v_s and v_a are the symmetric and antisymmetric parts of the potential under interchange of the two atoms. $v_a(\vec{G})=0$ for the group IV semiconductors.

The actual construction and diagonalization of the Hamiltonian is done by the subroutine EVAL. This routine is entered with the $\vec{k}$ vector of the desired Bloch states. EVAL calculates the

kinetic energy of the basis states $|\vec{k}+\vec{G}\rangle$ and calls the SORT routine which sorts the states in order of increasing energy. The basis states are then partitioned into the two sets required by the Löwdin procedure. The first set includes those states with $|k+G|^2 \leq E_1$ and the second includes those with $E_1 < |k+G|^2 \leq E_2$. EVAL then constructs the parts of the Hamiltonian required by the Löwdin procedure, and calls LOWDIN3, which performs that procedure, as modified by Brust [1964]. The higher-energy states are "folded down" as

$$H_{mn} \longleftarrow H_{mn} + \sum_j \frac{H_{mj}H_{jn}}{\bar{E}-H_{jj}} \qquad (B.4)$$

where m and n are states from the first set, j is a state from the second set, and $\bar{E}$ is either the average energy of the first eight states, for $m \neq n$, or H_{mn} for $n=m$. EVAL then calls library matrix diagonalization routines.

If the eigenvectors are required, EVAL calls a set of routines which perform that calculation. It then restores the folded-down components by

$$a_j = \sum_n \frac{H_{jn}}{\bar{E}-H_{jj}} a_n. \qquad (B.5)$$

The components must finally be rearranged so as to conform to the original numbering of the states as given in TABLE.

The calculation of the valence charge distribution is supervised by the subroutine VALCHG. It sets up the $\vec{k}$ vectors required

for the Chadi-Cohen [1973a] three-point Brillouin zone sample and then calls EVAL to calculate the eigenvectors. The subroutine ABSPSI2 calculates the absolute square of the Bloch function by

$$|\psi(\vec{x})|^2 = \sum_{\vec{G},\vec{G}'} a^*_{G'} a_G e^{i(\vec{G}-\vec{G}')\cdot\vec{x}} \qquad (B.6)$$

and then adds this to the charge density array in common block CHGDEN, with the appropriate multiplicative factor. After all of the wavefunctions have been calculated and squared, VALCHG calls SYMETRZ to symmetrize the charge density with respect to the point group operations. Since we have chosen the origin of our coordinate system at a point which does not exhibit the full point symmetry of the crystal, we must first translate the origin to one of the atomic sites. This is done by multiplying the Fourier coefficients of the charge density by a phase factor. The subroutine then runs through the 24-point group operations, which are represented as 3×3 matricies R, operating on each $\vec{G}$ and adding the $\vec{G}$ coefficient of the charge density to the $R\vec{G}$ coefficient of the symmetrized charge density array. The coordinate system must be finally translated back to the midpoint of the bond, again by multiplication by phase factors. If desired, the Fourier series for the charge density can be summed, and the results plotted out along the body diagonal, by the subroutine FSPLT.

AD-A032 078 COLORADO UNIV BOULDER F/G 20/12
A MODEL FOR THE PREDICTION OF SEMICONDUCTOR HETEROJUNCTION DISC--ETC(U)
SEP 76 W R FRENSLEY DAHC04-74-G-0114
UNCLASSIFIED ARO-12061.4-EL NL

2 OF 2
ADA032078



END

DATE
FILMED
1 -77

The Slater approximation for the exchange interaction is evaluated from the charge density by SLATER3. The quadratic approximation (II.9) for the cube root is used. The square of the charge density is calculated by CONVOL, which performs the discrete convolution needed to find the product of two Fourier series, given by

$$\sum_{\vec{G}} (ab)_{\vec{G}} e^{i\vec{G}\cdot\vec{x}} = \sum_{\vec{G},\vec{G}'} a_{\vec{G}} b_{\vec{G}'} e^{i(\vec{G}+\vec{G}')\cdot\vec{x}} . \qquad (B.7)$$

There are three subroutines which supervise the execution of the major tasks the program is intended to perform. ITERATE performs the self-consistency iterations. Using the current valence charge distribution, ITERATE calls MODELV to calculate the pseudopotential. It next calls VALCHG to perform the eigenvector and charge density calculations. The resulting charge density is taken in linear combination with the previous density, in order to provide a means for controlling oscillatory convergence of the band structure. Finally the average root-mean-square change in the electrostatic potential is calculated and printed out. The subroutine PRINGAP is used to calculate the principal gaps at the points Γ, L, and X. It calls EVAL to calculate the appropriate eigenvalues, assigns symmetry labels to the levels at Γ on the basis of the degeneracies, and prints out the resulting gaps. BZSAMPL does a more complete sampling of the Brillouin zone, calculating the bands

along the Λ, Δ, and Σ directions. It calls the subroutine BANDPLT, which is a straightforward printer plotting routine, to plot the results.

The main program BANDST performs none of the actual calculations. It handles the disk operations, modifies the parameter set in response to input data, decodes input instructions, and calls the subroutines to perform the calculations. It uses a number of features peculiar to CDC systems and the University of Colorado computing facilities in particular, so it would certainly have to be extensively rewritten in order to run successfully elsewhere.

2. Electrostatic Potential Program

The electrostatic potential is calculated according to the scheme described in Chapter II. This involves subtracting a fictitious charge distribution from the valence charge and adding it to the ion cores. The subroutine FOURCF subtracts the fictitious distribution (II.8) from the valence charge and divides the Fourier coefficients by $\vec{G}^2$ to find the electrostatic potential. The Fourier series for this part of the potential may be summed either by FSPT, if the value at only one point is desired, or by FRSUM, if the values along a line through the crystal are desired.

The ionic contribution to the electrostatic potential is calculated by the subroutine CLUSTER. It constructs the lattice points of the face-centered cubic structure, calculates the

distances from the given point to the two atomic sites, and calls the appropriate atomic potential function, VATOMA, etc. with these distances. It then adds the resulting contributions onto the total potential.

3. Program Listings

These programs have been written for, and successfully run on, the CDC 6400 system at the University of Colorado, operating under KRONOS 2.1 and using the RUN Fortran compiler.

As listed in the following pages, the program CRYSPOT and its associated subroutines assume locations for the anion and cation within the unit cell which are reversed from those locations assumed by BANDST and its associated routines. The following changes will make the two programs consistent. Note that this affects only the interchange of information between the programs; each will run successfully as listed.

Subroutine FOURCF Line above statement no. 200 should be

```
AR(I) = -(C/GSQ)*(CI(I) - (RHOA-RHOB)*SINGTAU(I))
```

Subroutine CLUSTER

Statement no. 100 should be

```
100   R2 = R2 + (Y(I) - TAU(I) - X(I))**2
```

Statement no. 170 should be

```
170   R2 = R2 + (Y(I) + TAU(I) - X(I))**2
```

TABLE OF PROGRAM LISTINGS

Name of Routine	Page	Name of Routine	Page
BANDST	88	CONVOL	123
FCCLAT	95	FSPLT	124
FRMFCTR	97	TYMER	127
MODELV	98	SORT	127
ITERATE	100	CRYSPOT	128
BZSAMPL	102	FOURCF	130
PRINGAP	104	CLUSTER	131
VALCHG	106	ERFC	133
EVAL	108	VATOMA	134
POTNTL	113	VATOMB	134
LOWDIN3	114	VATOMC	134
BANDPLT	116	VATOMD	134
ABSPSI2	118	FSPT	135
SYMETRZ	120	FRSUM	136
SLATER3	122	PLOTR	137

```
      PROGRAM BANDST (INPUT,OUTPUT,PUNCH,TAPE1=INPUT,TAPE7)
C
C
C
      LOGICAL INFOBIT
C
C
      COMMON/INFO/INFOBIT(16),E1,E2,A
C
C        THE INFO COMMON BLOCK CONTAINS LOGICAL VARIABLES CONTROLLING
C        THE OPERATION OF THE PROGRAM AND THE OUTPUT
C        INFOBIT(1) PRINTS OUT TIMING INFORMATION
C        INFOBIT(2) PRINTS OUT MILLER INDEX TABLE
C        INFOBIT(3) PRINTS OUT EIGENVALUES
C        INFOBIT(4) PRINTS OUT CHARGE COMPONENTS
C        INFOBIT(5) PRINTS OUT CHARGE PLOT
C        INFOBIT(6) INDICATES THAT AN EPM PSEUDOPOTENTIAL IS TO BE USED
C        E1 IS THE LIMIT OF THE INNER LOWDIN SET
C        E2 IS THE LIMIT OF THE OUTER LOWDIN SET
C        A IS THE LATTICE CONSTANT
C
C
      COMMON/LOCALV/VR(181),VI(181)
C
C        THE LOCALV COMMON BLOCK CONTAINS THE FOURIER COMPONENTS OF THE
C        LOCAL POTENTIAL.
C
C
      COMMON//VMNR(1600),VMNI(1600),VJMR(3200),VJMI(3200),VJJ(80)
C
C        THE BLANK COMMON BLOCK CONTAINS THE RELEVANT PARTS OF THE
C        UNPERTURBED HAMILTONIAN.  THE VMN CONTAIN THE SMALL SQUARE
C        MATRIX, THE VJM CONTAIN THE RECTANGULAR MATRIX, AND VJJ
C        CONTAINS THE DIAGONAL ELEMENTS OF THE LARGE SQUARE MATRIX.
C
C
      COMMON/HAMLT/HR(1600),HI(1600)
C
C        THE HAMLT COMMON BLOCK CONTAINS THE REAL AND IMAGINARY PARTS OF
C        THE PERTURBED HAMILTONIAN.
C
C
      COMMON/TABLE/ITAB(3,181),NTAB(11,11,11)
C
C        THE TABLE COMMON BLOCK CONTAINS THE INFORMATION REQUIRED TO
C        CONVERT FROM MILLER INDICIES TO A SINGLE SUBSCRIPT AND
C        VICE VERSA.
C
C
      COMMON/HEADING/NAME(8),IDATA(8)
C
C        THE HEADING COMMON BLOCK CONTAINS CHARACTERS USED IN OUTPUT
C        HEADINGS.
C
C
      COMMON/PTGROUP/GMN(3,3,24)
```

```
C
C       THE PTGROUP COMMON BLOCK CONTAINS THE 3X3 MATRICIES OF THE
C       OPERATIONS OF THE POINT SYMMETRY GROUP.
C
C
      COMMON/SFACTR/COSGTAU(181),SINGTAU(181)
C
C       THE SFACTR COMMON BLOCK CONTAINS THE STRUCTURE FACTORS
C       COS(G*TAU) AND SIN(G*TAU) FOR THE ZINC-BLENDE STRUCTURE.
C
C
      COMMON/BANDS/EK(8,40)
C
C       THE BANDS COMMON BLOCK CONTAINS THE ENERGIES (IN EV) AT EACH K.
C
C
      COMMON/CHGDEN/CR(181),CI(181)
C
C       THE CHGDEN COMMON BLOCK CONTAINS THE FOURIER COEFFICIENTS OF
C       THE VALENCE ELECTRON CHARGE DISTRIBUTION.
C
C
      COMMON/INCLUDE/INC(181)
C
C       THE INCLUDE COMMON BLOCK CONTAINS INFORMATION (COMPLEMENTED)
C       AS TO WHICH PLANE WAVES WERE INCLUDED IN THE EIGENVECTOR
C       CALCULATION.
C
C
      COMMON/PARAMTR/ZA,QA,ALPHAA,BETAA,GAMMAA,VOA,ZB,QB,ALPHAB,BETAB,
     1GAMMAB,VOB,XALPHA,RELAX
      COMMON/PRMTR2/ZC,QC,ALPHAC,BETAC,GAMMAC,VOC,ZD,QD,ALPHAD,BETAD,
     1GAMMAD,VOD,X1,Y1
C
C       THE PARAMTR COMMON BLOCK CONTAINS THE PARAMETERS OF THE MODEL
C       POTENTIAL.
C
C
      COMMON/EPMFF/NFF,IG2(10),VS(10),VA(10)
C
C       THE EPMFF COMMON BLOCK CONTAINS THE PSEUDOPOTENTIAL FORM
C       FACTORS FOR USE IN EPM CALCULATIONS.
C
C
C
      DIMENSION IMAGE(80),INSTRCT(10),ITEMP(2)
      DIMENSION PRMTR(14)
      DIMENSION PRMT2(14)
C
      EQUIVALENCE (PRMTR(1),ZA)
      EQUIVALENCE (PRMT2(1),ZC)
C
C
C
C
C
```

```
      CALL GET (5HTAPE7,7HPTGROUP,0,0)
      READ (7,50) (GMN(I),I=1,216)
   50 FORMAT (9F5.0)
      REWIND 7
C
C
      CALL GET (5HTAPE7,7HPARAMTR,0,0)
      READ (7,60) (PRMTR(I),I=1,14),E1,E2,A
      READ (7,61) (NAME(I),I=1,8),(IDATA(I),I=1,8)
      READ (7,60) (PRMT2(I),I=1,14)
   60 FORMAT (F12.4)
   61 FORMAT (8A10)
      REWIND 7
C
C
C        READ AND ENCODE COMMANDS
C
      READ 100,(IMAGE(I),I=1,80)
  100 FORMAT (80R1)
C
      IPOINT=0
C
      DO 120 J=1,10
C
      I1=IPOINT+1
C
C
      DO 110 I=1,11
C
      IPOINT=IPOINT+1
C
      IF (IMAGE(IPOINT).EQ.1R,) GO TO 115
      IF (IMAGE(IPOINT).EQ.1R.) GO TO 125
C
  110 CONTINUE
C
  115 NCHAR=IPOINT-I1
      IEND=IPOINT-1
      ENCODE (NCHAR,118,INSTRCT(J)) (IMAGE(IA),IA=I1,IEND)
  118 FORMAT (10R1)
C
C
  120 CONTINUE
C
  125 NCHAR=IPOINT-I1
      IEND=IPOINT-1
      ENCODE (NCHAR,118,INSTRCT(J)) (IMAGE(IA),IA=I1,IEND)
      J=J+1
      INSTRCT(J)=10HHALT
C
C
C        READ AND ENCODE OUTPUT INSTRUCTIONS
C
      READ 100,(IMAGE(I),I=1,80)
C
      DO 130 I=1,16
```

```
  130 INFOBIT(I)=.F.
C
      I1=1
C
      DO 140 I=1,80
C
      IF ((IMAGE(I).NE.1R,).AND.(IMAGE(I).NE.1R.)) GO TO 140
C
      NCHAR=I-I1
      IEND=I-1
      ENCODE (NCHAR,118,IWORD) (IMAGE(IA),IA=I1,IEND)
      I1=I+1
C
      IF (IWORD.EQ.10HTIMING    ) INFOBIT(1)=.T.
      IF (IWORD.EQ.10HTABLE     ) INFOBIT(2)=.T.
      IF (IWORD.EQ.10HENERGIES  ) INFOBIT(3)=.T.
      IF (IWORD.EQ.10HCHARGECOEF) INFOBIT(4)=.T.
      IF (IWORD.EQ.10HCHARGEPLOT) INFOBIT(5)=.T.
C
      IF (IMAGE(I).EQ.1R.) GO TO 145
C
  140 CONTINUE
C
C
C
C        READ HEADING,DATA,AND FORM FACTORS.
C
  145 READ 150,IWORD
C
  150 FORMAT (8A10)
C
      IF (EOF,1) 170,155
C
  155 IF (IWORD.EQ.10HHEADING   ) READ 150,(NAME(I),I=1,8)
      IF (IWORD.EQ.10HDATA      ) READ 150,(IDATA(I),I=1,8)
C
      IF (IWORD.NE.10HFORM FACTO) GO TO 165
C
      READ 160,NFF
      READ 160,(IG2(I),VS(I),VA(I),I=1,NFF)
  160 FORMAT (I5,2F10.4)
C
  165 GO TO 145
C
C
C        READ MODEL PARAMETERS
C
  170 READ 100,(IMAGE(I),I=1,80)
C
      IF (EOF,1) 200,175
C
  175 DO 180 IA=1,11
C
      IF (IMAGE(IA).EQ.1R=) GO TO 185
C
  180 CONTINUE
```

```
C
C
  185 NCHAR=IA-1
C
      ENCODE (NCHAR,118,IWORD) (IMAGE(I),I=1,NCHAR)
C
      IST=IA+1
      IEND=IST+19
C
      ENCODE (20,118,ITEMP) (IMAGE(I),I=IST,IEND)
      DECODE (20,190,ITEMP) X
  190 FORMAT (F20.6)
C
C
C        TEST NAMES AND REPLACE DATA
C
      IF (IWORD.EQ.10HZA          ) ZA=X
      IF (IWORD.EQ.10HZB          ) ZB=X
      IF (IWORD.EQ.10HQA          ) QA=X
      IF (IWORD.EQ.10HQB          ) QB=X
      IF (IWORD.EQ.10HALPHAA      ) ALPHAA=X
      IF (IWORD.EQ.10HALPHAB      ) ALPHAB=X
      IF (IWORD.EQ.10HBETAA       ) BETAA=X
      IF (IWORD.EQ.10HBETAB       ) BETAB=X
      IF (IWORD.EQ.10HGAMMAA      ) GAMMAA=X
      IF (IWORD.EQ.10HGAMMAB      ) GAMMAB=X
      IF (IWORD.EQ.10HVOA         ) VOA=X
      IF (IWORD.EQ.10HVOB         ) VOB=X
      IF (IWORD.EQ.10HA           ) A=X/.529177
      IF (IWORD.EQ.10HE1          ) E1=X
      IF (IWORD.EQ.10HE2          ) E2=X
      IF (IWORD.EQ.10HXALPHA      ) XALPHA=X
      IF (IWORD.EQ.10HRELAX       ) RELAX=X
      IF (IWORD.EQ.10HZC          ) ZC=X
      IF (IWORD.EQ.10HZD          ) ZD=X
      IF (IWORD.EQ.10HQC          ) QC=X
      IF (IWORD.EQ.10HQD          ) QD=X
      IF (IWORD.EQ.10HALPHAC      ) ALPHAC=X
      IF (IWORD.EQ.10HALPHAD        ) ALPHAD=X
      IF (IWORD.EQ.10HBETAC       ) BETAC=X
      IF (IWORD.EQ.10HBETAD        ) BETAD=X
      IF (IWORD.EQ.10HGAMMAC      ) GAMMAC=X
      IF (IWORD.EQ.10HGAMMAD      ) GAMMAD=X
      IF (IWORD.EQ.10HVOC         ) VOC=X
      IF (IWORD.EQ.10HVOD         ) VOD=X
      IF (IWORD.EQ.10HX           ) X1=X
      IF (IWORD.EQ.10HY           ) Y1=X
C
      GO TO 170
C
C
C
C        PRINT HEADING
C
  200 CALL DATE (I1)
      CALL TYME (I2)
```

```
      PRINT 205,I1,I2
      PRINT 210,(NAME(I),I=1,8)
  205 FORMAT (* RUN DATE *,A10,10X,*TIME *,A10,/)
  210 FORMAT (* BAND STRUCTURE FOR *,8A10,//)
C
C
C        PRINT POTENTIAL PARAMETERS
C
      PRINT 215,E1,E2
      PRINT 220,XALPHA,RELAX
C
      A1=.529177*A
C
      PRINT 225,A1
      PRINT 230
      PRINT 235,ZA,ZB,ZC,ZD
      PRINT 236,QA,QB,QC,QD
      PRINT 237,ALPHAA,ALPHAB,ALPHAC,ALPHAD
      PRINT 238,BETAA,BETAB,BETAC,BETAD
      PRINT 239,GAMMAA,GAMMAB,GAMMAC,GAMMAD
      PRINT 240,VOA,VOB,VOC,VOD
      PRINT 245,X1,Y1
C
  215 FORMAT (* CALCULATIONAL PARAMETERS*,/,* E1=*,F3.0,11X,*E2=*,F3.0)
  220 FORMAT (* XALPHA=*,F4.2,5X,*RELAXATION FACTOR=*,F4.2)
  225 FORMAT (//,* POTENTIAL PARAMETERS*,//,* LATTICE CONSTANT=*,F6.3,/)
  230 FORMAT (14X,*ATOM A*,9X,*ATOM B*,9X,*ATOM C*,9X,*ATOM D*,/)
  235 FORMAT (9X,*Z*,4(F10.0,5X))
  236 FORMAT (9X,*Q*,4(F10.0,5X))
  237 FORMAT (5X,*ALPHA*,4(F10.2,5X))
  238 FORMAT (6X,*BETA*,4(F10.2,5X))
  239 FORMAT (5X,*GAMMA*,4(F10.2,5X))
  240 FORMAT (8X,*VO*,4(F10.2,5X))
  245 FORMAT (//,8X,*X=*,F4.2,6X,*Y=*,F4.2,///)
C
C
C
      WRITE (7,60) (PRMTR(I),I=1,14),E1,E2,A
      WRITE (7,61) (NAME(I),I=1,8),(IDATA(I),I=1,8)
      WRITE (7,60) (PRMT2(I),I=1,14)
      CALL REPLACE (5HTAPE7,7HPARAMTR,0,0)
      REWIND 7
C
C
      CALL GET (5HTAPE7,7HCHGDATA,0,0)
      READ (7,295) (CR(I),CI(I),I=1,181)
  295 FORMAT (2F10.5)
      REWIND 7
C
C
C        EXECUTE THE TASKS SPECIFIED IN INSTRCT
C
  300 CALL FCCLAT
C
C
      DO 450 INST=1,10
```

```
C
C        IMPLEMENT THE INITIALIZE INSTRUCTION
C
      IF (INSTRCT(INST).NE.10HINITIALIZE) GO TO 350
C
      CALL FRMFCTR
      CALL VALCHG
C
C       IMPLEMENT THE EPM INSTRUCTION
C
  350 IF (INSTRCT(INST).EQ.10HEPM       ) INFOBIT(6)=.T.
C
C        IMPLEMENT THE GAPS INSTRUCTION
C
      IF (INSTRCT(INST).NE.10HGAPS      ) GO TO 370
C
      IF (INFOBIT(6)) CALL FRMFCTR
      IF (.NOT.INFOBIT(6)) CALL MODELV (CR,CI)
      CALL PRINGAP
C
C        IMPLEMENT THE FULL ZONE INSTRUCTION
C
  370 IF (INSTRCT(INST).NE.10HFULL ZONE ) GO TO 390
C
      IF (INFOBIT(6)) CALL FRMFCTR
      IF (.NOT.INFOBIT(6)) CALL MODELV (CR,CI)
      CALL BZSAMPL
C
C        IMPLEMENT THE ITERATE N INSTRUCTION
C
  390 I1=INSTRCT(INST).AND.07777777777777000000
      IF (I1.NE.7LITERATE) GO TO 420
C
      I2=(INSTRCT(INST).AND.0777777).OR.7L
      DECODE (9,400,I2)N1
  400 FORMAT (7X,I2)
      CALL ITERATE (N1,RELAX)
C
C        IMPLEMENT THE HALT INSTRUCTION
C
  420 IF (INSTRCT(INST).EQ.10HHALT      ) GO TO 500
C
  450 CONTINUE
C
  500 CONTINUE
C
C
C        STORE CHARGE DENSITY ON DISK
C
      WRITE (7,295) (CR(I),CI(I),I=1,181)
      CALL REPLACE (5HTAPE7,7HCHGDATA,0,0)
C
C
C
      END
```

```
      SUBROUTINE RECLAT
C
C
C
C        THIS SUBROUTINE SETS UP THE TABLE OF RECIPROCAL LATTICE VECTORS
C        FOR THE FCC STRUCTURE AND CALCULATES THE STRUCTURE FACTORS.
C
C
      COMMON/TABLE/ITAB(3,181),NTAB(11,11,11)
      COMMON/SFACTR/COSGTAU(181),SINGTAU(181)
      COMMON/INFO/INFOBIT(16)
C
C
      DIMENSION IGSQ(181)
C
      INTEGER GSQ
C
C
C     SET UP TABLE TO CONVERT MILLER INDICIES TO SINGLE SUBSCRIPT
C
C        MA=1 CALCULATES ODD MILLER INDICIES, MA=2 CALCULATES EVEN ONES
C
      N=1
      DO 210 MA=1,2
      MAX=5
      MIN=MA-MAX-1
C
C        THESE LOOPS CONSTRUCT THE G VECTORS
C
      DO 210 I=MIN,MAX,2
      DO 210 J=MIN,MAX,2
      DO 210 K=MIN,MAX,2
C
      GSQ=I*I+J*J+K*K
      IF (GSQ.GT.32) GO TO 210
C
C        THIS SORT ROUTINE ORDERS THE VECTORS IN INCREASING MAGNITUDE
C
      L=N-1
      IF(N.EQ.1) GO TO 206
  204 IF(L.LE.0) GO TO 206
      IF(IGSQ(L).LE.GSQ) GO TO 206
      IGSQ(L+1)=IGSQ(L)
      DO 205 IA=1,3
  205 ITAB(IA,L+1)=ITAB(IA,L)
      L=L-1
      GO TO 204
  206 IGSQ(L+1)=GSQ
      ITAB(1,L+1)=I
      ITAB(2,L+1)=J
      ITAB(3,L+1)=K
      N=N+1
  210 CONTINUE
C
C        SET UP TABLE OF N AS A FUNCTION OF MILLER INDICIES
C
```

```
      DO 212 N=1,181
      I=ITAB(1,N)
      J=ITAB(2,N)
      K=ITAB(3,N)
      NTAB(I+6,J+6,K+6)=N
  212 CONTINUE
C
C
C        PRINT OUT INDEX TABLE IF INFOBIT(2) IS TRUE.
C
      IF (.NOT.INFOBIT(2)) GO TO 280
C
      PRINT 250
      PRINT 255
      PRINT 260,(I,(ITAB(J,I),J=1,3),IGSQ(I),I=1,181)
C
  250 FORMAT (///,42X,*TABLE OF RECIPROCAL LATTICE VECTORS*C//)
  255 FORMAT (5(* INDX ( I J K) GSQ*,7X),/)
  260 FORMAT (5(I5,* (*,3I2,*) *,I3,7X))
C
C
C        SET UP STRUCTURE FACTOR TABLE.
C
C
  280 DO 300 I=1,181
C
      GTAU=0.785398*(ITAB(1,I)+ITAB(2,I)+ITAB(3,I))
C
      COSGTAU(I)=COS(GTAU)
      SINGTAU(I)=SIN(GTAU)
C
C
  300 CONTINUE
C
C
      RETURN
C
      END
```

```
      SUBROUTINE FRMFCTR
C
C        THIS SUBROUTINE CALCULATES THE FOURIER COMPONETS OF THE
C        PSEUDOPOTENTIAL FROM THE FORM FACTOR INFORMATION STORED IN E
C        EPMFF.
C
C
      COMMON/EPMFF/NFF,IG2(10),VS(10),VA(10)
      COMMON/SFACTR/COSGTAU(181),SINGTAU(181)
      COMMON/LOCALV/VR(181),VI(181)
      COMMON/TABLE/IT(3,181),NT(11,11,11)
C
C
      DO 100 I=1,181
      VR(I)=0.
  100 VI(I)=0.
C
C
      DO 200 I=2,181
C
      IGSQ=0
      DO 120 J=1,3
  120 IGSQ=IGSQ+IT(J,I)**2
C
      DO 150 J=1,NFF
C
      IF (IGSQ.NE.IG2(J)) GO TO 150
C
      VR(I)=COSGTAU(I)*VS(J)
      VI(I)=SINGTAU(I)*VA(J)
C
  150 CONTINUE
  200 CONTINUE
C
      RETURN
      END
```

```
      SUBROUTINE MODELV (CR,CI)
C
C        THIS SUBROUTINE CALCULATES THE POTENTIAL FROM THE MODEL
C        PARAMETERS.
C
C
      COMMON/TABLE/IT(3,181),NT(11,11,11)
      COMMON/LOCALV/VR(181),VI(181)
      COMMON/SFACTR/COSGTAU(181),SINGTAU(181)
      COMMON/INFO/DUMMY(18),A
      COMMON/PARAMTR/ZA,QA,ALPHAA,BETAA,GAMMAA,VOA,ZB,QB,ALPHAB,BETAB,
     1GAMMAB,VOB,XALPHA,RELAX
      COMMON/PRMTR2/ZC,QC,ALPHAC,BETAC,GAMMAC,VOC,ZD,QD,ALPHAD,BETAD,
     1GAMMAD,VOD,X1,Y1
C
      DIMENSION CR(181),CI(181)
C
      REAL KSQ
C
C
C
      CALL SLATER3 (XALPHA,CR,CI,VR,VI)
C
C
      C=39.4784/(A**2)
      VOL=(A**3)/4.
      C1=25.1327/VOL
C
      C2A=VOA/VOL
      C2B=VOB/VOL
      C2C=VOC/VOL
      C2D=VOD/VOL
C
      ALPHAA2=ALPHAA**2
      BETAA2=BETAA**2
      GAMMAA2=GAMMAA**2
C
      ALPHAB2=ALPHAB**2
      BETAB2=BETAB**2
      GAMMAB2=GAMMAB**2
C
      ALPHAC2=ALPHAC**2
      BETAC2=BETAC**2
      GAMMAC2=GAMMAC**2
C
      ALPHAD2=ALPHAD**2
      BETAD2=BETAD**2
      GAMMAD2=GAMMAD**2
C
C
C        CALCULATE THE G=0 COMPONENT
C
      VC=0.
      VD=0.
      VA=C1*(-(ZA-QA)/(2.*BETAA2)-QA/ALPHAA2+(ZA**2)/(QA*ALPHAA2))+C2A
      VB=C1*(-(ZB-QB)/(2.*BETAB2)-QB/ALPHAB2+(ZB**2)/(QB*ALPHAB2))+C2B
```

```
C
      IF (X1) 100,110,100
  100 VC=C1*(-(ZC-QC)/(2.*BETAC2)-QC/ALPHAC2+(ZC**2)/(QC*ALPHAC2))+C2C
C
  110 IF (Y1) 120,130,120
  120 VD=C1*(-(ZD-QD)/(2.*BETAD2)-QD/ALPHAD2+(ZD**2)/(QD*ALPHAD2))+C2D
C
  130 VR(1)=(1.-X1)*VA+(1.-Y1)*VB+X1*VC+Y1*VD+VR(1)
      VI(1)=0.
C
C
C        CALCULATE OTHER COMPONENTS
C
      IGSQ1=0
C
      DO 350 I=2,181
C
      IGSQ=IT(1,I)**2+IT(2,I)**2+IT(3,I)**2
      IF (IGSQ.EQ.IGSQ1) GO TO 300
      IGSQ1=IGSQ
      KSQ=C*IGSQ
C
      VC=0.
      VD=0.
      VA=C1*(ZA/(KSQ+(QA*ALPHAA2)/ZA)-(ZA-QA)/KSQ-QA/(KSQ+ALPHAA2))
      VA=VA+C2A*EXP(-KSQ/(2.*GAMMAA2))
C
      VB=C1*(ZB/(KSQ+(QB*ALPHAB2)/ZB)-(ZB-QB)/KSQ-QB/(KSQ+ALPHAB2))
      VB=VB+C2B*EXP(-KSQ/(2.*GAMMAB2))
C
      IF (X1) 150,160,150
  150 VC=C1*(ZC/(KSQ+(QC*ALPHAC2)/ZC)-(ZC-QC)/KSQ-QC/(KSQ+ALPHAC2))
      VC=VC+C2C*EXP(-KSQ/(2.*GAMMAC2))
C
  160 IF (Y1) 170,300,170
  170 VD=C1*(ZD/(KSQ+(QD*ALPHAD2)/ZD)-(ZD-QD)/KSQ-QD/(KSQ+ALPHAD2))
      VD=VD+C2D*EXP(-KSQ/(2.*GAMMAD2))
C
C
  300 CONTINUE
C
      VCATION=(1.-X1)*VA+X1*VC
      VANION=(1.-Y1)*VB+Y1*VD
C
      VR(I)=(VCATION+VANION)*COSGTAU(I)+C1*CR(I)/KSQ+VR(I)
      VI(I)=(VCATION-VANION)*SINGTAU(I)+C1*CI(I)/KSQ+VI(I)
C
C
  350 CONTINUE
C
C
      RETURN
      END
```

```
      SUBROUTINE ITERATE (N,X)
C
C
C        THIS SUBROUTINE PERFORMS N ITERATIONS OF THE BAND STRUCTURE-
C        CHARGE DENSITY CALCULATION.
C        X IS A RELAXATION FACTOR TO IMPROVE CONVERGENCE.
C
C
      COMMON/CHGDEN/CR(181),CI(181)
      COMMON/INFO/DUMMY(18),A
      COMMON/TABLE/IT(3,181),NT(11,11,11)
C
      DIMENSION CRIN(181),CIIN(181)
C
C
C
      C=25.1327*4./A**3
C
C
      DO 500 ITERAT=1,N
C
C
      DO 100 I=1,181
      CRIN(I)=CR(I)
  100 CIIN(I)=CI(I)
C
C
      CALL MODELV (CR,CI)
C
      CALL VALCHG
C
C        AVERAGE OVER THE LAST ITERATION WITH RELAXATION FACTOR.
C
      Y=1.-X
C
      DO 150 I=1,181
      CR(I)=X*CR(I)+Y*CRIN(I)
  150 CI(I)=X*CI(I)+Y*CIIN(I)
C
C        GENERATE CONSISTENCY DATA.
C
      DELVSQ=0.
C
      DO 175 I=2,181
C
      GSQ=0.
      DO 170 J=1,3
  170 GSQ=GSQ+IT(J,I)**2
C
      DELTAVR=(CR(I)-CRIN(I))/GSQ
      DELTAVI=(CI(I)-CIIN(I))/GSQ
C
      DELVSQ=DELVSQ+DELTAVR**2+DELTAVI**2
C
  175 CONTINUE
C
```

```
      DELV=C*SQRT(DELVSQ)
C
      PRINT 200,DELV
  200 FORMAT (/,* AVERAGE RMS CHANGE IN POTENTIAL=*,F6.3,* RYDBERGS*)
C
C
  500 CONTINUE
C
      RETURN
      END
```

```
      SUBROUTINE BZSAMPL
C        THIS SUBROUTINE SETS UP A STANDARD SET OF K VECTORS AND CALLS
C        EVAL TO FIND THE ENERGIES.
C
      DIMENSION AK(3)
      COMMON/BANDS/EK(8,40)
      COMMON/INFO/ INFOBIT(16),AMAG1,AMAG2
C
C        GAMMA POINT
C
      AK(1)=0.
      AK(2)=0.
      AK(3)=0.
      CALL EVAL (11,AK,.F.)
      DO 20 I=1,8
   20 EK(I,31)=EK(I,11)
C
C        GAMMA TO L
C
      DO 30 I=1,10
      N=11-I
      AK(1)=I*.05
      AK(2)=I*.05
      AK(3)=I*.05
      CALL EVAL (N,AK,.F.)
   30 CONTINUE
C
C        GAMMA TO X
C
      AK(1)=0.
      AK(2)=0.
      DO 40 I=1,10
      N=I+11
      AK(3)=.1*I
      CALL EVAL (N,AK,.F.)
   40 CONTINUE
C
C        X TO K
C
      AK(1)=1.
      AK(2)=.125
      AK(3)=.125
      CALL EVAL (22,AK,.F.)
C
C        K TO GAMMA
C
      AK(3)=0.
      DO 50 I=1,8
      N=31-I
      AK(1)=.09375*I
      AK(2)=.09375*I
      CALL EVAL (N,AK,.F.)
   50 CONTINUE
C
C
C
```

```
      RANGE=20.
      AZERO=5.*AINT(EK(3,11)/5.)-10.
C
      CALL BANDPLT (AZERO,RANGE)
C
C
      RETURN
C
      END
```

```
      SUBROUTINE PRINGAP
C
C
C        THIS SUBROUTINE CALCULATES THE PRINCIPAL BAND GAPS AT GAMMA,
C        L AND X.
C
C
      DIMENSION AK(3)
      DIMENSION GAP(8)
      COMMON/BANDS/E(8,40)
      COMMON/HEADING/NAME(8),IDATA(8)
      REAL L3V,L1C,L3C
C
C
      DO 20 I=1,3
   20 AK(I)=0.
C
      CALL EVAL (11,AK,.F.)
C
      AK(3)=1.
C
      CALL EVAL (21,AK,.F.)
C
      DO 30 I=1,3
   30 AK(I)=.5
C
      CALL EVAL (1,AK,.F.)
C
C
      ENTRY GAPS
C
C
C        SORT OUT GAMMA LEVELS
C
      G15V=E(3,11)
      G1C=E(5,11)
      G15C=E(6,11)
C
      IF(ABS(E(2,11)-G15V).LE.0.01) GO TO 100
C
      G1C=E(2,11)
      PRINT 80
   80 FORMAT (* METAL BAND STRUCTURE*)
C
  100 IF (ABS(G1C-G15C).LE.0.01) G1C=E(8,11)
C
C        L AND X LEVELS
C
      L3V=E(4,1)
      L1C=E(5,1)
      L3C=E(6,1)
C
      X4V=E(4,21)
      X1C=E(5,21)
      X3C=E(6,21)
C
```

```
C        CALCULATE GAPS
C
      GAP(1)=G1C-G15V
      GAP(2)=G15C-G15V
      GAP(3)=L1C-G15V
      GAP(4)=X1C-G15V
      GAP(5)=L1C-L3V
      GAP(6)=L3C-L3V
      GAP(7)=X1C-X4V
      GAP(8)=X3C-X1C
C
C
      PRINT 200
      PRINT 210,(GAP(I),I=1,8)
      PRINT 220,(IDATA(I),I=1,8)
C
  200 FORMAT (//,12X,*G1C-G15V G15C-G15V  L1C-G15V  X1C-G15V   L1C-L3V
     1 L3C-L3V   X1C-X4V   X3C-X1C*,/)
C
  210 FORMAT (* RESULTS  *,8F10.2)
  220 FORMAT (/,* DATA     *,8A10)
C
C
      RETURN
      END
```

```
      SUBROUTINE VALCHG
C
C
C        THIS SUBROUTINE EVALUATES THE VALENCE CHARGE DISTRIBUTION USING
C        THE CHADI-COHEN 3 POINT BRILLOUIN ZONE SAMPLE.
C
C
C
      COMMON/CHGDEN/CR(181),CI(181)
      COMMON/INFO/INFOBIT(16)
      COMMON/TABLE/IT(3,181),NT(11,11,11)
      LOGICAL INFOBIT
C
      DIMENSION AK(3)
C
C
      DO 100 I=1,181
      CR(I)=0.
  100 CI(I)=0.
C
C
      AK(1)=.5
      AK(2)=0.
      AK(3)=0.
C
      CALL EVAL (33,AK,.T.)
C
      CALL ABSPSI2 (.25)
C
C
      AK(2)=.5
C
      CALL EVAL(34,AK,.T.)
C
      CALL ABSPSI2 (.5)
C
C
      AK(1)=1.
C
      CALL EVAL (35,AK,.T.)
C
      CALL ABSPSI2 (.25)
C
C
      CALL SYMETRZ
C
C
C        PRINT CHARGE COEFFICIENTS IF INFOBIT(4) IS TRUE
C
      IF (.NOT.INFOBIT(4)) GO TO 300
C
      PRINT 200
      PRINT 205
      PRINT 210,(I,(IT(J,I),J=1,3),CR(I),CI(I),I=1,181)
C
  200 FORMAT (///,20X,*FOURIER COMPONENTS OF THE VALENCE CHARGE DENSITY*
```

```
     1,//)
  205 FORMAT (4(*  NO ( I J K)*,7X,*CR*,6X,*CI*,4X),/)
  210 FORMAT (4(I4,* (*C3I2,*) *,2F8.4,4X))
C
  300 CONTINUE
C
C        PLOT CHARGE DENSITY IF INFOBIT(5) IS TRUE
C
      IF (INFOBIT(5)) CALL FSPLT(0.,40.)
C
C
      RETURN
      END
```

```
      SUBROUTINE EVAL (NO,AK,CONTROL)
C
C        THIS SUBROUTINE EVALUATES THE BAND ENERGIES FOR A GIVEN K USING
C        THE POTENTIAL PART OF THE HAMILTONIAN CALCULATED PREVIOUSLY AND
C        STORED IN POTNTL.
C
C        N IS THE INDEX UNDER WHICH THE RESULTS ARE STORED IN 'BANDS'
C        AK IS THE K VECTOR AT WHICH THE ENERGIES ARE EVALUATED.
C        A IS THE LATTICE CONSTANT.
C
C
      LOGICAL CONTROL
      LOGICAL INFOBIT
      LOGICAL INC
C
      DIMENSION AK(3)
      DIMENSION T(181),AKSQ(181),INDX(181)
      DIMENSION D(40),E1(40),E2(40),TAU(2,40)
      DIMENSION ZR(1600),ZI(1600)
      DIMENSION AR(181,8),AI(181,8),BR(181,8),BI(181,8)
C
      COMMON/INFO/INFOBIT(16),AMAG1,AMAG2,A
      COMMON/BANDS/EK(8,40)
      COMMON/LOCALV/VR(181),VI(181)
      COMMON/TABLE/ITAB(3,181),NTAB(11,11,11)
      COMMON/HAMLT/HR(1600),HI(1600)
      COMMON//VMNR(1600),VMNI(1600),VJMR(3200),VJMI(3200),VJJ(80)
      COMMON/INCLUDE/INC(181)
C
      EQUIVALENCE (VMNR,AR),(VMNI,AI),(HR,BR),(HI,BI)
      EQUIVALENCE (VMNR,ZR),(VMNI,ZI)
      EQUIVALENCE (T,AKSQ)
C
C
C
      DO 20 I=1,181
      AKSQ(I)=0.
      INDX(I)=I
      DO 20 J=1,3
   20 AKSQ(I)=AKSQ(I)+(AK(J)+ITAB(J,I))**2
C
C
      CALL SORT (181,AKSQ,INDX)
C
      CONST=(6.2832/A)**2
      DO 25 I=1,181
      IF(AKSQ(I).LE.AMAG1) N1=I
      IF(AKSQ(I).LE.AMAG2) MAX=I
   25 T(I)=CONST*AKSQ(I)
C
      N2=MAX-N1
C
      IF (N1.LE.40) GO TO 35
C
      PRINT 30,NO
   30 FORMAT (* INNERSET OVERRANGE ON *,I5)
```

```
      N1=40
      N2=MAX-N1
C
   35 IF (N2.LE.3200/N1) GO TO 40
C
      PRINT 37,NO
   37 FORMAT (* OUTER SET OVERRANGE ON *,I5)
      N2=3200/N1
C
   40 CONTINUE
C
C
      IF(INFOBIT(1)) CALL INTYME
C
C
C        SET UP HAMILTONIAN FOR LOWDIN3
C
C
C        SMALL SQUARE MATRIX
C
      DO 60 N=1,N1
      DO 60 M=1,N
      NM=N1*(M-1)+N
      MN=N1*(N-1)+M
      CALL POTNTL(INDX(M),INDX(N),VMNR(MN),VMNI(MN))
      VMNR(NM)=VMNR(MN)
      VMNI(NM)=-VMNI(MN)
   60 CONTINUE
C
C        ADD KINETIC ENERGY TO DIAGONAL ELEMENTS
C
      DO 65 N=1,N1
      NN=N1*(N-1)+N
   65 VMNR(NN)=VMNR(NN)+T(N)
C
C        DIAGONAL ELEMENTS OF LARGE SQUARE MATRIX
C
      DO 70 J=1,N2
   70 VJJ(J)=VR(1)+T(N1+J)
C
C        RECTANGULAR MATRIX
C
      DO 80 J=1,N2
      DO 80 M=1,N1
      I1=INDX(J+N1)
      I2=INDX(M)
      JM=N2*(M-1)+J
      CALL POTNTL(I1,I2,VJMR(JM),VJMI(JM))
   80 CONTINUE
C
C        EBAR IS THE AVERAGE OF THE FIRST 8 ENERGY LEVELS OF THE EMPTY
C        LATTICE.
C
      EBAR=0.
      DO 85 J=1,8
   85 EBAR=EBAR+VMNR(N1*J-N1+J)/8.
```

```
C
      IF(INFOBIT(1)) CALL TYMER(5HSETUP)
      CALL LOWDIN3(N1,N2,EBAR)
      IF(INFOBIT(1)) CALL TYMER(7HLOWDIN3)
C
C
C        CALL DIAGONALIZATION ROUTINES
C
      IF (CONTROL) GO TO 300
C
C
      CALL HTRIDI(N1,N1,HR,HI,D,E1,E2,TAU)
      IF (INFOBIT(1)) CALL TYMER (6HHTRIDI)
C
      CALL IMTQL1(N1,D,E1,IERR)
      IF (INFOBIT(1)) CALL TYMER (6HIMTQL1)
C
C
C        IF ERROR CODE INDICATES EIGENVALUE DID NOT CONVERGE, PRINT OUT
C        MESSAGE AND TERMINATE EXECUTION.
C
      IF (IERR.NE.0) GO TO 900
C
C
C        CONVERT ENERGIES TO EV AND STORE IN OUTPUT ARRAY
C
  140 DO 150 I=1,8
  150 EK(I,NO)=13.605*D(I)
C
      IF (.NOT.INFOBIT(3)) GO TO 190
C
      PRINT 170,NO,(AK(J),J=1,3)
      PRINT 171,N1,N2
      PRINT 172,(EK(I,NO),I=1,8)
  170 FORMAT(//,* NO.*,I5,10X,*K= *,3F5.2)
  171 FORMAT(I5,* PLANE WAVES TREATED DIRECTLY,*,I5,* PLANE WAVES TREATE
     1D BY PERTURBATION*)
  172 FORMAT (/,* ENERGIES *,8F10.2)
  190 CONTINUE
C
      RETURN
C
C
C        EIGENVECTOR CALCULATION
C
C        INITIALIZE Z
C
  300 DO 305 I=1,1600
      ZR(I)=0.
  305 ZI(I)=0.
C
      DO 310 I=1,N1
  310 ZR(I+N1*I-N1)=1.
C
      IF (INFOBIT(1)) CALL INTYME
```

```
C
C        CALL DIAGONALIZATION ROUTINES
C
      CALL HTRIDI (N1,N1,HR,HI,D,E1,E2,TAU)
      IF (INFOBIT(1)) CALL TYMER (6HHTRIDI)
C
      CALL IMTQL2 (N1,N1,D,E1,ZR,IERR)
      IF (INFOBIT(1)) CALL TYMER (6HIMTQL2)
C
      CALL HTRIBK (N1,N1,HR,HI,TAU,4,ZR,ZI)
      IF (INFOBIT(1)) CALL TYMER (6HHTRIBK)
C
C
C        TRANSFORM AND OUTPUT EIGENVECTORS
C
C
      NBAND=4
      IF (INFOBIT(16)) NBAND=8
      NWAVE=181*NBAND
C
      DO 315 I=1,NWAVE
C
      BR(I)=0.
  315 BI(I)=0.
C
C
      MDISP=0
      NDISP=0
C
C
      DO 325 IBAND=1,NBAND
C
      DO 320 I=1,N1
C
C
      BR(I+MDISP)=ZR(I+NDISP)
  320 BI(I+MDISP)=ZI(I+NDISP)
C
      MDISP=MDISP+181
  325 NDISP=NDISP+N1
C
C
C        UNFOLD THE LOWDIN TRANSFORMATION.
C
      DO 350 J=1,N2
C
      DENOM=1./(EBAR-VJJ(J))
      MDISP=0
C
C
      DO 345 IBAND=1,NBAND
C
      CR=0.
      CI=0.
      JM=J
C
```

```
      DO 340 MDEX=1,N1
C
      M=MDISP+MDEX
C
      CR=CR+VJMR(JM)*BR(M)-VJMI(JM)*BI(M)
      CI=CI+VJMI(JM)*BR(M)+VJMR(JM)*BI(M)
C
  340 JM=JM+N2
C
C
      BR(J+N1+MDISP)=CR*DENOM
      BI(J+N1+MDISP)=CI*DENOM
C
  345 MDISP=MDISP+181
C
  350 CONTINUE
C
C
C        REARRANGE COMPONENTS.
C
C
      DO 380 I=1,181
C
      J=INDX(I)
C
      INC(J)=I.GT.MAX
      ID=I
C
C
      DO 380 IBAND=1,NBAND
C
      AR(J)=BR(ID)
      AI(J)=BI(ID)
C
      J=J+181
      ID=ID+181
C
  380 CONTINUE
C
C
      GO TO 140
C
  900 PRINT 910,NO
  910 FORMAT (//,* DIAGONALIZATION ROUTINE FAILED ON *,I5,* K VECTOR*)
  999 FORMAT (/////)
      END
```

```
      SUBROUTINE POTNTL(M,N,V1R,V1I)
C
C
C        THIS SUBROUTINE CALCULATES THE M,N ELEMENT OF THE POTENTIAL
C        MATRIX AND STORES THE RESULT IN V1.  NOTE THAT M,N HERE REFER
C        TO INDICIES AS ORIGINALLY DEFINED IN 'TABLE'.
C
C
      COMMON/LOCALV/VR(181),VI(181)
      COMMON/TABLE/I(3,181),NTAB(11,11,11)
C
C
C        INDEX MANIPULATIONS
C
      L1=I(1,M)-I(1,N)
      L2=I(2,M)-I(2,N)
      L3=I(3,M)-I(3,N)
C
      IF ((L1**2+L2**2+L3**2).GT.24) GO TO 20
C
C
   10 NA=NTAB(L1+6,L2+6,L3+6)
      V1R=VR(NA)
      V1I=VI(NA)
      GO TO 30
C
C
   20 V1R=0.
      V1I=0.
   30 CONTINUE
C
      RETURN
      END
```

```
      SUBROUTINE LOWDIN3 (N1,N2,EBAR)
C
C
C        N1 IS THE DIMENSION OF THE SMALL SQUARE MATRIX AND N2 IS THE
C        DIMENSION OF THE RECTANGULAR MATRIX.  N1 MUST BE LE 40 AND
C        N2 MUST BE LE 80.
C
C
      DIMENSION DENOM (80)
      COMMON//VMNR(1600),VMNI(1600),VJMR(3200),VJMI(3200),VJJ(80)
      COMMON/HAMLT/HR(1600),HI(1600)
C
C
C
      DO 25 J=1,N2
      DENOM(J)=EBAR-VJJ(J)
   25 CONTINUE
C
C
C        CALCULATE THE OFF DIAGONAL PERTURBATION TERMS
C
C        TRIANGULAR NESTED DO LOOPS
C
      DO 40 M=2,N1
      MAX=M-1
      INDXM=N2*MAX
      DO 40 N=1,MAX
      INDXN=N2*(N-1)
C
      PERTR=0.
      PERTI=0.
      DO 30 J=1,N2
      MJ=J+INDXM
      NJ=J+INDXN
      PERTR=PERTR+(VJMR(MJ)*VJMR(NJ)+VJMI(MJ)*VJMI(NJ))/DENOM(J)
      PERTI=PERTI+(VJMR(MJ)*VJMI(NJ)-VJMI(MJ)*VJMR(NJ))/DENOM(J)
   30 CONTINUE
C
C        ADD PERTURBATION TERM TO HAMILTONIAN
C
      MN=N1*(N-1)+M
      NM=N1*(M-1)+N
      HR(MN)=VMNR(MN)+PERTR
      HR(NM)=HR(MN)
      HI(MN)=VMNI(MN)+PERTI
      HI(NM)=-HI(MN)
   40 CONTINUE
C
C        CALCULATE THE DIAGONAL MATRIX ELEMENTS
C
      DO 60 N=1,N1
      E=VMNR(N1*(N-1)+N)
      PERT=0.
      DO 50 J=1,N2
      JN=N2*(N-1)+J
      PERT=PERT+(VJMR(JN)**2+VJMI(JN)**2)/(E-VJJ(J))
```

```
   50 CONTINUE
      NN=N1*N-N1+N
      HR(NN)=VMNR(NN)+PERT
      HI(NN)=0.
   60 CONTINUE
C
C
      RETURN
      END
```

```
      SUBROUTINE BANDPLT (AZERO,RANGE)
C
C        THIS SUBROUTINE GENERATES A PRINTER PLOT OF THE BAND STRUCTURE
C
C
      COMMON/BANDS/EK(8,40)
      COMMON/HEADING/NAME(8)
      COMMON//ICHAR(31,51),ESCALE(51)
C
      DELTA=RANGE/50.
      DO 25 I=1,1581
   25 ICHAR(I)=0.
C
C        SET UP EACH COLUMN
C
      DO 50 N=1,31
C
C        SCAN UP THE COLUMN
C
      DO 50 I=1,51
      AMIN=AZERO+(I-1.5)*DELTA
      AMAX=AZERO+(I-.5)*DELTA
C
      DO 50 J=1,9
      X=EK(J,N)
      IF((X.LE.AMAX).AND.(X.GT.AMIN)) ICHAR(N,I)=ICHAR(N,I)+1
   50 CONTINUE
C
      DO 55 I=1,51
   55 ESCALE(I)=AZERO+(I-1)*DELTA
C
C        CONVERT INTEGERS TO CHARACTERS
C
      DO 70 I=1,1581
      ICHAR(I)=ICHAR(I)+0000033
      IF(ICHAR(I).EQ.0000033) ICHAR(I)=0000055
   70 CONTINUE
C
C        GENERATE OUTPUT
C
      PRINT 100,(NAME(I),I=1,8)
  100 FORMAT (*1BAND STRUCTURE FOR *,8A10,//)
      I=51
      DO 150 NA=1,51
      N=52-NA
      IF(N.EQ.I) GO TO 120
      PRINT 200,(ICHAR(J,N),J=1,31)
      GO TO 150
  120 PRINT 201,ESCALE(I),(ICHAR(J,N),J=1,31)
      I=I-5
  150 CONTINUE
C
  200 FORMAT(13X,*I*,R1,30(3X,R1))
  201 FORMAT(2X,F10.2,* I*,R1,30(3X,R1))
C
      PRINT 210
```

```
      PRINT 212
      PRINT 211
C
  210 FORMAT(14X,*I*,39(*.*),*I*,39(*.*),*I*,7(*.*),*I*,31(*.*),*I*)
  211 FORMAT(14X,*L*,17X,*(111)*,15X,*GAMMA*,15X,*(100)*,17X,*X*,7X,
     1*K*,11X,*(110)*,12X,*GAMMA*)
  212 FORMAT(/)
C
      RETURN
      END
```

```
      SUBROUTINE ABSPSI2 (ALFA)
C
C
C        THIS SUBROUTINE CALCULATES THE ABSOLUTE SQUARE OF A BLOCH
C        FUNCTION.
C
C
      LOGICAL INC
      COMMON/TABLE/IT(3,181),NT(11,11,11)
      COMMON /HAMLT/HR(1600),HI(1600)
      COMMON//VMNR(1600),VMNI(1600)
      COMMON/CHGDEN/CR(181),CI(181)
      COMMON/INCLUDE/INC(181)
C
      DIMENSION AR(181,8),AI(181,8),BR(181,8),BI(181,8)
C
      EQUIVALENCE (VMNR,AR),(VMNI,AI),(HR,BR),(HI,BI)
C
C
      DO 80 I=1,724
      BR(I)=0.
   80 BI(I)=0.
C
C
C
      ID=0
      DO 210 I=1,181
      IF (INC(I)) GO TO 210
C
C
      JD=0
      DO 200 J=1,181
      IF (INC(J)) GO TO 200
C
C
      I1=IT(1+ID)-IT(1+JD)
      I2=IT(2+ID)-IT(2+JD)
      I3=IT(3+ID)-IT(3+JD)
C
      ISQ=I1**2+I2**2+I3**2
C
      IF (ISQ-32) 100,100,200
C
  100 M=NT(I1+6,I2+6,I3+6)
C
      I1=I
      J1=J
C
      DO 150 IBAND=1,4
C
C
      BR(M)=BR(M)+AR(I1)*AR(J1)+AI(I1)*AI(J1)
      BI(M)=BI(M)+AI(I1)*AR(J1)-AR(I1)*AI(J1)
C
      M=M+181
      I1=I1+181
```

```
      J1=J1+181
C
  150 CONTINUE
C
C
  200 TD=JD+3
C
  210 ID=ID+3
C
C
C        NORMALIZE TO 1 ELECTRON PER STATE.
C
      ID=0
      DO 250 IBAND=1,4
C
      CONST=ALFA/BR(1,IBAND)
C
      DO 240 I=1,181
C
      CR(I)=CR(I)+CONST*BR(I+ID)
      CI(I)=CI(I)+CONST*BI(I+ID)
C
  240 CONTINUE
C
  250 ID=ID+181
C
C
      RETURN
      END
```

```
      SUBROUTINE SYMETRZ
C
C
C        THIS SUBROUTINE AVERAGES THE CHARGE DENSITY OVER THE POINT
C        GROUP OPERATIONS.
C
C
      COMMON/TABLE/IT(3,181),NT(11,11,11)
      COMMON/SFACTR/COSGTAU(181),SINGTAU(181)
      COMMON/CHGDEN/CR(181),CI(181)
      COMMON/PTGROUP/ GMN(3,3,24)
      COMMON//AR(200),AI(200),BR(200),BI(200)
C
      DIMENSION L(3)
C
      EQUIVALENCE (L(1),L1),(L(2),L2),(L(3),L3)
C
C
C        TRANSLATE THE COORDINATE SYSTEM TO A SYMMETRY POINT.
C
      DO 100 I=1,181
C
      BR(I)=CR(I)*COSGTAU(I)-CI(I)*SINGTAU(I)
      BI(I)=CR(I)*SINGTAU(I)+CI(I)*COSGTAU(I)
C
      AR(I)=0.
  100 AI(I)=0.
C
C
C        AVERAGE OVER THE GROUP OPERATIONS.
C
      JD=0
      DO 250 J=1,24
C
C
      ID=0
      DO 200 I=1,181
C
C
      KD=0
      DO 180 K=1,3
C
      L(K)=6
C
C
      DO 150 M=1,3
C
  150 L(K)=L(K)+GMN(M+KD+JD)*IT(M+ID)
C
  180 KD=KD+3
C
C
      N=NT(L1,L2,L3)
C
      AR(I)=AR(I)+BR(N)/12.
      AI(I)=AI(I)+BI(N)/12.
```

```
C
  200 ID=ID+3
C
  250 JD=JD+9
C
C
C        TRANSLATE THE COORDINATE SYSTEM BACK.
C
      DO 300 I=1,181
C
      CR(I)=AR(I)*COSGTAU(I)+AI(I)*SINGTAU(I)
  300 CI(I)=AI(I)*COSGTAU(I)-AR(I)*SINGTAU(I)
C
C
      RETURN
      END
```

```
      SUBROUTINE SLATER3 (ALPHA,CR,CI,XSR,XSI)
C
C
C        THIS SUBROUTINE CALCULATES A QUADRATIC APPROXIMATION TO THE
C        SLATER EXCHANGE APPROXIMATION.
C
C        THE INPUT MUST BE IN UNITS OF ELECTRONS PER PRIMITIVE UNIT CELL
C        AND THE OUTPUT IS IN RYDBERGS.
C
C
      DIMENSION XSR(181),XSI(181),CR(181),CI(181)
C
      COMMON/INFO/DUMMY(18),A
      C0=0.847
      C1=0.142
      C2=-0.00209
C
      CONST=-4.68956*ALPHA/A
C
C
      CALL CONVOL (181,CR,CI,CR,CI,XSR,XSI)
C
C
      DO 100 I=1,181
C
      XSR(I)=CONST*(C1*CR(I)+C2*XSR(I))
      XSI(I)=CONST*(C1*CI(I)+C2*XSI(I))
C
  100 CONTINUE
C
      XSR(1)=XSR(1)+CONST*C0
C
C
      RETURN
C
      END
```

```
      SUBROUTINE CONVOL (N,AR,AI,BR,BI,CR,CI)
C
C
C
C        THIS SUBROUTINE CALCULATES THE FOURIER SERIES FOR THE PRODUCT
C        OF TWO FOURIER SERIES.
C
C        AR AND AI ARE THE REAL AND IMAGINARY PARTS OF THE FIRST SERIES.
C        BR AND BI ARE THE REAL AND IMAGINARY PARTS OF THE SECOND SERIES
C        CR AND CI ARE THE REAL AND IMAGINARY PARTS OF THE PRODUCT
C        SERIES.
C
C
      DIMENSION AR(N),AI(N),BR(N),BI(N),CR(N),CI(N)
C
      COMMON/TABLE/IT(3,181),NT(11,11,11)
C
C
      MAX=0
      DO 110 I=1,3
  110 MAX=MAX+IT(I,N)**2
C
C
      DO 120 I=1,N
      CR(I)=0.
  120 CI(I)=0.
C
C
      DO 200 I=1,N
      DO 200 J=1,N
C
C
      I1=IT(1,I)+IT(1,J)
      I2=IT(2,I)+IT(2,J)
      I3=IT(3,I)+IT(3,J)
C
      ISQ=I1*I1+I2*I2+I3*I3
      IF (ISQ.GT.MAX) GO TO 200
C
      M=NT(I1+6,I2+6,I3+6)
C
      CR(M)=CR(M)+AR(I)*BR(J)-AI(I)*BI(J)
      CI(M)=CI(M)+AR(I)*BI(J)+AI(I)*BR(J)
C
  200 CONTINUE
C
C
      RETURN
      END
```

```
      SUBROUTINE FSPLT (ZERO,RANGE)
C
C
C        CR IS THE ARRAY OF THE REAL COEFICIENTS.
C        CI IS THE ARRAY OF THE IMAGINARY COEFICIENTS.
C        A IS THE STARTING POINT IN THE UNIT CELL.
C        B IS THE FINAL POINT.
C
C
      COMMON/CHGDEN/CR(181),CI(181)
      COMMON/TABLE/I(3,181),NTAB(11,11,11)
      COMMON/HEADING/NAME(8)
      COMMON//X(101),Y(101),ICHAR(101)
C
      DIMENSION A(3),B(3),DELX(3)
C
C
      N=181
C
      DO 110 J=1,3
      A(J)=0.
      B(J)=1.
  110 DELX(J)=(B(J)-A(J))/100.
C
      DO 115 L=1,101
  115 Y(L)=0.
C
C
C
      DO 200 K=1,N
      GDX=0.
C
      DO 130 J=1,3
  130 GDX=GDX+I(J,K)*DELX(J)
C
      CSGDX=COS(6.2832*GDX)
      SNGDX=SIN(6.2832*GDX)
C
C
C        CALCULATE TERM AT A
C
      GX=0.
      DO 135 J=1,3
  135 GX=GX+I(J,K)*A(J)
C
      CSGX=COS(6.2832*GX)
      SNGX=SIN(6.2832*GX)
C
      Y(1)=Y(1)+CR(K)*CSGX-CI(K)*SNGX
C
C        CALCULATE TERMS FROM A TO B
C
      DO 200 L=2,101
C
      CSTEMP=CSGX
      SNTEMP=SNGX
```

```
      CSGX=CSTEMP*CSGDX-SNTEMP*SNGDX
      SNGX=SNTEMP*CSGDX+CSTEMP*SNGDX
C
      Y(L)=Y(L)+CR(K)*CSGX-CI(K)*SNGX
C
C
  200 CONTINUE
C
C
C
C        GENERATE OUTPUT
C
      PRINT 205,(NAME(J),J=1,8)
  205 FORMAT (*1PLOT OF *,8A10,/)
      PRINT 206,(A(J),J=1,3),(B(J),J=1,3)
  206 FORMAT(* FROM (*,F6.3,*,*,F6.3,*,*,F6.3,*)   TO (*,F6.3,*,*,
     1F6.3,*,*,F6.3,*)*,//)
C
C
      DELY=RANGE/50.
      IFLG=50
C
      DO 300 INDX=1,51
C
      M=51-INDX
      YM=M*DELY+ZERO
      YMIN=YM-.5*DELY
      YMAX=YM+.5*DELY
C
C
      DO 220 K=1,101
C
      ICHAR(K)=0000055
      IF ((Y(K).LE.YMAX).AND.(Y(K).GT.YMIN)) ICHAR(K)=0000047
C
  220 CONTINUE
C
C
C
      IF (M.EQ.IFLG) GO TO 230
C
      PRINT 225,(ICHAR(K),K=1,101)
  225 FORMAT (15X,*I*,101R1)
      GO TO 300
C
C
  230 PRINT 235,YM,(ICHAR(K),K=1,101)
  235 FORMAT (5X,F10.2,*I*,101R1)
      IFLG=IFLG-5
C
  300 CONTINUE
C
C
      PRINT 310
  310 FORMAT (15X,20(*I....*),*I*)
C
```

```
      PRINT 311,(J,J=1,9)
  311 FORMAT (13X,*0.0*,9(7X,*0.*,I1),7X,*1.0*)
C
C
      DO 350 L=1,101
  350 X(L)=(L-1)/100.
C
      PRINT 999
      PRINT 355,(X(L),Y(L),L=1,101)
  355 FORMAT (1X,5(F5.2,F10.3,10X))
C
  999 FORMAT (/////)
C
C
      RETURN
      END
```

```
      SUBROUTINE TYMER (NAME)
C
C        THIS SUBROUTINE GENERATES TIMING INFORMATION
C
C
      CALL CPELAP(I)
      T=(IMILLI(I)-K)/1000.
      PRINT 10,T,NAME
   10 FORMAT (5X,F10.3,* SECONDS REQUIRED TO EXECUTE *,A10)
C
      ENTRY INTYME
      CALL CPELAP(I)
      K=IMILLI(I)
      RETURN
      END
```

```
      SUBROUTINE SORT(N,X,I)
C
C        THIS SUBROUTINE SORTS A ONE-DIMENSIONAL ARRAY X IN ORDER OF
C        INCREASING MAGNITUDE AND SIMULTANEOUSLY PERMUTES AN INDEX ARRAY
C        I.  N IS THE LENGTH OF THE ARRAY
C
C
      DIMENSION X(N),I(N)
      DO 50 J=2,N
      XT=X(J)
      IT=I(J)
      DO 40 K=2,J
      L=J-K+1
      IF(XT.GE.X(L)) GO TO 50
      X(L+1)=X(L)
      I(L+1)=I(L)
      X(L)=XT
      I(L)=IT
   40 CONTINUE
   50 CONTINUE
      RETURN
      END
```

```
      PROGRAM CRYSPOT (INPUT,OUTPUT,TAPE1=INPUT,TAPE6)
C
C
C
      COMMON/TABLE/IT(3,181),NT(11,11,11)
      COMMON/PARAMTR/ZA,QA,ALPHAA,BETAA,GAMMAA,VOA,ZB,QB,ALPHAB,BETAB,
     1GAMMAB,VOB,XALPHA,RELAX,E1,E2,A
      COMMON/SFACTR/COSGTAU(181),SINGTAU(181)
      COMMON/DIFF/AR(181),AI(181)
      COMMON/CHGDEN/CR(181),CI(181)
      COMMON/HEADING/NAME(8),IDATA(8)
      COMMON/INFO/INF(16)
      COMMON/PRMTR2/ZC,QC,ALPHAC,BETAC,GAMMAC,VOC,ZD,QD,ALPHAD,BETAD,
     1GAMMAD,VOD,X1,Y1
C
      DIMENSION XA(3),XB(3),X(3)
      DIMENSION PRMTR(17)
      DIMENSION PRMT2(14)
C
      EQUIVALENCE (PRMTR(1),ZA)
      EQUIVALENCE (PRMT2(1),ZC)
C
C
      LOGICAL INF
      DO 10 I=1,16
   10 INF=.F.
C
C
C
      READ 60,(NAME(I),I=1,8)
      IF (EOF,1) 100,50
   50 READ 60,(IDATA(I),I=1,8)
      READ 80,(PRMTR(I),I=1,17)
      READ 90,(J,CR(J),CI(J),I=1,181)
C
   60 FORMAT (8A10)
   80 FORMAT (8F10.4)
   90 FORMAT (4(I4,2F8.5))
C
      DO 95 I=1,14
   95 PRMT2(I)=0.
C
      GO TO 150
C
  100 CALL GET (5HTAPE6,7HPARAMTR,0,0)
C
      READ (6,110) (PRMTR(I),I=1,17)
      READ (6,120) (NAME(I),I=1,8),(IDATA(I),I=1,8)
      READ (6,110) (PRMT2(I),I=1,14)
      REWIND 6
C
      CALL GET (5HTAPE6,7HCHGDATA,0,0)
      READ (6,130) (CR(I),CI(I),I=1,181)
C
```

```
  110 FORMAT (F12.4)
  120 FORMAT (8A10)
  130 FORMAT (2F10.5)
C
C
  150 CONTINUE
C
      CALL FCCLAT
C
C
      CALL DATE (I1)
      CALL TYME(I2)
      PRINT 170,I1,I2
      PRINT 175,(NAME(I),I=1,8)
      PRINT 180,ZA,QA
      PRINT 185,ALPHAA,BETAA,GAMMAA,VOA
      PRINT 190,ZB,QB
      PRINT 185,ALPHAB,BETAB,GAMMAB,VOB
      PRINT 195,X1,Y1
      PRINT 999
C
  170 FORMAT (10X,*RUN DATE *,A10,10X,*TIME *,A10,//)
  175 FORMAT (* ELECTROSTATIC POTENTIAL OF *,8A10,//)
  180 FORMAT (* A ATOM*,/,* Z=*,F2.0,5X,*Q=*,F2.0)
  185 FORMAT (* ALPHA=*,F5.2,5X,*BETA=*,F5.2,5X,*GAMMA=*,F5.2,5X,*VO=*,F6.
     16.2)
  190 FORMAT (//,* B ATOM*,/,* Z=*,F2.0,5X,*Q=*,F2.0)
  195 FORMAT (/,5X,*X=*,F4.2,10X,*Y=*,F4.2)
C
C
C
      CALL FOURCF
C
      DO 350 J=1,3
  350 X(J)=.375
      CALL CLUSTER (A,X,10.,X1,Y1,VREF1)
      CALL FSPT (181,X,AR,AI,VREF1)
C
      DO 360 J=1,3
  360 X(J)=.625
      CALL CLUSTER (A,X,10.,X1,Y1,VREF2)
      CALL FSPT (181,X,AR,AI,VREF2)
C
      VREF1=-13.605*VREF1
      VREF2=-13.605*VREF2
C
      PRINT 375,VREF1,VREF2
  375 FORMAT (* VREF1=*,F10.2,10X,*VREF2=*,F10.2)
C
C
  900 CONTINUE
  999 FORMAT (/////)
C
      END
```

```
      SUBROUTINE FOURCF
C
C
C
      COMMON/PARAMTR/ZA,QA,ALPHAA,BETAA,GAMMAA,VOA,ZB,QB,ALPHAB,BETAB,
     1GAMMAB,VOB,XALPHA,RELAX,E1,E2,A
      COMMON/SFACTR/COSGTAU(181),SINGTAU(181)
      COMMON/TABLE/IT(3,181),NT(11,11,11)
      COMMON/DIFF/AR(181),AI(181)
      COMMON/CHGDEN/CR(181),CI(181)
      COMMON/PRMTR2/ZC,QC,ALPHAC,BETAC,GAMMAC,VOC,ZD,QD,ALPHAD,BETAD,
     1GAMMAD,VOD,X1,Y1
C
C
C
      AR(1)=0.
      AI(1)=0.
C
      C=2.5465/A
C
      C1A=(1.-X1)*(ZA-QA)+X1*(ZC-QC)
      C1B=(1.-Y1)*(ZB-QB)+Y1*(ZD-QD)
C
      C2A=-19.7392*((1.-X1)/(BETAA*A)**2+X1/(BETAC*A)**2)
      C2B=-19.7392*((1.-Y1)/(BETAB*A)**2+Y1/(BETAD*A)**2)
C
C
      DO 200 I=2,181
      GSQ=IT(1,I)**2+IT(2,I)**2+IT(3 I)**2
C
      RHOA=C1A*EXP(C2A*GSQ)
      RHOB=C1B*EXP(C2B*GSQ)
C
      AR(I)=-(C/GSQ)*(CR(I)-(RHOB+RHOA)*COSGTAU(I))
      AI(I)=-(C/GSQ)*(CI(I)-(RHOB-RHOA)*SINGTAU(I))
C
C
  200 CONTINUE
C
C
      RETURN
      END
```

```
      SUBROUTINE CLUSTER (A,XA,RMAX,X1,Y1,Z)
C
C
C        THIS SUBROUTINE EVALUATES A CLUSTER SUMMATION OVER A RADIUS
C        RMAX ABOUT A POINT X OF FUNCTIONS FTN LOCATED ON ZINC-BLENDE
C        LATTICE POINTS.
C        A IS THE CUBIC LATTICE CONSTANT.
C
C
      DIMENSION X(3),XA(3),Y(3),TAU(3)
C
C
      LOGICAL IX,IY
C
      IX=X1.NE.0.
      IY=Y1.NE.0.
C
C
      Z=0.
C
      DO 50 I=1,3
      X(I)=A*XA(I)
   50 TAU(I)=.125*A
C
      RMAX2=RMAX**2
      C=A/2.
      MAX=8
      MIN=-8
C
C
C        CONSTRUCT THE LATTICE VECTORS.
C
      DO 300 I1=MIN,MAX
      DO 300 I2=MIN,MAX
      DO 300 I3=MIN,MAX
C
      Y(1)=C*(I2+I3)
      Y(2)=C*(I1+I3)
      Y(3)=C*(I1+I2)
C
C        A ATOM
C
      R2=0.
      DO 100 I=1,3
  100 R2=R2+(Y(I)+TAU(I)-X(I))**2
      IF (R2-RMAX2) 120,120,150
  120 R=SQRT(R2)
      Z=Z+(1.-X1)*VATOMA(R)
C
      IF (IX) Z=Z+X1*VATOMC(R)
C
C        B ATOM
C
  150 R2=0.
      DO 170 I=1,3
  170 R2=R2+(Y(I)-TAU(I)-X(I))**2
```

```
      IF (R2-RMAX2) 200,200,300
  200 R=SQRT(R2)
      Z=Z+(1.-Y1)*VATOMB(R)
C
      IF(IY) Z=Z+Y1*VATOMD(R)
C
C
  300 CONTINUE
C
C
      RETURN
      END
```

```
      FUNCTION ERFC (X)
C
C         THIS FUNCTION EVALUATES THE COMPLEMENTARY ERROR FUNCTION.
C
C
      T=1./(1.+.47047*X)
      ERFC=T*(.3480242+T*(-.0958798+T*.7478556))*EXP(-X**2)
C
      RETURN
      END
```

```
      FUNCTION VATOMA (R)
C
C
      COMMON/PARAMTR/ZA,QA,ALPHAA,BETAA,GAMMAA,VOA,ZB,QB,ALPHAB,BETAB,
     1GAMMAB,VOB,XALPHA,RELAX,E1,E2,A
C
      X=.707107*BETAA*R
      VATOMA=(2./R)*(QA*EXP(-ALPHAA*R)+(ZA-QA)*ERFC(X))
C
      RETURN
      END


      FUNCTION VATOMB (R)
C
C
      COMMON/PARAMTR/ZA,QA,ALPHAA,BETAA,GAMMAA,VOA,ZB,QB,ALPHAB,BETAB,
     1GAMMAB,VOB,XALPHA,RELAX,E1,E2,A
C
      X=.707107*BETAB*R
      VATOMB=(2./R)*(QB*EXP(-ALPHAB*R)+(ZB-QB)*ERFC(X))
C
      RETURN
      END


      FUNCTION VATOMC (R)
C
C
      COMMON/PRMTR2/ZC,QC,ALPHAC,BETAC,GAMMAC,VOC,ZD,QD,ALPHAD,BETAD,
     1GAMMAD,VOD,X1,Y1
C
      X=.707107*BETAC*R
      VATOMC=(2./R)*(QC*EXP(-ALPHAC*R)+(ZC-QC)*ERFC(X))
C
      RETURN
      END


      FUNCTION VATOMD (R)
C
C
      COMMON/PRMTR2/ZC,QC,ALPHAC,BETAC,GAMMAC,VOC,ZD,QD,ALPHAD,BETAD,
     1GAMMAD,VOD,X1,Y1
C
      X=.707107*BETAD*R
      VATOMD=(2./R)*(QD*EXP(-ALPHAD*R)+(ZD-QD)*ERFC(X))
C
      RETURN
      END
```

```
      SUBROUTINE FSPT (N,X,AR,AI,Z)
C
C
      COMMON/TABLE/IT(3,181),NT(11,11,11)
C
      DIMENSION AR(N),AI(N)
      DIMENSION X(3)
C
C
      DO 200 I=1,N
      GX=0.
      DO 100 J=1,3
  100 GX=GX+IT(J,I)*X(J)
      GX=6.28319*GX
C
      Z=Z+AR(I)*COS(GX)-AI(I)*SIN(GX)
C
  200 CONTINUE
      RETURN
      END
```

```
      SUBROUTINE FRSUM (N,XA,XB,AR,AI,Z)
C
C
C
      COMMON/TABLE/IT(3,181),NT(11,11,11)
C
C
      DIMENSION XA(3),XB(3),DELX(3)
      DIMENSION AR(181),AI(181)
      DIMENSION Z(N)
C
C
      C=6.28319
C
C        CALCULATE DELX
C
      DO 50 I=1,3
   50 DELX(I)=(XB(I)-XA(I))/N
C
C        DO FOR ALL G
C
      DO 400 J=1,229
C
C        INITIALIZE COSGX,SINGX,COSGDX,SINGDX
C
      GX=0.
      GDX=0.
C
      DO 100 I=1,3
      GX=GX+IT(I,J)*XA(I)
  100 GDX=GDX+IT(I,J)*DELX(I)
C
      COSGX=COS(C*GX)
      SINGX=SIN(C*GX)
      COSGDX=COS(C*GDX)
      SINGDX=SIN(C*GDX)
C
C         DO FOR ALL X
C
      DO 300 K=1,N
C
      COST=COSGX
      SINT=SINGX
C
      COSGX=COST*COSGDX-SINT*SINGDX
      SINGX=COST*SINGDX+SINT*COSGDX
C
      Z(K)=Z(K)+AR(J)*COSGX-AI(J)*SINGX
C
C
  300 CONTINUE
C
  400 CONTINUE
C
      RETURN
      END
```

```
      SUBROUTINE PLOTR (Y,ZERO,RANGE)
C
C
C
      DIMENSION Y(100),NAME(8)
      DIMENSION ICHAR(100)
C
C
      READ 100,(NAME(I),I=1,8)
  100 FORMAT (8A10)
C
      PRINT 110,(NAME(I),I=1,8)
  110 FORMAT (*1*,10X,8A10,///)
C
C
      DELY=RANGE/50.
      IFLG=50
C
C
C
      DO 300 INDX=1,51
C
      M=51-INDX
      YM=M*DELY+ZERO
      YMIN=YM-.5*DELY
      YMAX=YM+.5*DELY
C
C
      DO 220 K=1,100
C
      ICHAR(K)=0000055
C
      IF ((Y(K).LE.YMAX).AND.(Y(K).GT.YMIN)) ICHAR(K)=0000047
C
  220 CONTINUE
C
C
      IF (M.EQ.IFLG) GO TO 230
C
      PRINT 225,(ICHAR(K),K=1,100)
  225 FORMAT (15X,*I*,100R1)
C
      GO TO 300
C
C
  230 PRINT 235,YM,(ICHAR(K),K=1,100)
  235 FORMAT (5X,F10.2,*I*,100R1)
      IFLG=IFLG-5
C
C
  300 CONTINUE
C
C
C
      PRINT 310
  310 FORMAT (15X,20(*I....*),*I*)
```

```
C
      PRINT 320,(I,I=10,100,10)
  320 FORMAT (15X,*0*,10I10)
C
C
      RETURN
      END
```